Università degli Studi di Ferrara

DOTTORATO DI RICERCA IN
"FARMACOLOGIA ED ONCOLOGIA MOLECOLARE"

CICLO XXVI

COORDINATORE Chiar.mo Prof. Antonio Cuneo

Extracellular ATP modulates Myeloid Derived Suppressor Cells functions

Settore Scientifico Disciplinare Patologia Clinica /MED 05

Dottorando
Dott.ssa Marta Vuerich
Marta Vuerich

Tutore
Chiar.mo Prof. Francesco Di Virgilio

Anni 2011/2013

INDEX

ABBREVIATIONS **5**

INTRODUCTION **7**

TUMOR AND IMMUNE SYSTEM 7

MYELOID DERIVED SUPPRESSOR CELLS 9

MDSCs accumulation in cancer 10

MDSCs: Mechanisms of Suppression 11

Factors involved in MDSCs immunosuppression 12

Other immunosuppressive mechanisms 15

MDSCs and T cells 16

MDSCs and Treg 16

MDSCs and $CD8^+$ Lymphocytes 16

MDSCs and $CD4^+$ Lymphocytes 18

ATP **20**

Functions of ATP as extracellular messenger 21

CD39 and CD73 22

PURINERGIC RECEPTORS **24**

P2X7 RECEPTOR 26

AIM OF THE WORK **29**

MATERIAL AND METHODS 30

MSC-1 and MSC-2 Cell Lines 30

Generation of BM-MDSC in vitro 30

Reverse transcriptase polymerase chain reaction 31

Western blot analysis 32

Cytosolic Ca^{2+} concentration measurement 33

Changes in plasma membrane permeability 33

Lucifer yellow uptake assay 33

Plasma membrane potential measurement 34

LDH assay 34

IL-1β secretion measurement 35

TGF-β1 secretion measurement 35

Intracellular ROS concentration measurement 35

Measurement of extracellular ATP 36

Thin Layer Chromatography (TLC) 36

Flow Cytometry Analysis 36

CFSE assay 37

Microscopic analyses 37

Immunofluorescence analysis 38

Evaluation of extracellular ATP levels in neuroblastoma microenvironment 38

RESULTS 39

MSC-1 and MSC-2 express the mRNA and the protein of purinergic receptors ... 39

The stimulation of MSC-1 and MSC-2 with ATP increases $[Ca^{2+}]_i$ 40

The stimulation with BzATP is most effective in MSC-2 41

The stimulation of P2Y receptors with UTP induces a transient calcium response 42

In MSC-2 cell line different P2 subtypes are functional 43

The stimulation with ATP and BzATP induces ethidium bromide uptake in both cell lines 44

The pore associate to the P2X7R is permeable to lucifer yellow in both cell lines 46

The stimulation of MSC-2 with ATP or BzATP induces depolarization of the plasma membrane 49

The stimulation with ATP and BzATP induces cell swelling and blebbing in MSC-1 and MSC-2 cell lines 51

The stimulation of P2 receptors induces a moderate LDH release by MSC-1 and MSC-2 54

The stimulation of P2X7R triggers IL-1β release in both cell lines 58

P2X7R stimulation induces the release of TGF-β1 in MSC-1 and MSC-2 59

The stimulation of P2X7R increases the intracellular ROS concentration in both cell lines 60

The stimulation of P2X7R increases ARG-1 expression in both cell lines..... 61

Extracellular ATP is detectable in neuroblastoma tumor microenvironment 62

MSC-1 and MSC-2 cell lines release ATP in the extracellular microenvironment. 64

MSC-2 cell line express the protein of CD39 65

In vitro generation of BM-MDSC 66

MDSCs express the protein of PX3, P2X5, P2Y6 AND P2X7R 67

MDSCs release ATP in the extracellular microenvironment..... 68

ATP and UTP have chemotactic effect on MDSC 69

MDSCs express the protein of CD39 and CD73 70

The stimulation with ATP or adenosine increases the expression of CD39 71

MDSCs express functional CD39 and CD73..... 72

The stimulation of MDSCs with ATP or adenosine increases their immunosuppressive activity in vitro..... 73

Identification of Myeloid Derived Suppressor Cells from neuroblastoma-bearing mice 78

Identification of Granulocytic and Monocytic Myeloid Derived Suppressor Cells subsets from neuroblastoma-bearing mice 79

P2X7R is expressed in Granulocytic and Monocytic Myeloid Derived Suppressor Cells subsets in neuroblastoma-bearing mice..... 80

P2X7 receptor is more functional in M-MDSCs..... 81

Functional characterization of Granulocytic and Monocytic Myeloid Derived Suppressor Cells subsets from neuroblastoma-bearing mice..... 82

M-MDSCs are more tumorigenic than G-MDSCs 84

DISCUSSION 85

REFERENCES 90

FULL PAPERS..... 105

POSTERS 105

ABBREVIATIONS

ADO:	Adenosine
AMP:	Adenosine monophosphate
ADP:	Adenosine diphosphate
ATP:	Adenosine triphosphate
Arg-1:	Arginase-1
BM:	Bone marrow
BM-MDSC:	Bone marrow generated myeloid derived suppressor cells
BSA:	Bovine Serum Albumin
BzATP:	2',3'-(4-benzoil)-benzoic-ATP
Ca^{2+}:	Ion calcium
C/EBP-b:	CAAT/enhancer binding protein-beta
CD:	Cluster of Differentiation
Da:	Dalton
DC:	Dendritic cells
Dig:	Digitonin
DNA:	Deoxyribosenucleic acid
cDNA:	Complementary-double stranded DNA
dsDNA;	Double stranded DNA
ELISA:	Enzyme linked immunoabsorbant assay
FACS:	Flow cytometry
GM-CSF:	Granulocyte macrophage colony stimulating factor
HEK:	Human Embryonic Kidney
IFN-β:	Interferon beta
IFN-γ:	Interferon gamma
IL:	Interleukin
iNOS:	Inducible nitric oxide synthase
Iono:	Ionomycin
LPS:	Lipopolysaccharide
2-MeSATP:	2-metiltio-ATP
MDSCs:	Myeloid derived suppressor cells

MHC:	Major Histocomptability complex
NB:	Neuroblastoma
NF-kB:	Nuclear factor kappa light chain enhancer of activated B cells
NO:	Nitric oxide
PCR:	Polymerase chain reaction
RT-PCR:	Reverse transcriptase- polymerase chain reaction
PBS:	Phosphate Buffered Saline
PGE2:	Prostaglandin E2
RNA:	Ribosenucleic acid
ROS:	Reactive oxygen species
SP:	Sulfinpyrazone
STAT:	Signal Transducer and Activator of Transcription
TCR:	T-cell receptor
T eff:	T effector cell
TLR:	Toll-like receptor
Th1:	T helper cells (Type 1)
Th2:	T helper cells (Type 2)
Treg:	Regulatory T cell
TNF-α:	Tumor necrosis factor-alfa
UDP:	Uridin diphosphate
UTP:	Uridin triphosphate
WT:	Wildtype

INTRODUCTION

TUMOR AND IMMUNE SYSTEM

The first evidence of the power of the immune system to recognize and destroy cancer cells, dates back 1809 when William Coley found that injection of erysipelas directly into the tumor produced remission in some sarcoma patients [1].

This and other observations led nearly a century later, the development of the "Immunosorveillance theory" purposed by Brunet and Thomas. According to this theory the specific neo-antigens expressed by tumor cells would have induced an immune stimulation, leading the elimination of the malignancy [2]. In addition both researchers hypothesized that the higher organisms would have developed some mechanisms protecting them from tumors in allogenic rejection-like manner.

Unfortunately discordant results obtained in the subsequent years, and increasing evidences of the inability of the immune system to effectively destroy the tumor, led the abandonment of the theory. Furthermore there was a growing conviction that the nature of the immune response in cancer is a complex comprised of highly orchestrated and integrated innate and adaptive responses, that reveal a delicate balance between positive and negative stimuli [3].

On the other hand the tumor develops escaping mechanisms able to induce a potent suppression of the immune response, acting at localized and systemic level. An important role in this phenomenon is played by the genetic instability of cancer cells, that affects antigens expression, components of the MHC or the IFN-γ signaling pathway.

Taken together these observations led a review of the Brunet and Thomas' theory, introducing the "cancer immunoediting" hypothesis, that summarizes the complex relationship between the immune system and cancer cells in three main events:

1) Elimination: in the beginning the immune system can recognize and destroy tumor cells.
2) Equilibrium: the tumor growth arrests and the immune response selects and/or promotes tumor cell variants with increasing capacities to survive the immune attack.

3) Escaping: the survived tumor cell variants expand in an uncontrolled manner. In this phase the malignancy is clinically detectable.

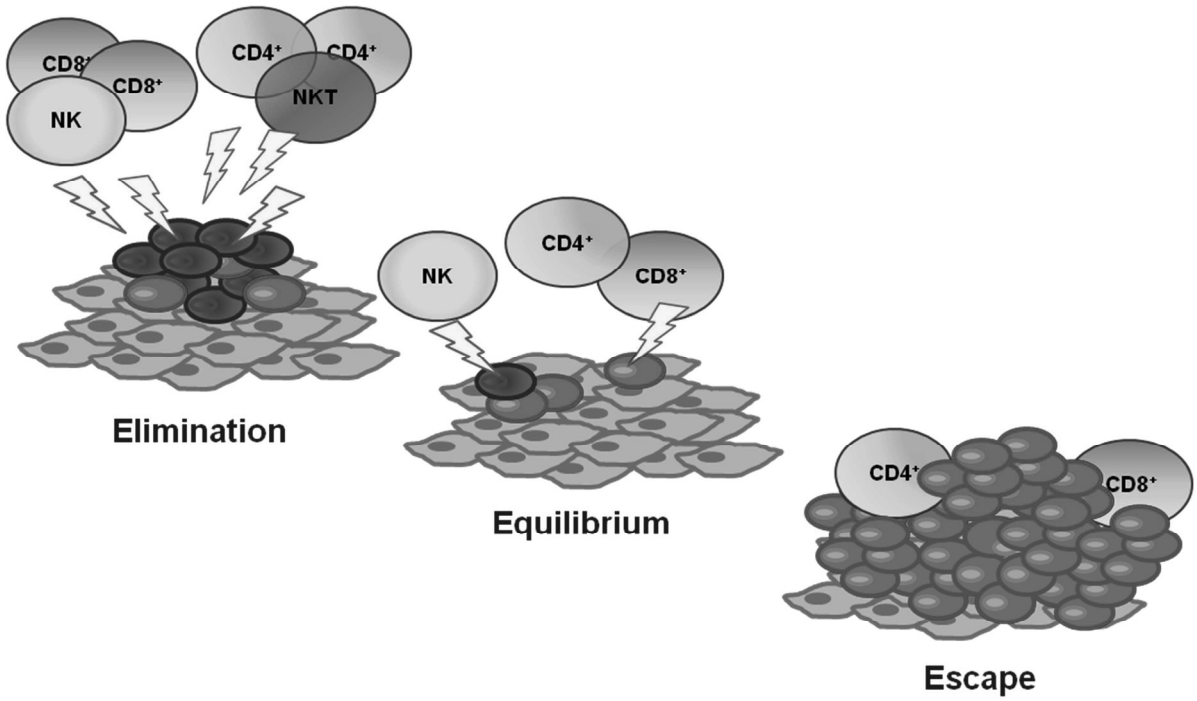

Figure 1. Three phases of the "cancer immunoediting"

Elimination, Equilibium and Escape. In the first and second phases tumor cells (blue) and tumor cell variants (red) are underlyed stroma cells (gray): immune cells limit the growth of the neoplasm. In the last phase, as result of the equilibrium process, the selected tumor cell variants (red) expand in an uncontrolled manner. Different lymphocyte populations are as marked.

The tumor immune escape is mediated by different mechanisms dealing with structural and functional changes, both in tumor and stroma cells, leading finally to the inability of even activated effectors immune cells to reject the tumor.

For example tumor cells can affect the differentiation of DCs, inhibiting their functionality. This causes a reduction in the number of APCs (antigen presenting cells), resulting in a deficiency in T cells stimulation. Gabrilovich ad colleague have also found that this inhibition in the DCs maturation is probably due to the constitutive activation of STAT3 and inactivation of NF-Kb (nuclear factor B), consequence of the exposure to vascular endothelial growth factor (VEGF), IL-6 and M-CSF [4].

Moreover an intensive secretion of several factors, such as transforming growth factor (TGF)-β, interleukin (IL)-10, reactive oxygen and nitrogen species, prostaglandins [5] and IL-1β led a rapid recruitment in the tumor microenvironment of immunosuppressive cells of lymphoid and myeloid origin.

The cellular populations with regulatory effect on the immune response are: regulatory T cells (Tregs) ($CD4^+$, $CD25^+$, $FOXP3^+$, $CD39^+$, $CD73^+$) [6, 7], tumor-associated M2 macrophages (TAMs) [8], N2 neutrophiles, regulatory/tolerogenic dendritic cells (DCs) [9] and myeloid-derived suppressor cells (MDSCs) [10,11,12].

Most of these populations in physiological conditions play an important role in the maintenance of the immune system homeostasis, for example Tregs dysfunctions are associated to autoimmune diseases with at times fatal outcome.

Unfortunately the tumor can use these same mechanisms to its advantage. In fact the accumulation of Tregs and MDSCs in tumor microenvironment is widely stated and there are evidences of an increased role of MDSCs in the tumor-escape phenomenon.

MYELOID DERIVED SUPPRESSOR CELLS

The term Myeloid Derived Suppressor Cells (MDSCs) was reported for the first time in a letter to the editor of the journal Cancer Research, signed by Gabrilovich and colleague in 2007 [13].

From that moment MDSCs has been used to define a cell population that accumulates under inflammatory conditions such as infections, chronic inflammation, autoimmune disease and cancer, with the peculiarity to exert a potent suppression of T cells response both *in vitro* and *in vivo*.

Characteristic of these cells is the ability to change their mediators expression (e.g. iNOS and Arginase I (ARG1)) and their differentiation state in response to environmental influences. MDSCs are also distinguished by their partially undifferentiated (immature) state and by the high capacity to release cytokines, reactive oxygen and nitrogen species [14].

A low amount of MDSCs is detectable also in an non-inflamed state, present predominantly in the bone marrow where participate in the normal process of

myelopoiesis (controlled by a complex network of soluble factors including GM-CSF, G-CSF, M-CSF, SCF, FLT3 and IL-3) [15].

In mice, MDSCs are commonly identified for the co-expression of the cell surface markers CD11b and Gr-1 [16]. Moreover, due to their partial undifferentiated state, these cells express several different markers and recently some groups have divided mouse MDSCs in two major subsets, based on the expression of Ly6C and Ly6G.
As result of this classification we have:

- "monocytic" MDSCs ($CD11b^{+}Ly6G^{+}Ly6C^{low}$)
- "granulocytic/ neutrophil-like" MDSCs ($CD11b+Ly6G^{-}Ly6C^{high}$) [17, 18]

these two cell subsets even differ in their immunosuppressive mechanism [19].
As regard human MDSCs the same two subpopulations have been observed:

- $Lin^{-}HLA^{-}DR^{-}CD33^{+}$ or $CD11b^{+}CD14^{-}CD15^{+}$ for "granulocytic" MDSCs
- $CD14^{+}HLA^{-}DR^{neg/lo}$ or $CD11b^{+}CD14^{+}HLADR^{neg/\ lo}$ for "monocytic" cells [11, 20, 21].

MDSCs accumulation in cancer

It is strongly stated that tumor milieu is an highly inflammatory environment, rich on nucleotides and inflammatory mediators [22].
It has been reported that many of these factors could stimulate the MDSCs recruitment and expansion [11, 12]. Interestingly, also in the absence of tumor cells, chronic inflammation has been shown to provide the conditions for MDSCs accumulation and stimulation [23]. Furthermore there are evidences that anti-inflammatory conditions cause a significant reduction of frequencies and immunosuppressive functions of tumor-infiltrating MDSCs [24, 25, 26].
The chronic inflammatory factors associated to the expansion of suppressor cells are:

- cytokines: IL-1β, IL-4, IL-5, IL-6, IL- 10, IL-13, tumor necrosis factor (TNF)-α, and interferon (IFN)-γ
- growth factors: VEGF, TGF-β, granulocyte/macrophage colony-stimulating factor (GM-CSF), granulocyte colony-stimulating factor (G-CSF), and macrophage colony-stimulating factor (M-CSF)
- chemokines C-C motif ligand: (CCL) 2, CCL4, CCL5, C-X-C motif ligand (CXCL) 1, CXCL8, and CXCL12

- cyclooxygenase-2 (COX-2) as well as prostaglandin E2 (PGE2) [20, 21, 24, 51].

All these mediators exert their effects in combination and in dose-dependent manner. In physiological conditions GM-CSF drives myelopoiesis, whereas G-CSF and M-CSF induce further differentiation of myeloid cells to granulocytes or macrophages respectively [27]. However in tumor lesions, all three growth factors have been shown to be overproduced [28, 29]. Tumor-derived GM-CSF has been recently reported to be one of the key factors involved in the generation of MDSCs in a dose-dependent manner [30]. Low GM-CSF concentrations, without IL-4, induce a robust generation of MDSCs and immature DCs from bone marrow hematopoietic precursor cells *in vitro*, on the contrary high concentrations of the growth factor stimulates the development of neutrophiles and mature DCs. Furthermore, GM-CSF in combination with IL-6, IL-1β, PGE2, TNF-α or VEGF has been shown to mediate the *in vitro* generation of highly suppressive MDSCs from $CD33^+$ mononuclear cells isolated from the peripheral blood of healthy donors [31].

MDSCs: Mechanisms of Suppression

Due to their heterogeneous phenotype, MDSCs can contribute to the tumor progression in several ways including inhibition of both innate and adaptive immunity and induction of angiogenesis [32, 33].

At this regard some groups have found that the hypoxic conditions of the tumor microenvironment induce MMP and VEGF production by suppressor cells [34] regulated by the hypoxia inducible transcription factor HIF-1α [35].

The role of MDSCs in perturbing innate immunity is currently less defined, however observations suggest that MDSCs may suppress NK cells [36, 37] and polarize tissue macrophage differentiation toward a type 2/‘alternatively activated’ phenotype, (associated with tissue remodeling and pro-angiogenic activities) [38] thus enhancing tumor progression. It has also been suggested that MDSCs limit the availability of mature and functional DCs, which bridge the gap between innate and adaptive immunity.

On the other hand the importance of the adoptive immunity suppression for cancer immune escape is well stated, therefore a robust investigation to elucidated how MDSCs inhibit T cells responses is now ongoing. Several studies have found that the T cells suppression requires cell-to-cell contact and can be antigen-specific or non-specific. Moreover the mechanism is strongly associated to the involved MDSCs

subpopulation, suggesting a role for surface receptor interactions and/or short-lived soluble mediators.

MDSCs activation is reflected by an intensive NO production and ARG-1 expression, resulting in a strong inhibition of T cell reactivity [39, 40]. One of the major effects of MDSCs on T cell is the remarkable decrease in the TCR ζ-chain expression, which plays a central role in coupling the TCR-mediated antigen recognition to various signaling pathways [41]. A profound down-regulation of TCR ζ-chain expression has been detected in T lymphocytes infiltrating melanoma lesions from ret transgenic mice, in T cells from cancer patients [42, 43] and also from chronically inflamed mice, [44] suggesting a resemblance of both pathological processes. Moreover, a direct inhibition of TCR ζ-chain expression has been observed upon an *in vitro* co-culture of MDSCs isolated from tumor-bearing mice or animals affected by chronic inflammatory conditions with normal T lymphocytes [45].

Factors involved in MDSCs immunosuppression

Arginase (ARG1)

The disruption of the metabolism of L-arginine, to affect the T cells functions has been extensively described in MDSCs [46].

The availability of arginine is a key factor for T-cells metabolism and it has been shown that the L-arginine depletion induces loss of CD3-ζ chain, blocks cell proliferation (being arrested in the G0-G1 phase of the cell cycle) and decreases cytokines production by lymphocytes *in vitro*.

This important amino-acid is the substrate for two enzymes: iNOS (that generates NO) and arginase (ARG1) which converts L-arginine into urea and L-ornithine. MDSCs express high levels of both enzymes whose direct role in the inhibition of T-cell function is well established [47].

The expression of ARG1 is regulated by Th2 cytokines, especially IL-4 and IL-13.

The increased activity of the enzyme in MDSCs enhances L-arginine catabolism, causing the depletion of this non-essential amino acid from the tumor microenvironment. This phenomenon has been described in patients with colon, breast, lung, and prostate cancer [48].

Usually the amino acids deprivation is an important mechanism for regulating of the lymphocyte response, in fact some data show that the CTLs suppression correlate even with the depletion of cysteine, phenylalanine and tryptophan [49, 50, 51].

Tryptophan

Tryptophan metabolism is increased in a tumor-conditioned microenvironment [54, 52]. The enzyme involved in the metabolism of this amino-acid is the indoleamine 2,3-dioxygenase (IDO), that catalyzes the degradation of the L-tryptophan to N-formylkynurenine. It was interestingly shown that human monocyte-derived macrophages and in vitro-derived DC expressing IDO, inhibit T cell proliferation, [53,54] and has been suggested that the IDO expression by Myeloid Derived Suppressor Cells might protect tumor from T cells (inducing tolerance through tryptophan catabolism) [55].

Cysteine

Cysteine is another amino-acid important for T cell proliferation and activation. Mammalian cells generate cysteine via two different pathways:

- expression of plasma membrane cystine transporter xc: imports disulfide-bonded cystine from the oxidizing extracellular milieu to the intracellular reducing environment, where it can be reduced to cysteine [56, 57]
- intracellular expression of cystathionase: it converts intracellular methionine to cysteine [58]

Unfortunately T cells do not contain cystathionase or the xCT chain of the xc– transporter [59, 60], so they so can neither produce cysteine nor import cystine from the extracellular environment, making them dependent on other cells for production of the amino-acid (which is then imported through their ASC neutral amino acid plasma membrane transporter).

Under physiological conditions DCs and macrophages, expressing both cystathionase and the xc–transporter, synthesize cysteine of which surplus is released and subsequently imported by T cells during antigen presentation.

Interestingly MDSCs express the xc–plasma membrane transporter (permitting enhanced cystine uptake), but do not express neither cystathionase nor ASC neutral amino acid transporter (so are unable to import and export cysteine). Hence MDSCs are fully dependent on importing cystine from the extracellular environment, competing for, and depleting the necessary amino acid required for T cell activation and proliferation. This results in the inhibition of anti-tumor T cell responses [49].

Reactive Oxygen and Nitrogen Species

One of the major characteristics of MDSCs has been shown to be the high production of ROS. The up-regulation of this pathway, as well the molecular mechanism to which this underlies are strictly related to exposure of the cells at the tumor derived factors and the inflammatory mediators. Szuster-Ciesielska and colleagues have compared the ROS production by PMN isolated from the blood of 16 patients affected by larynx carcinoma, with that of neutrophils obtained from 15 healthy individuals. They have interestingly observed that the levels of ROS, especially spontaneous and PMA inducible superoxide, were substantially higher in cancer patients than in healthy volunteers. They also found that the rise was associated with the tumor stage. Moreover they have shown how, after partial or total laryngectomy, a significant decrease in ROS production and in the serum activity of catalase and peroxidase, occurred [61].

Several known tumor-derived factors, like TGF-β, IL-10, a number of other cytokines and growth factors released by tumor can induce ROS production, including IL-6, IL-3, PDGF, GMCSF [62].

It was even observed that ARG and iNOS can synergistically operate to inhibit antigen-specific T cell responses *in vitro* [63]. When both enzymes are induced at sufficient levels, under conditions of limited L-arginine availability, reactive nitrogen oxide species are produced by NOS2 [46].

Studies have shown that oxidative stress, caused by MDSCs, inhibited ζ-chain expression in T cells and antigen-induced cell proliferation [64, 66, 67]. ROS are also known to trigger signaling related to angiogenesis.

Moreover both *in vitro* and *in vivo,* the inhibition of ROS production in MDSCs, completely abrogated the negative effect of these cells in mice and cancer patients [65].

Peroxynitrite

Peroxynitrite (PNT), the product of interaction between NO and superoxide, is one of the most powerful oxidants. The main effect of the accumulation on PNT is the nitration of several amino acids such as cysteine, methionine, tryptophane and most prominently tyrosine. An increased concentration of PNT has been detected in inflammatory sites, characterized by accumulation of MDSCs or ongoing immune reactions. It has been shown that this phenomenon is directly implicated in the

promotion of tumor progression as it is documented for pancreatic cancer, malignant gliomas, head and neck cancer, breast cancer, melanoma and mesothelioma.
It has been shown that the peroxynitrite production by MDSCs, during direct contact with T cells, resulted in nitration of the T-cell receptor (TCR) and CD8 molecules [68], leading conformational changes in the TCR-CD3 complex. This reduces the physical interaction between CD8 and TCR, abrogating the antigen-specific response. On the contrary, non-specific TCR-CD3 complexes remained relatively intact and the same T cells were able to respond to non-specific stimuli. These data suggest that the MDSC-induced defect, via releasing of peroxynitrites, is only specific to cells bearing TCR and involved in the interaction with the peptide presented by MDSCs.
Interestingly the scavenger of PNT completely eliminated the MDSC-induced T cell tolerance, suggesting that ROS and peroxynitrite in particular, could be responsible for MDSCs mediated $CD8^+$ T cell tolerance [69].

Other immunosuppressive mechanisms

Several other mechanisms by which MDSCs lead tumor progression and immune escape have been identified:

- Sakuishi and colleague have found that MDSCs express galactin 9, which binds TIM3 on lymphocytes and induces T cell apoptosis [70].
- MDSCs inhibit the homing to tumor draining lymph nodes of naïve T cells, reducing the activation of $CD4^+$ and $CD8^+$ cells. This effect is due to the ADAM17 expression (disintegrin and metalloproteinase domain 17) that decreases the L-selectin (CD62L) expression on the surface of naïve T cells, thus limiting T cell recirculation [71].
- MDSCs can also induce a tumor-promoting type 2 response. They lead this effect down-regulating IL-12 production by macrophages and increasing their production of IL-10 in response to signals from macrophages [72].
- MDSCs mediated immune suppression in ovarian carcinoma was suggested to involved a member of the B7 family of surface receptors (CD80) [73]. The up-regulation of CD80 is critical for antigen presenting cells. Paradoxically, it was shown that this protein suppress T cells, when expressed by MDSCs. Moreover MDSCs from spleen and ascites of 1D8 ovarian carcinoma bearing mice, expressed high levels of CD80. The suppression was mediated by $CD4^+CD25^+$ T regulatory cells and required CD152. Other members of the B7 family inhibitory

molecules, like PD-L1 and PD-L2 receptors, are expressed on a variety of myeloid cells and were shown to be directly involved in the suppression of immune response [74].

MDSCs and T cells

MDSCs and Treg

In addition to MDSCs tumor harbors thymus-derived natural Treg and locally induced Treg (iTreg), both $CD4^+$ $CD25^{hi}$ $FoxP3^+$ immunosuppressive populations. Naive $CD4^+$ $CD25^-$ can be converted into iTreg cells as a consequence of exposure to antigen, in the presence of TGF-β or IL-10 [75, 76]. There are increasing evidences that MDSCs are involved in the induction of iTreg and in the attraction and activation of Treg-cell subsets in general. Moreover it has been suggested that this mechanisms require cell-to-cell contact, including CD40–CD40L interactions [77], production of soluble factors such as IFNγ and IL-10 [79], and expression of ARG [78].

Some *in vivo* studies have found that MDSCs support the development of Treg cells through TGF-β-dependent and –independent pathways [79]. Moreover it has been reported that the suppressive activity of Gr-$1^+$$CD11b^+$ MDSCs isolated from ovarian-carcinoma bearing mice was dependent on the presence of CD80 on the MDSC and involved $CD4^+$$CD25^+$ Treg cells, suggesting a relationship between MDSC and Treg cells.

In a B-cell lymphoma model, Serafini and colleague have identified MDSC as tollerogenic APCs, capable of antigen uptake and presentation to tumor-specific Treg cells. These $CD11b^+$$CD11c^{lo}$ $MHCII^{lo}$ MDSCs expressed ARG-1 to mediate the expansion of Treg cells [79].

MDSCs and $CD8^+$ Lymphocytes

The suppressive role of MDSCs on $CD8^+$ T cells is well established. However the major unsolved question is if MDSCs mediate antigen-specific or non specific suppression of T cell responses. Recent findings suggest that both mechanisms actually occur and the discriminating factor seems to be the environment where the suppression takes place.

In the peripheral lymphoid organs the mechanism is antigen-specific and requires the presence of three factors:

- MDSCs
- activated antigen-specific $CD8^+$ T cells
- tumor-associated antigen.

It was shown both *in vitro* and *in vivo*, that MDSCs inhibit IFN-γ production by $CD8^+$ T cells in response to peptide epitopes presented by MHC class I [80]. This antigen-specific T cell tolerance is not operated by soluble factors, requires direct cell-to-cell contact and is probably mediated by reactive oxygen species [81, 82].

Moreover MDSCs can uptake soluble antigens, including tumor associated antigens, to process and present them to T cells [83, 84]. Furthermore the blockade of MDSC–T cell interactions with a MHC-class-I-specific antibody completely abrogated the MDSC-mediated inhibition of T cell responses *in vitro* [85].

Nagaraj and colleague have recently demonstrated that MDSCs caused $CD8^+$ T cell tolerance only against the peptide they presented. In a system with $CD8^+$ T cells expressing two different transgenic TCR on the same cells, MDSC did not affect the T-cell response against the peptide which was not presented by them [86].

The main subset of MDSCs responsible for $CD8^+$ T cells tolerance is G-MDSCs, because of their prevalence in lymphoid organs of tumor bearing hosts and because of the nature of the immune suppression mediated by these cells.

G-MDSCs in fact contain high levels of ROS and PNT, both instable molecules that can act only in short distance. The interface of MDSCs and $CD8^+$T cells, interacting during the antigen-TCR recognition phase, provides the conditions of this suppressive event [60].

As regard the MDSCs suppressive activity at the tumor site, evidences suggest that the phenomenon is quite different and that could be antigen non-specific. When MDSCs migrate into the tumor, up-regulate the expression of ARG1 and iNOS, down-regulating the production of ROS and stimulating tumor-associated macrophages (TAMs) [87]. These MDSCs cells produce higher levels of NO and arginase compared to those detected in peripheral lymphoid organs of the same animals. Moreover TAMs produce several cytokines [88, 89] that suppress T-cell responses in a non-specific manner.

MDSCs and $CD4^+$ Lymphocytes

The main controversy about the suppressive activity of MDSCs, regards their role in $CD4^+$ T cells suppression.

Studies described different effects of MDSCs on T cells in cancer patients and tumor bearing mice and there are some evidences that although MDSCs induce antigen specific tolerance of $CD8^+$, it does not occur for $CD4^+$ T cells. However in different experimental systems, MDSCs induce inhibition of IFN-γ production by $CD4^+$ T cells [91].

An important thing to be considered in this argument is that in most of the experiments with MDSCs form patients' peripheral blood, the specific nature of T cell suppression was not investigated.

Recent studies have found that the antigen-specific $CD4^+$ T cell tolerance *in vivo* was dependent on the expression of MHC class II by MDSCs [92].

The exact mechanism of MHC class II regulation in MDSCs is not clear, STAT3 may play a role because its up-regulation is a common finding in myeloid cells of tumor bearing hosts and it is known that it leads reduction of MHC class II expression in DCs [93, 94, 95]. Moreover many cytokines produced by the tumor may trigger STAT3 signaling in myeloid cells.

Low expression of MHC class II (HLA-DR) was also reported in MDSC of patients with melanoma, leukemia and several solid tumors [97, 98].

On the contrary was also found that in tumor-bearing mice the antigen-specific $CD4^+$ T cell suppression occurs only if MDSCs express a sufficient level of MHC class II. Moreover the antigen-specific $CD4^+$ T cells, but not the $CD8^+$ T cells, were able to convert MDSCs to non-specific suppressor cells both *in vitro* and *in vivo* (in a MHC class II dependent manner). The phenomenon was observed only in the presence of specific peptide and required direct cell-to-cell contact [92].

Gabrilovich and colleague have demonstrated that this effect involved MHC class II cross-linking, leading to up-regulation of COX-2 and PGE2, which were implicated in MDSCs mediated immune suppression [99].

Prostaglandins E (PGE) are pro inflammatory modulators, secreted in the course of immune response by many types of myeloid cells. Autocrine production of PGEs is indirectly involved in the regulation of IL-12 production, depending IL-10 release [100] also implicated in the regulation of myeloid cell differentiation. The enzyme which underlies the production of PGE2 is cyclooxygenase-2 (COX-2) and there are

evidences of its expression in human lung, colon, breast and prostate cancers. Moreover in cancers with up-regulation of COX-2, prostanoids have been shown to induce arginase I expression, thereby contributing to tumor escape [47]. It is well stated that PGE2 induces MDSC differentiation and it is probably due to the interaction with E1 and E2 receptors. In fact EP2 receptor knockout mice show a delayed growth of 4T1 mammary carcinoma, associated to a lower number of MDSCs compared to relative wild type mice [101].

ATP

Adenosine thriphosphate is a key nucleotide involved in several important cell mechanisms.

The intracellular role as energy source for the cells has been recognized for many years: cells have mechanisms for synthesizing, maintaining or rapidly restoring the intracellular level of ATP. In mammalian the ATP concentration in the intracellular compartment is 5-10 mM, but can reach much higher levels in specific intracellular stores, where the nucleotide concentration reach 100 mM.

On the contrary, the extracellular ATP concentration in physiological conditions, is in the nanomolar range (50-20 nM).

In case of plasma membrane damage such as in necrosis, cells leak their cytosolic content leading an immediate increase of the extracellular ATP concentration [102].

ATP can also be actively released by many different cell types, such as activated platelets [103], vascular endothelial cells [104], leukocytes and T lymphocytes [105].

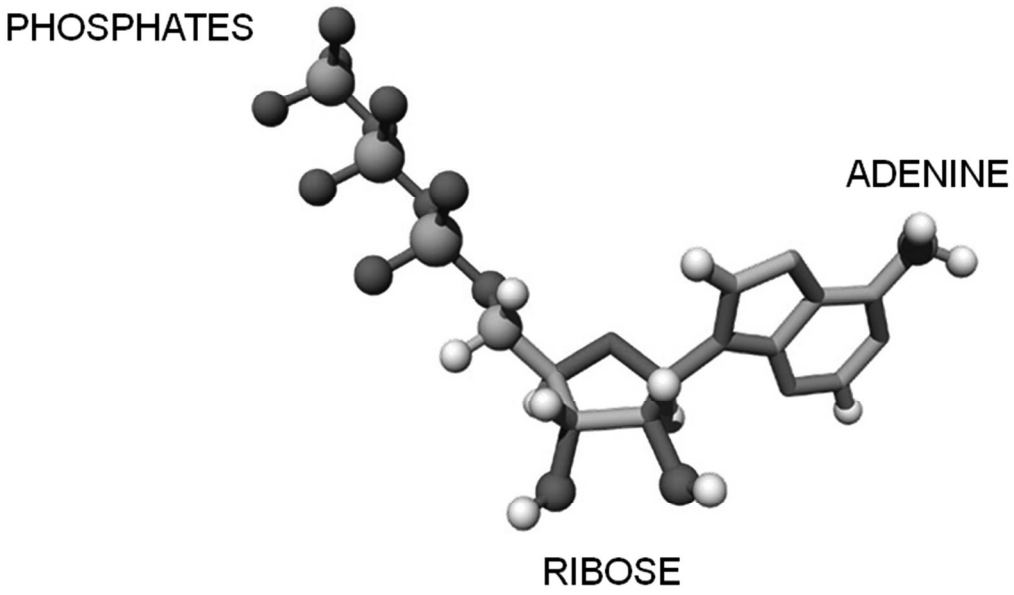

Figure 2. Structure of ATP

ATP consists of adenosine, composed of an adenine ring and a ribose sugar, and three phosphate groups (triphosphate).

The mechanisms of active ATP secretion by cells depends on the nature of the stimulus and/or the pathophysiological condition.
The main ways to release the nucleotide in the extracellular microenvironment are:

- opening of volume-sensitive channels [106]
- purinergic X receptors (P2X)-gated channels
- opening of connexin channels upon mechanical stress
- release of the nuocleotide stored in cytoplasmic vesicles, such as in neurons and platelets [107]
- pannexin (panx)-1 hemichannels, in response to increased cytosolic calcium concentration [108]

The biological rationale of the release of ATP in extracellular microenvironment is the role of the nucleotide as extracellular messenger.
This phenomenon was demonstrated for the first time in 1929 by Drury and Szent-Gyorgyi who observed that extracellular ATP induces decrease of the strength and the velocity of cardiac muscle contraction.
Moreover thirty years later was found that during antidromic stimulation of sensory nerves of the ear artery, the ATP was released in sufficient concentration to affect the muscular tone [109].
Anyway the effective breakthrough came in 1972 when Geoffrey Burnstock demonstrated that ATP act as neurotransmitter, released by purinergic terminations in CNS neurons or in smooth muscle cells, and binds membrane receptors.
Moreover Burnstock purposed the existence of two families of purinergic receptors, P1 and P2, capable to mediate effects of respectively adenosine and ATP.

Functions of ATP as extracellular messenger

When released in the extracellular milieu ATP mediates several different effects, depending on the nucleotide concentration and the nature of the cells involved in the phenomenon.
Low concentration of nucleotide promotes proliferation of epithelial cells, fibroblasts and hematopoietic stem cells. This release also affects biological process such as platelet aggregation, neurotransmission, muscle contraction and cardiac function.

Low ATP concentration can affect several responses as pain sensation, cytokines secretion and NO production [110].
Recent studies have also found that T cells, macrophages and microglial cells release ATP in extracellular environment after stimulation with different antigens or with LPS [111].
Quite interestingly Lazarowski and colleague have shown that a notable release of the nucleotide can also occur without effective cell stimulation [112].
Some studies have found that ATP have also chemotactic effect: tumor cells, attacked by T cells, release ATP form membrane lesions, leading the recruitment of phagocytic cells [113].
Endothelial cells increase proliferation after stimulation with ATP. In these cells the effect is associated to a rise in the intracellular calcium concentration, diacil-glicerol and inositol 1-4-5 triphosphate production, MAP kynase activation, protein-kynase Cδ traslocation and ERK kynase stimulation.
In keratynocites, vascular smooth muscle cells [114], mesangial cells and astocytes, the observed proliferative effect of ATP depends on the activation of purinergic receptors P2Y.
ATP and UTP act *in vitro* as potent growth factors for human hematopoietic stem cells, increasing the stimulatory effect of other growth factors [115].
The release of the nucleotide occurs also during the early stages of apoptosis, inducing monocyte/macrophages recruitment, acting as a “find me” signal to exert an efficient cell clearance [116].
High concentrations of extracellular ATP are associated to inflammatory conditions, since the nucleotide is released by injured cells and by activated immune system cells [117].

CD39 and CD73

Two important membrane-bound enzymes involved in the metabolism of extracellular nucleotides are CD39/(ENTPD1) and CD73/ecto-5’-nucleotidase. CD39 catalyzes the hydrolysis of ATP and ADP in adenosine–monophosphate (AMP), that is then converted in adenosine by CD73.

Interestingly CD39 and CD73 are simultaneously expressed in murine T regulatory lymphocytes (Tregs) and in a subset of human Tregs and monocyte-derived dendritic cells [118].

Deaglio et al. have shown that the adenosine produced by CD39/73-mediated cleavage of ATP, acts on T-effector cells resulting in cell cycle arrest [119]. Effects due to ATP catabolites rather than to ATP itself can be distinguished using non-hydrolyzable ATP analogues (e.g. ATP-γ-S), adenosine deaminase (ADA; that converts adenosine into inosine) or exogenous apyrases that hydrolyzes extracellular ATP.

PURINERGIC RECEPTORS

Purinergic receptors are membrane receptors activated by extracellular nucleotides [120]. The family includes P1 receptors, activated by adenosine, and P2 receptors whose physiological agonist is ATP. The intracellular signaling pathways activated by P2 receptors depend on the cell type, the pattern of receptors expressed and the nature of the stimulation.

Two P2 receptor subfamilies have been described: P2X and P2Y [121].

P2Y are seven membrane-spanning, G-protein-coupled receptors whose activation triggers calcium release from intracellular stores. Moreover effects of the activation depends on the G protein subtype involved. P2Y1, 2,4,6, and 11 are coupled to Gq/11 proteins that trigger the generation of inositol 1,4,5-trisphosphate and the release of Ca^{2+} from the intracellular stores. P2Y12, 13 and 14 are associated with Gi/0 proteins, which inhibit adenylate cyclases [122].

P2X receptors are ligand-gated ion channels that modulate membrane permeability for monovalent and divalent cations [123].

P2X receptors are constituted by two hydrophobic transmembran domains (TM1 and TM2), an extracellular region composed by 10 cysteins and cytoplasmic amino- and carboxyl- terminal domains.

Upon activation P2X subunits aggregate to form homo- or in some cases hetero-multimers and determine low molecular weight cation influx, plasma membrane depolarization and increase of intracellular Ca^{2+} concentration [124].

Asapragin residues of P2X subunits are glicosilated and the deletion of al least two of them inhibits the formation of the channel.

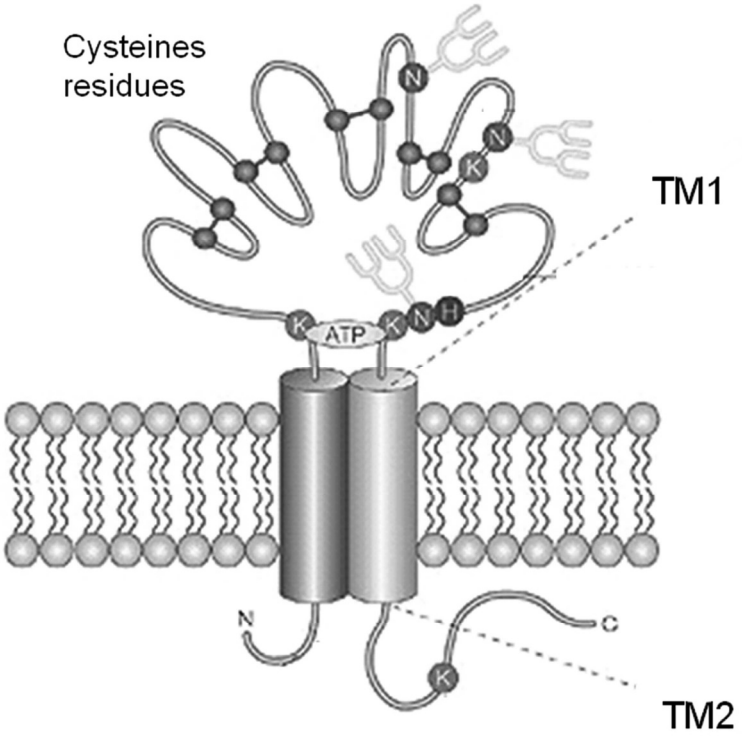

Figure 3. Structure of P2X receptor

In red is represented the transmembrane region 1 (TM1) and in blue the transmembrane region 2 (TM2). Are also highlighted the cysteine residues that form the disulfide bridges, the three sites of N-glycosylation (yellow) and the binding site with ATP.

Amino-terminal domain is constituted by twenty-thirty residues and is similar in all P2 subtypes. On the contrary the carboxyl-terminal has a considerable variability in length. Mutations or deletions in the C-terminal domain affects kinetics, permeability and desentization of the ionic channel [125].

The extracellular domain contains two disulfide-bonded loops (S-S) and three N-linked glycosyl chains. Between Lys 69 and Lys 71 is localized the ATP binding site.

The P2X subfamily is composed of seven members named P2X1-P2X7 [120].

P2X2, P2X4 and P2X7 receptors can make the transitions from channel to pore and have two opening states called I_1 and I_2 [126].

The only known physiological agonist for P2X receptors is ATP, but this subfamily can also be activated by pharmacological analogues such as αβ-metilene-ATP that unlike ATP, resists to enzymatic degradation.

P2X7 RECEPTOR

Cloned in 1996 P2X7 receptor was included in the P2X subfamily because, under stimulation in physiological conditions, is selectively permeable to small cations. Moreover, in case of continued exposure to ATP, the cation channel can convert to a pore, permeable to small molecules as well as ions [127].

In human the P2X7R gene includes 13 exons and is located on chromosome 12q24.

Expressed by different cell types such as neurons, dendritic cells [128], macrophages [129], microglial cells[130], fibroblasts, lymphocytes [131] and endothelial cells the protein of P2X7 receptor can be over-expressed under stimulation with inflammatory mediators like INF-g, TNF-a and LPS**.** These observations suggest an involvement of the receptor in inflammatory response. Stimulation with high concentration of agonist or for prolonged period, have been shown to induce apoptosis [132].

P2X7 is also over-expressed by several malignant tumors [133, 134] and it has been shown to induce proliferative effect on T-cells [135]. Over the last years evidence has accumulated in support of an important role of P2X7 as an immunomodulatory receptor involved in IL-1β maturation and release, Ag presentation, graft-versus-host reaction and contact hypersensitivity [136].

The P2X7 receptor is a 595 aa protein structurally similar to other P2X receptors except for the fact that it has a significantly longer intracellular C-terminal (240 amino acids).

P2X7R does not readily desensitize, therefore the pore remains open as long as the agonist is present in the extracellular environment. Although the molecular mechanism leading the pore formation is still unclear, in 1996 Surprenant and colleague have demonstrated the importance of the long C-terminal intracellular domain of which at least the last 177 amino acids are crucial for the induction of the non-selective pore [137].

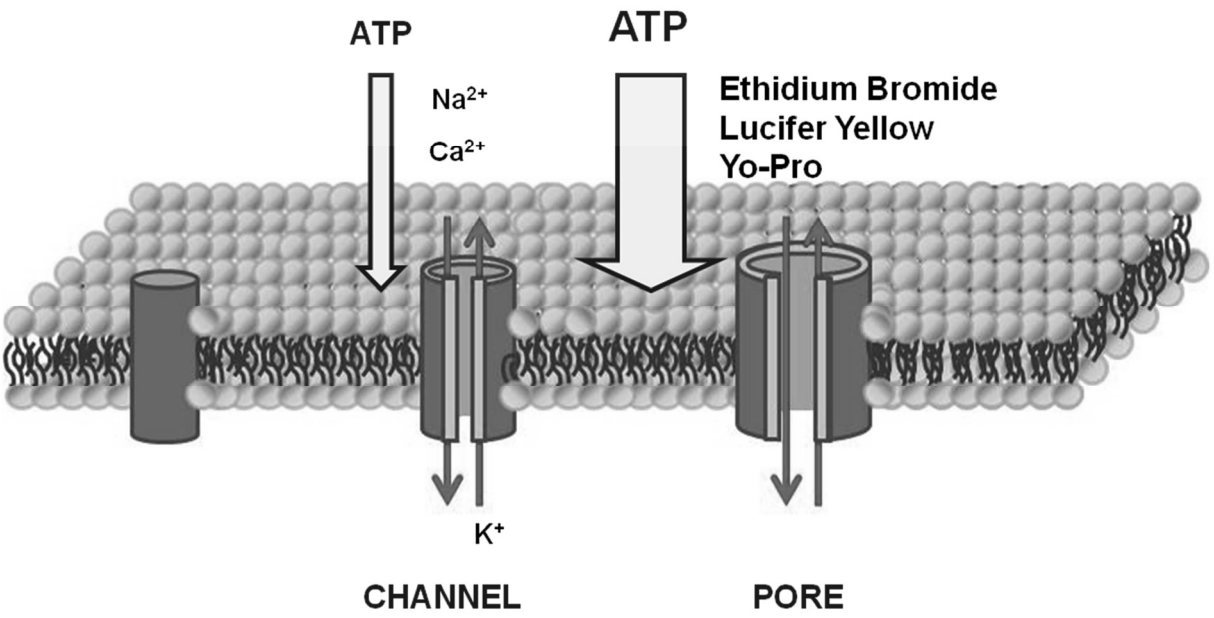

Figure 4. P2X7 receptor stimulation

In presence of ATP, P2X7R mediates Na^+ e Ca^{2+} influx and K^+ efflux through plasma membrane. Repeated stimulation with the agonist or higher concentrations of the same, result in the opening of a pore that allows the passage of molecules up to 900 Da.

In human lymphocytes B and T the stimulation with ATP induces Na^+ and Ca^{2+} flux throw plasma membrane and increases the permeability to ethidium bromide (314 Da) [138]. Moreover in lymphocytes, the stimulation leads the formation of a smaller pore than in other cells, permeable to molecules of MW up to 320 Da.

In peritoneal macrophages the P2X7 receptor makes multimerics complexes, on the contrary in glial cells and astrocytes the receptor was found only as a monomer [139].

Experiments of immunoprecipitation have shown that 11 proteins interact with the receptor. Two of them, RPTPβ (*receptor protein tyrosine phosphatase-beta*) and HSP 90, are able to modulate P2X7R funciotns [140].

Experiments with P2X7R truncated expressed in HEK293 and in Xenophus Laenis oocytes, have shown the importance of the C-term for the formation of the pore. On the contrary the channel functionality is not affected even if the receptor is truncated at 380 position. All these data suggest that unlike the pore, the channel formation requires only a short portion of the C-term [141].

P2X7 is an highly polymorphic protein and in last years four different aminoacid substitution that affect its functionality, have been identified. Both in human and in

mouse Glu 496 is important for the pore formation, in fact its substitution with an Alanine affects or, in case of homozygosity, completely abrogates the P2X7R functionality [142].

Moreover the substitution on an Isoleucyne with an Alanine in the C-term inhibits the membrane receptor expression [143], and the substitution of Glu 307 with an Arginine, abolishes the binding of the ATP to the extracellular domain. In our lab was identified in chronic lymphatic leukemia (CLL), the first polymorphism (His 155 –Tyr) that increases the receptor functionality [144].

The physiologic P2X7R agonist is ATP, in particular its tetra-anionic form (ATP^{4-}). In physiological conditions ATP^{4-} is associated to Mg^{2+}, Ca^{2+} or H^{-}, forming $MgATP^{2-}$, $CaATP^{2-}$ and $HATP^{3-}$. The removal of Mg2+ and Ca2+, or the alcalinization of the colture medium, increase the ATP affinity for the receptor [158]. The preferential agonist for P2X7 is 2'-3'-4(benzoil)-benzoic-ATP (BzATP), an pharmacological ATP analog with high affinity. Other, less effective than ATP P2X7 agonists, are 2-MeSATP and ATPγS.

AIM OF THE WORK

Although many therapies are currently available, cancer is still an unsolved problem. The main event supporting the growth of the malignancy is a well stated tumor-induced tolerance. The major contributor to this phenomenon is a cell population identified in 2007 and defined Myeloid Derived Suppressor Cells. MDSCs accumulates under inflammatory conditions and induce a potent suppression of tumor immunity (innate and adaptative). Many laboratories are now working to understand the exact mechanism of the immunosuppressive activity of these cells, some models have been described and there are evidences that ROS and Arg-1 are involved but other molecules may probably play a role. Two of these additional agents might be extracellular ATP and adenosine.

To explore the role of these factors in tumor-mediated immunosuppression I have carried out an extensive characterization of purinergic signaling in two MDSCs cell lines (MSC-1 and MSC-2) and in BM-MDSCs. Based on evidences that P2X7R supports the growth of several malignancies, my study was particularly focused on the expression and the functionality of this receptor. Moreover in the second part of the work I investigated the activity of two ecto-enzymes CD39 and CD73, responsible of the hydrolysis of ATP in adenosine.

MATERIAL AND METHODS

MSC-1 and MSC-2 Cell Lines

I worked on murine immortalized MDSCs cell lines: MSC-1 and MSC-2. Cells were originated by Prof. Bronte's group in Padova as described in Apolloni et al. [151]. Briefly, the MSC-1 line originated from Gr-11 splenocytes from mice bearing a 1-moold TS/A tumor, while the MSC-2 line originated from Gr-11 splenocytes from mice immunized 6 days earlier with a recombinant vaccinia virus encoding mouse IL-2. Both lines were immortalized with the insertion of the viral recombinant oncongenic sequences v-myc and v-raf.

I cultured cells in RPMI 1640 (Euroclone, Milan, Italy) supplemented with 100 IU/ml penicillin, 50 µg/ml streptomycin (all from Sigma-Aldrich, Milano, Italy) 1% L-glutamine, 1% Sodium Pyruvate (Euroclone, Milan, Italy) and 10% fetal bovine serum superior (Biochrom, Cambridge, UK) at 37℃, in an a tmosphere of 5% CO^2.

Generation of BM-MDSC in vitro

I isolated tibia and femur from C57black6 wild type and P2X7 KO mice, I flushed BM and I removed red blood cells with an ammonium chloride solution. $5x10^6$ cells were cultured in 100 mm petri dish (Falcon, Beccton Dickinson) for 4 days with 40 ng/ml GM-CSF and 40 ng/ml IL-6 (both from Peprotech, London, UK) as suggested in Marigo and colleague's work [149]. On day 4 some cells were stimulated with 300 µM / 1 mM ATP or adenosine. To confirm the differentiation in MDSCs at day 5 I assessed whether cells expressed surface antigens CD11b and Gr-1.

I stained MDSCs for at least 20 min. at 4 ℃ with 1 :100 PerCp Cy5.5 anti CD11b and 1:100 APC anti Ly6G (Gr-1). After two washes I acquired data with FACSCalibur (BD Biosciences, Mountain View, CA, U.S.A.) and analyzed them with the program FlowJo (Tree Star, Inc.).

Reverse transcriptase polymerase chain reaction

I extracted total RNA using Trizol reagent (Invitrogen, Monza, Italy) following the manufacturer's instructions. I carried out the reverse transcription reaction using the following specific primer sequences:

P2X1	sense: 5'-CGCCTTCCTCTTCGAGTATG-3' antisense: 5'-GGAAGACGTAGTCAGCCACA-3'
P2X3	sense: 5'-GAGAGTGAGAATACCG-3' antisense:5'-CACTGGTCCCACGCCTTG-3'
P2X4	sense: 5'-TGCATTTATGATGCTAAAACAG-3' antisense: 5'-CAAGACCCTGCTCGTAATC-3'
P2X5	sense: 5'-CCGGGAGCGACTTCCAGGATATAG-3' antisense: 5'-GGCATGGGATCACTGGGTGCTAGAC-3'
P2X6	sense: 5'-AAAAACAGGCCAGTGTGTGGTGTTC-3' antisense: 5'-TGCCTGCCCGGTGACGAGG-ATGTCGA-3'
P2X7	sense: 5′-ATATCCACTTCCCCGGCCAC-3′ antisense: 5′-TACCACGGTACTGACGCT-3'
P2Y1	sense: 5'-AGCAGAATGGAGACACGAGTTTG-3 antisense: 5'-GGGATGTCTTGTGACCATGTTACA-3'
P2Y2	sense: 5'-GAAGAACTGGAGCAGGCGCT-3' antisense: 5'-CCATTGCCCTGGACCTGATC-3'
P2Y4	sense: 5'-CTGCAAGTTCGTCCGCTTTC-3' antisense: 5'- GTATTGCCCGCAGTGGATG-3'
P2Y6	sense: 5'-TGAAAACAACGAGGAACACCAA-3' antisense: 5'-CAGCCTTTCCTATGCTCGGA-3'
P2Y12	sense: 5'-CACAGAGGGCTTTGGGAACTTA-3' antisense: 5'-TGGTCCTGCTTCTGCTGAATC-3'
P2Y13	sense: 5'-CAGCTGAGTCTCTTCCAAAACAAA-3' antisense: 5'-TGCATCCCAGTGGTGTTGAT-3'
P2Y14	sense: 5'-CCACCACAGACCCTCCAAAC-3 antisense: 5'-CAACACGGGAATGATCTGCTTT-3'

The RNA samples (100 ng) were reversed transcribed using the ACCESS RT-PCR kit (Promega, Monza, Italy), with the following conditions: denaturation at 95℃ for 2 min (1 cycle) and reverse transcription at 48℃ for 45 seconds (1 cycle); 33 cycles of denaturation at 94℃ for 45 seconds, annealing at 5 6.5℃ for 30 seconds, extension at 68℃ for 1 min, followed by a final extension at 68℃ for 4 min. As control I

evaluated Glyceraldehyde 3-phosphate dehydrogenase (GAPDH) amplification, using the following primers: forward 5′-CAAGGAGTAAGAAACCCTGAC-3′; reverse 3′-AATTGTGAGGGAGATGCTCAGT-5′. PCR products (100ng) were separated by agarose gel electrophoresis using an Agarose Electrophoresis Grade (Invitrogen) and then visualized by Gel Red staining. A 100-bp DNA Ladder (Fermentas, Thermo Scientific, Cornaredo, Italy) was used as a molecular weight. marker. PCR products were run on a 1.5% agarose gel containing 0.5 µg/ml ethidium bromide and photographed under UV light.

Western blot analysis

MSC-1 and MSC-2 cell lines were cultured in flasks and when 70% confluence was reached cells were detached with Cell Dissociation Solution (Gibco-Life Technologies, Monza, Italy) and centrifuged at 160 g for 5 min. The pellets were resuspended in sucrose saline containing benzamidine and PMSF and kept at -80℃. A 7.5% acrilamide gel was run by loading in each lane 30 µg of protein solubilized in O solution (10% w/v glycerol, 5% v/v 2-mercaptoethanol, 2.3% w/v SDS, 62.5 mM Tris-Cl, 0.003% bromophenol blue). Western blotting was performed by transferring proteins onto a nitrocellulose membrane (Amersham Biosciences, Little Chalfont, UK). Blocking of non-specific binding sites was achieved by incubating the membrane with 10% skim-milk in TBS buffer (10 mM Tris-Cl, 150 mM NaCl, pH 8.0) for 1 hour. The primary antibody was used overnight at respective dilution in TBS-t buffer.

- anti mouse P2X7 (Sigma Aldrich, Milano, Italy): 1:200 in TBS-t + 2% BSA
- anti mouse P2X3 (Alomone, Jerusalem, Israel): 1:400 in TBS-t
- anti mouse P2X4 (Alomone, Jerusalem, Israel): 1:400 in TBS-t
- anti mouse P2X5 (Alomone, Jerusalem, Israel) 1:400 in TBS-t
- anti mouse CD39 (Abcam, Cambridge, UK) 1:500 in TBS-t
- anti mouse CD73 (Abcam, Cambridge, UK) 1:500 in TBS-t
- anti mouse β-actin (Sigma Aldrich, Milano, Italy) 1:1000 in TBS-t

Antibody binding was visualized by the protein A peroxidase-linked process (GE Healthcare, Milan, Italy).

Cytosolic Ca^{2+} concentration measurement

Cells were loaded with the Ca^{2+} indicator fura-2/AM (2 μM) (Molecular Probes, Leiden, Netherlands) for 20 min at 37℃ in a standa rd saline solution containing: 125 mM NaCl, 5 mM KCl, 1 mM $MgSO_4$, 1 mM NaH_2PO_4, 20 mM HEPES, 5.5 mM glucose, 5 mM $NaHCO_3$, 1 mM $CaCl_2$ and 250 μM sulfinpyrazone (Sigma Aldrich, Milan, Italy), pH 7.4. Cells (1x106) were stimulated with BzATP (Sigma Aldrich, Milan, Italy) in a temperature-controlled magnetically stirred cuvette at 37℃ and intracellular Ca^{2+} concentration ($[Ca^{2+}]_i$) changes were measured with a Perkin Elmer fluorometer (Perkin Elmer Ltd., Beaconsfield, United Kingdom). The excitation was at 340-380 nm, and emission at 510 nm. Ca^{2+} concentration was calculated using the FLwinlab software (Perkin Elmer).

Changes in plasma membrane permeability

ATP and BzATP-dependent increases in plasma membrane permeability were measured by monitoring the uptake of the dye ethidium bromide (Sigma Aldrich, Milan, Italy). Briefly, 5 x 10^5 cells were resuspended in a Na+-free saline solution containing: 300 mM sucrose, 1 mM $MgSO_4$, 1 mM K_2HPO_4, 5.5 mM glucose, 1 mM $CaCl_2$ and 20 mM HEPES (pH 7.4 with KOH). Cells were kept in a magnetically stirred fluorometric cuvette, thermostatted at 37℃ and incubated in the presence of 20 μM ethidium bromide (Sigma Aldrich, Milan, Italy). To achieve complete permeabilization of the cells, 100 μM digitonin was added at the end of the experiment (100% fluorescence signal). Fluorescence was measured at an excitation/emission wavelength couple of 360/580 nm.

Lucifer yellow uptake assay

ATP and BzATP-dependent increases in plasma membrane permeability were measured by monitoring the uptake of the fluorescent dye lucifer yellow (Molecular Probes, Inc.). 2 x 10^5 cells were seeded in 12-well pate in a standard saline solution containing: 125 mM NaCl, 5 mM KCl, 1 mM $MgSO_4$, 1 mM NaH_2PO_4, 20 mM HEPES,

5.5 mM glucose, 5 mM $NaHCO_3$, 1 mM $CaCl_2$ and 250 μM sulfinpyrazone (Sigma Aldrich, Milan, Italy), pH 7.4. Cell were then incubated for 30 minutes at 37 ℃ in the presence of 1 mg/ml lucifer yellow and 300 μM BzATP or 1 mM ATP respectively. After stimulation and several washings to remove the extracellular dye, cells were analyzed with an inverted fluorescence microscope (Olympus IMT-2, Olympus Optical Co. Ltd., Tokyo, Japan) equipped with a 20X objective. Images were acquired both in phase-contrast and fluorescence with a NIKON DS-2MV digital sight camera.

Plasma membrane potential measurement

Changes in plasma membrane potential were measured with the fluorescent dye bis[1,3-diethylthiobarbiturate)trimethineoxonal (bisoxonol) (Molecular Probes, Leiden, The Netherlands), at the wavelength pair 540/580 nm, as previously described (Falzoni et al., 1995). Experiments were performed in a spectrofluorometer (model LS50, Perkin Elmer Ltd., Beaconsfield, UK) equipped with a thermostat-controlled (37℃) cuvette holder and magnetic stirrer.

LDH assay

Lactate dehydrogenase (LDH) activity was measured according to standard methods. Briefly, MSC-1 (1 x 105) and MSC-2 (5 x 105) were plated overnight in 24 wells plates, rinsed and incubated in culture medium in the presence of increasing ATP (Roche Diagnostics, Monza, Italy) concentrations for 8 h. Supernatants were then collected, cleared by centrifugation (10 min at 149 x g) and added to a solution containing, 0.63 mM pyruvate, 11.3 mM NADH, 44.4 mM K2HPO4, 16.8 mM KH2PO4 (pH 7.5). Absorbance was measured in a spectrofluorometer (Ultrospec 3000, Pharmacia Biotech, Milan, Italy) at a wavelength of 340 nm. Cells were also lysed with 0.1% Triton X-100 (JT Baker, Milan, Italy) and cleared by centrifugation. Absorbance of these samples was considered as 100% of lactic dehydrogenase release.

IL-1β secretion measurement

MSC-1 (5 x 104) and MSC-2 (2 x 105) were seeded in a polylisinezed (Sigma Aldrich, Milan, Italy) 24-well plates. Cells were primed with 1µg/ml LPS (Sigma Aldrich, Milan, Italy) for 4 h at 37℃, 5% CO2, fol lowed by stimulation with 100 µM or 300 µM BzATP for 30 minutes. After stimulation the whole medium (300 µl) was collected and centrifuged at 160 g for 5 minutes, to remove any detached cells, followed by transfer of the supernatant to a fresh tube. Supernatants were stored at -80℃ and assayed with Mouse IL-1 β, Quantikine ELISA (RandD Systems, Abingdon, UK)

TGF-β1 secretion measurement

MSC-1 (5 x 104) and MSC-2 (2 x 105) were seeded in a polylisinezed (Sigma Aldrich, Milan, Italy) 24-well plates. Cells were primed with 1µg/ml LPS for 4 h at 37℃, 5% CO2, followed by stimulation with 100µM or 300 µM BzATP for 30 minutes. BzATP stimulations were performed also without the priming with LPS. After stimulation the whole medium (300 µl) was collected and centrifuged at 160 g for 5 minutes, to remove any detached cells, followed by transfer of the supernatant to a fresh tube. Supernatants were stored at -80℃ and a ssayed with Mouse TGF-β1 Quantikine ELISA (RandD Systems, Abingdon, UK).

Intracellular ROS concentration measurement

Intracellular ROS levels were measured using dichlorodihydro- fluorescein diacetate oxidation. Cells (6 x 105) were plated in petri dish (MSC-1) or 6-well plates (MSC-2) and primed with 1µg/ml LPS for 4 h at 37℃, 5% CO2, followed by stimulation with 100µM or 300 µM BzATP for 30 minutes. 4 h co-stimulation with BzATP and LPS were performed too. After stimulation cells were detached and incubated with 10 µM CM-H2 DCFDA (Invitrogen, San Diego, CA) for 30 min. at 37℃. Cells were then analyzed using a Tali Image Cytometer (Life Technologies, Monza, Italy) set at 458 nm excitation with a 525/20 nm emission filter (green channel). MSC-1 and MSC-2

were also incubated with 500μM H2O2 (Sigma Aldrich, Milan, Italy) for 4 h at 37℃, absorbance of these samples was considered as 100%.

Measurement of extracellular ATP

Extracellular ATP was measured in the culture supernatants with the luciferase/luciferin method. Briefly, MSC-1 and MSC-2 were plated in 96-well plates, supernatants were withdrawn and 100 μl of ATP-stabilizing diluent buffer (sucrose/EDTA solution) was added to the culture wells. Luminescence was measured in a Victor2 Wallac Perkin Elmer luminometer (Perkin Elmer, Wellesley, MA, USA) equipped with an automatic dispenser of an Enliten rluciferase/luciferin solution (100 μl) (Promega, Madison, USA). The level of the fluorescence detected was compared with a standard ATP curve created for every single experiment.

Thin Layer Chromatography (TLC)

Enzymatic modification of nucleotide and nucleoside substrates was evaluated utilizing [^{14}C]ADP (PerkinElmer Life Sciences). 2 mCi/ml [^{14}C]ADP was added to cell cultures; aliquots were removed and analyzed for the presence of [^{14}C]ADP hydrolysis products by TLC samples were then applied to silica gel matrix thin layer chromatography plates (Sigma-Aldrich) and migrated until the solvent (6:3:1, 2-propanol/ ammonium hydroxide/ distilled H_2O) front reached 4 cm beyond the application site. Plates were dried and incubated in a storage phosphor screen cassette overnight, after which the screens were analyzed on a GE Storm 860 Imager.

Flow Cytometry Analysis

Quantitative flow cytometric analyses were performed using standard procedures. Cells were collected and stained for at least 20 minutes at 4℃ in a PBS + 5% FBS solution with the respective antibody:

- allophycocyanin (APC) anti mouse CD39 (1:100)
- PerCp anti mouse CD4 (1:400)
- allophycocyanin (APC) anti CD8 (1:400)

After the stimulation and two washings, data acquisition was performed using FACSCalibur flow cytometer (BD Biosciences, Mountain View, CA, U.S.A.) and analyzed by using FlowJo (Tree Star, Inc.).

CFSE assay

A CFSE stock (5 mM in DMSO; Invitrogen, USA) was thawed and diluted in phosphate-buffered saline (PBS) to the 10 μM working concentrations. Freshly isolated splenocytes from C57blasck6 mouse were resuspended in PBS (0.1% BSA) at 1×10^6 cells/ml and incubated with CFSE (final concentration: 10 μM) for 10 min at 37 ℃. Reaction was stopped with the addiction of 20 ml of cold medium and incubation at 4 ℃ for 5 minutes. Cells were then washed twice and resuspended in culture medium at 2×10^6 cells/ml.

CFSE labeled T cells were cultured in 96-well flat bottom plates (Nunc Roskilde, Denmark) at 2×10^4 cells/well in the presence of different MDSCs concentrations (ratio T cells: MDSC: 1:1, 1:2, 1:4, 1:8). Cell cultures were stimulated with CD3/CD28 Dynabeads (Invitrogen, Carlsbad, CA). In a parallel experiment CFSE labeled T cells were cultured alone with and without stimulation. After 3 days, cells were harvested and stained with 1:400 anti-CD8 allophycocyanin and 1:400 anti-CD4 PerCP Abs for at least 20 min at 4℃. CFSE signal of gated lymphocytes was analyzed by flow cytometry.

Microscopic analyses

MSC-1 and MSC-2 were plated in 24 mm round coverslips. Slips were then placed in a thermostatted Leyden chamber (model TC-202A, Medical Systems Corp., Greenfield, WI, USA) on the stage of an inverted Nikon Eclipse TE300 microscope (Nikon, Tokyo, Japan) equipped with epifluorescence and a 100X objective (Physik Instrumente, GmbH & Co., Karlsruhe, Germany). The bright field or fluorescence

images were captured with a back-illuminated CCD camera (Pricenton Instruments, Tucson, AZ, USA) using the Metamorph software (Universal Imaging Corporation, Downingtown, PA, USA).

Immunofluorescence analysis

MSC-1 and MSC-2 were centrifuged on polylisine slides, and fixed in 2% paraformaldehyde (pH 7.4). After washing with PBS, the slides were incubated with ammonium cloride 100 mM for 20 min at 4C°, permeabi lized with Triton X-100 (0.1% in PBS) for 8 min and blocked with BSA (2% in PBS). Cells were then incubated for 1 anti-ARG-1 Ab. Binding of primary antibodies was detected with fluorescein goat anti-rabbit IgG (Invitrogen). After rinsing, the slides were counterstained with DAPI (Vectashield mounting, Vector Laboratories, Peterborough, UK). Digital images were acquired using a Nikon E-1000 fluorescence microscope equipped with appropriate filter sets and the Genikon imaging system software (Nikon Instruments, Tokyo, Japan).

Evaluation of extracellular ATP levels in neuroblastoma microenvironment

Six-week-old female immunocompetent syngeneic A/J mice (n=5) were intravenously (i.v.) injected in the tail vein with pmeLUC-NXS2 cells ($2x10^5$ cells/mouse). Bioluminescence imaging (BLI) was performed evaluating the stably pmeLUC–transfected NB cell, by highly sensitive, cooled CCD camera mounted in a light-tight specimen box (IVISTM; Xenogen) as previously described(Bianchi et al.). BLI was performed after 7, 12, 19 and 26 days after tumor cell inoculum. In some experiments, immunocompetent syngeneic A/J mice were i.v. co-injected with murine NB NXS2 cells trasfected with firefly luciferase gene (NXS2-LUC) [158] and Gr-1high or Gr-1low MDSCs (1:1; $2x10^5$ cells/mouse). The animals were imaged 8, 14, 20, 26 days after tumor cell inoculum by BLI.

RESULTS

MSC-1 and MSC-2 express the mRNA and the protein of purinergic receptors

To evaluate whether MSC-1 and MSC-2 cell lines expressed P2 receptors, total RNA was isolated and probed by RT-PCR with specific primers for all P2X and P2Y subtypes. Figure 5 A shows the expression of P2X3, P2X4, P2X5, P2X7, P2Y6, P2Y12 and P2Y13 in both cell lines. On the contrary the mRNA of P2X6 was detected only in MSC-2.

Moreover, as shown in Figure 5 B, by Western Blot I verified the expression of the proteins of P2X3, P2X4, P2X5 and P2X7 receptors. Quite interestingly, the P2X7R protein was more expressed in MSC-2 than MSC-1 (Fig. 5 C).

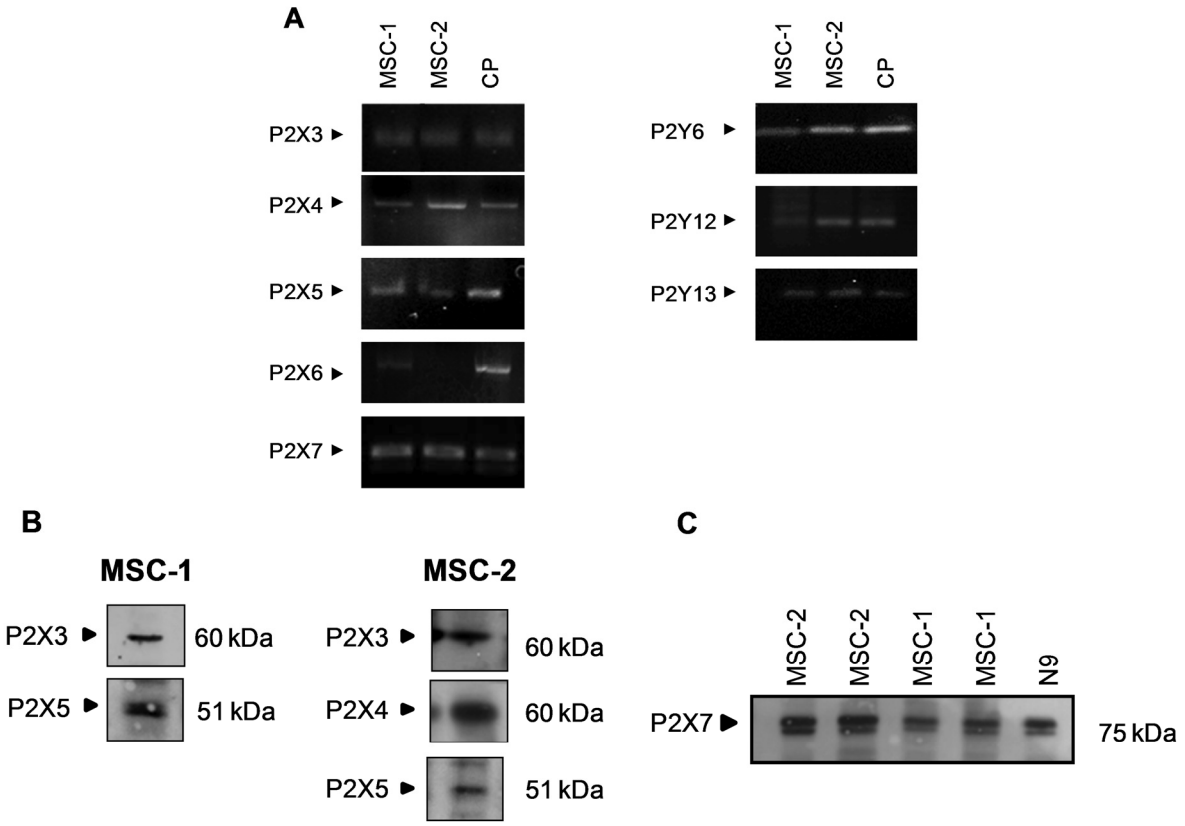

Figure 5. Identification of P2 receptors transcripts and proteins.

Panel A shows the mRNA expression of different P2Rs subtypes. Comparison with a 100-bp nucleotide ladder was used to determine the approximate size of the various P2 PCR products, detected by ethidium bromide staining. Panel B shows the protein expression of P2Rs subtypes and panel C shows the P2X7R expression in MSC-1 and MSC-2. Equal amounts of protein (30 µg) were loaded in each lane and incubated with either primary antibody. Mouse microglial lysates (N9) served as a positive control.

The stimulation of MSC-1 and MSC-2 with ATP increases $[Ca^{2+}]_i$

I have studied the activity of P2Rs expressed by MSC-1 and MSC-2. At first I have measured the intracellular calcium response after stimulation with several ATP concentrations (0, 3, 10, 100, 300 µM and 1-3 mM), both in presence and in absence of extracellular Ca^{2+}. P2Rs were fully functional as both cell lines (Fig. 6 A) showed a large $[Ca^{2+}]_i$ increase in response to the stimulation. It is worth of notice that the rise was mainly due to the influx of the ion from the extracellular space, as it was almost entirely abrogated by chelation of extracellular Ca^{2+} (Fig. 6 B). The dose-dependence curves show that the most effective concentration of ATP for MSC-1 and MSC-2 was in the range of 1 mM (Fig. 6 C). Moreover in MSC-1 the dose-dependency curve is biphasic, witnessing the activation of at least two P2 receptor subtypes: one with higher affinity, responsible for the $[Ca^{2+}]_i$ increase at lower agonist concentrations, and another with lower affinity, responsible for the response at higher agonist concentrations [145].

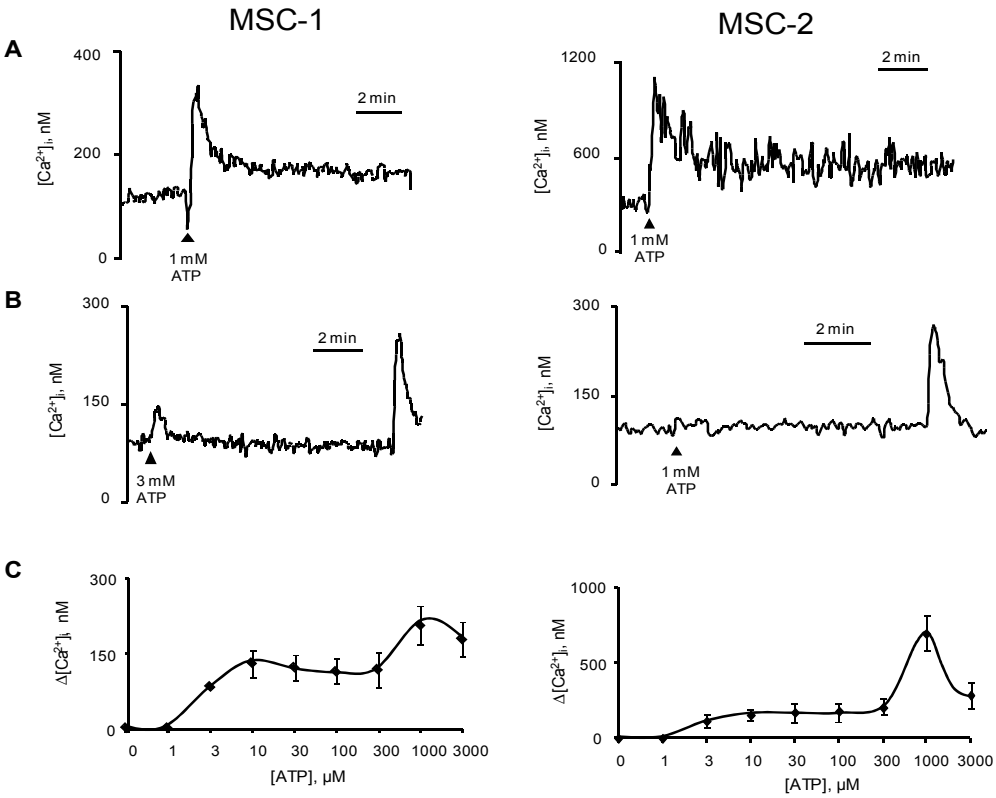

Figure 6. Calcium response to the stimulation with ATP.

Panel A shows the $[Ca^{2+}]_i$ increase in MSC-1 and MSC-2. Panel B shows the $[Ca^{2+}]_i$ response after stimulation in absence of extracellular calcium. Panel C shows ATP dose dependency curves in both cell lines.

The stimulation with BzATP is most effective in MSC-2

I have measured the intracellular calcium concentration also in response to the stimulation with BzATP, the preferential P2X7R agonist. As shown in Figure 7A, P2X7R was fully functional in both lines. Quite interestingly the $[Ca^{2+}]_i$ rise was over 10 times larger in MSC-2 than in MSC-1 and was mainly due to the influx of the ion from the extracellular space, as it was almost entirely abrogated by chelation of extracellular Ca^{2+} (Fig. 7B). Dose-dependency curves show that the most effective BzATP concentration for MSC-1 and MSC-2 was in the range of 300 µM (Fig. 7C). Also in this case the BzATP dose-dependency curve is biphasic for MSC-1 line, suggesting the activation of at least two P2 receptor subtypes with different affinity for the agonist.

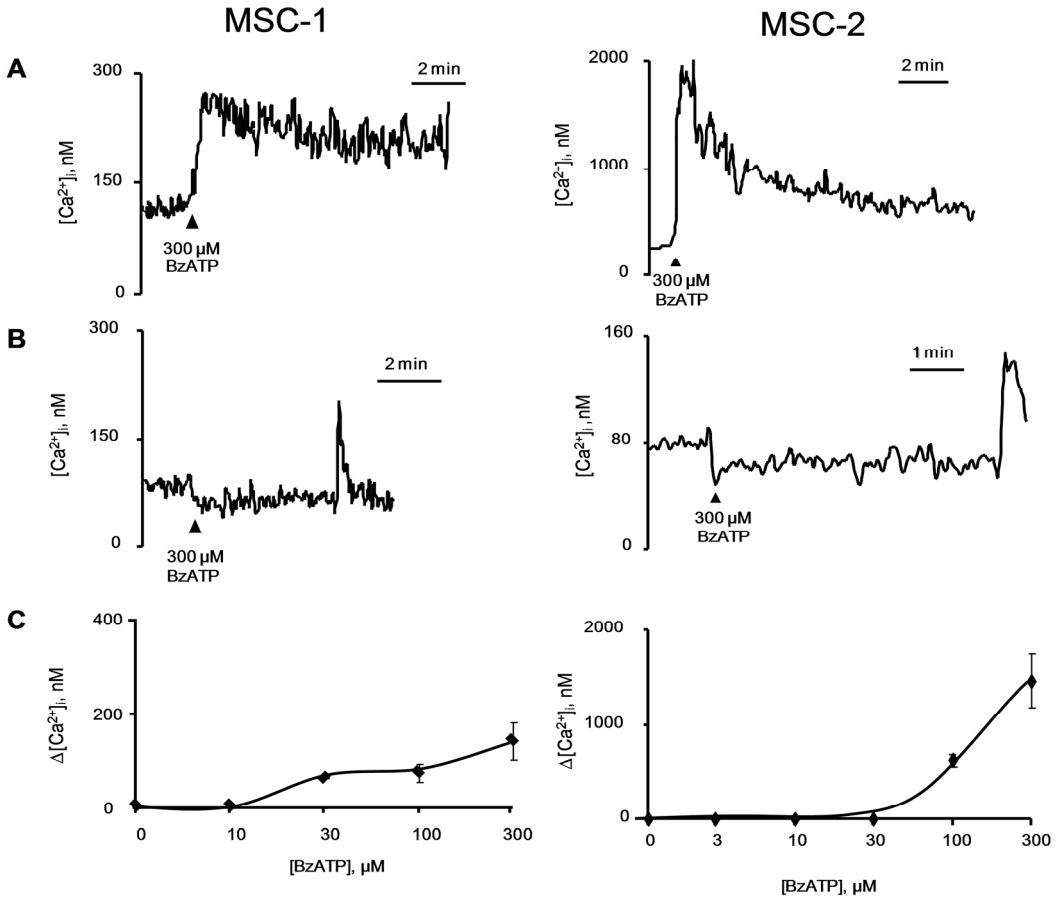

Figure 7. Calcium response to the stimulation with BzATP.

Panel A shows $[Ca^{2+}]_i$ increases in MSC-1 and MSC-2. Panel B shows $[Ca^{2+}]_i$ response after stimulation in absence of extracellular calcium. Panel C shows BzATP dose dependency curves of both cell lines.

The stimulation of P2Y receptors with UTP induces a transient calcium response

In both cell lines I have studied the activity of P2Y receptors in response to the stimulation with UTP. The activation of P2YRs induces calcium release from the intracellular stores, resulting in an increase of the $[Ca^{2+}]_i$. Figure 8A shows that in MSC-1 and MSC-2, in the presence of extracellular calcium, UTP induced a transient $[Ca^{2+}]_i$ increase, typical P2Y response. Moreover both curves of Figure 8A show that the moderate amount of the ion released from the stores was quickly reported to physiological levels. As shown in Figure 8C (MSC-2), even in case of chelation of extracellular Ca^{2+} a weaker response was detectable.

The most effective concentration of UTP was in the range of 100 µM for MSC-1 and 1 mM for MSC-2 (Figure 8B).

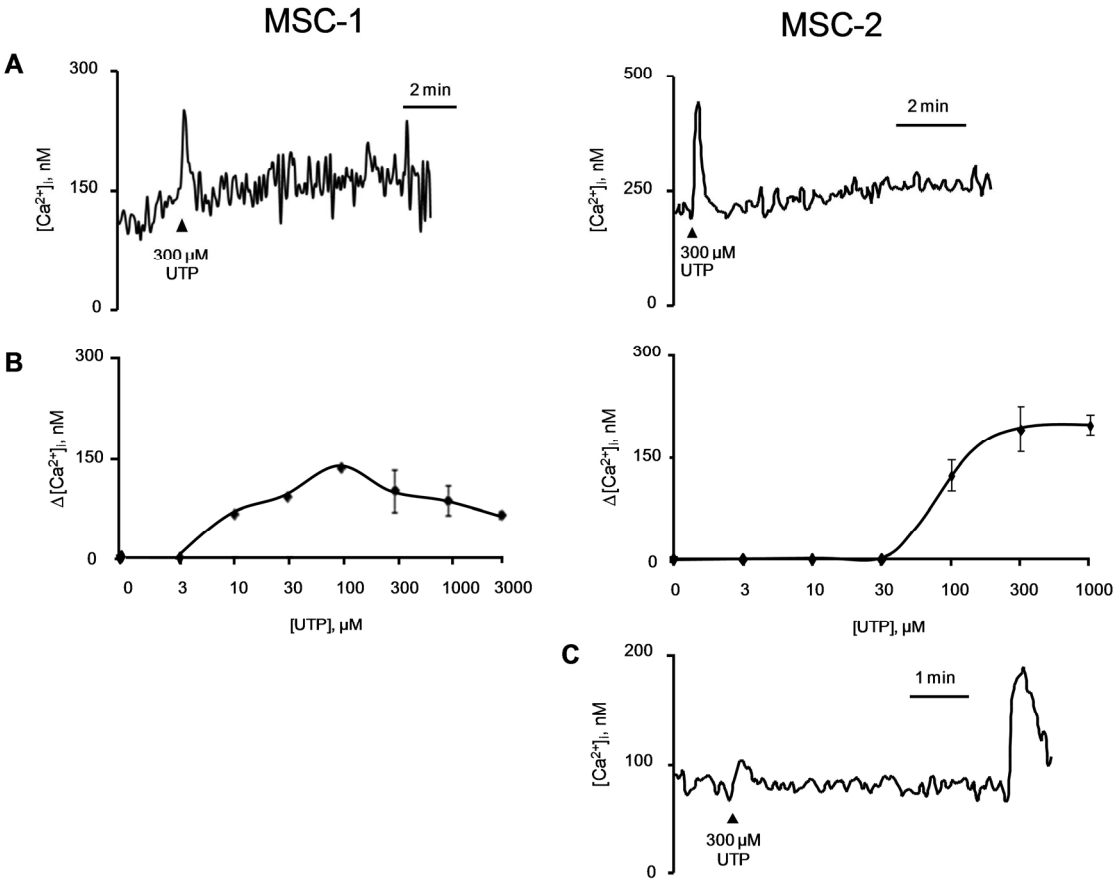

Figure 8. Calcium response to the stimulation with UTP.

Panel A shows the calcium response in MSC-1 and MSC-2. Panel B shows UTP dose-dependency curve in both cell lines and Panel C shows the $[Ca^{2+}]_i$ increases after stimulation of MSC-2 in absence of extracellular calcium.

In MSC-2 cell line different P2 subtypes are functional

In the presence of extracellular calcium I have stimulated MSC-2 line with different P2Rs subtypes agonists. Figure 9A and 9B show that the stimulation with UDP and 2MetSATP induced a transient calcium response. On the contrary the stimulation with UDP-glucose and αβMetATP were not effective (Figure 9C and 9D).

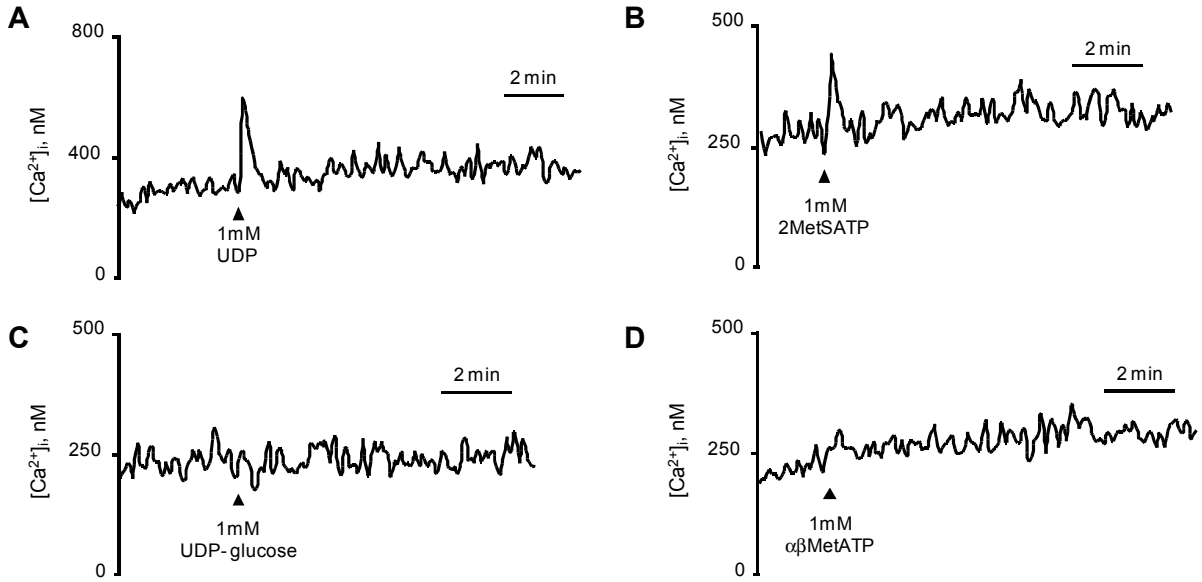

Figure 9. Calcium response in MSC-2.

Panels A-D show $[Ca^{2+}]_i$ response in MSC-2 after the stimulation with UDP (Panel A), 2MetSATP (Panel B), UDP-glucose (Panel C) and αβMetATP (Panel D).

The stimulation with ATP and BzATP induces ethidium bromide uptake in both cell lines

The hallmark of P2X7R activation is an ATP-dependent permeabilization of the plasma membrane to large molecules including the fluorescent dyes lucifer yellow, YO-PRO and ethidium bromide [146].

As shown in Figure 10 (A, MSC-1 and B, MSC-2) the stimulation of both cell lines with 1 mM ATP triggered Et-Br uptake, 56 % +- 14 and for MSC-1 and 69 % +- 13 for MSC-2. The most effective concentration of the nucleotide was in the range of 1 mM.

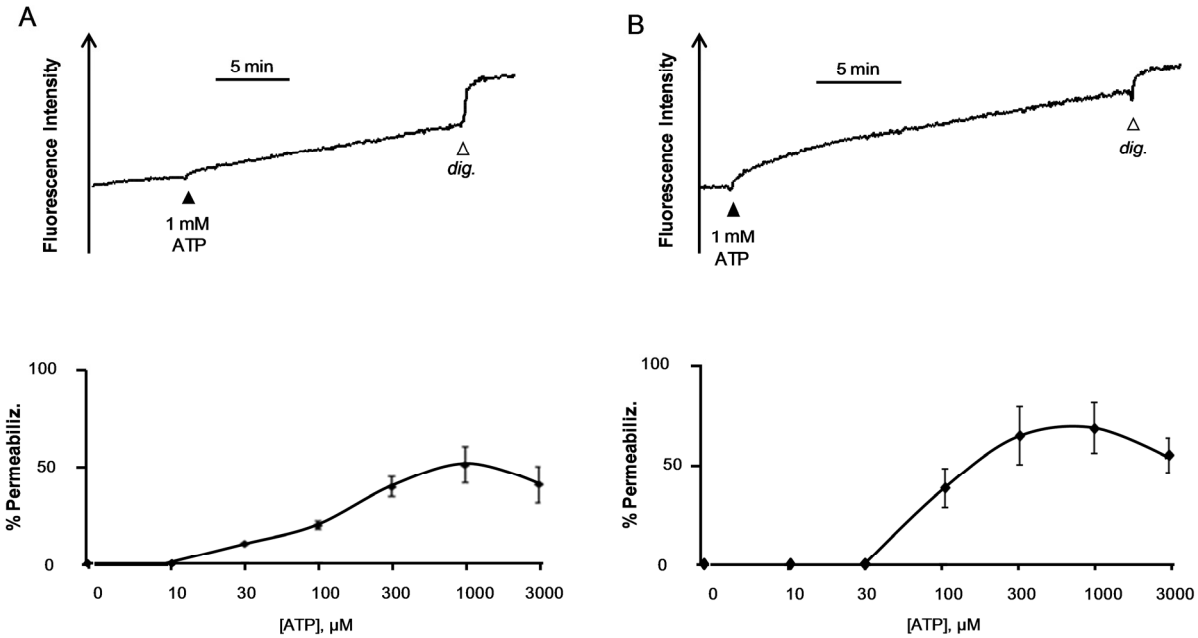

Figure 10. Ethidium Bromide uptake in MSC-1 and MSC-2 after stimulation with ATP.
Figure 10 shows the EtBr uptake and the ATP dose dependency curves for MSC-1 (Panel A) and MSC-2 (Panel B) cell lines.

Based on these data I focused my attention on the activity of P2X7R, stimulating cells with BzATP. As shown in Figure 11 A and B, the agonist lead an uptake of ethidium bromide even higher than ATP. The P2X7-mediated effect was particularly evident in MSC-2 where the level of permeabilization reach 83%.

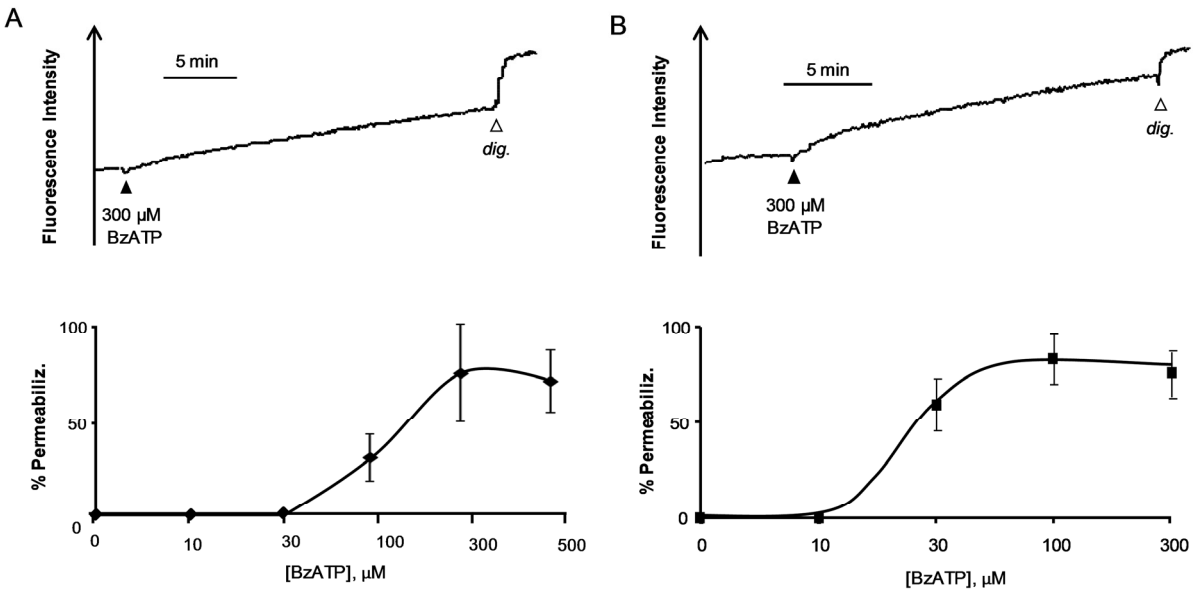

.

Figure 11. **Ethidium Bromide uptake in MSC-1 and MSC-2 after stimulation with BzATP.** Figure 11 shows the EtBr uptake and BzATP dose dependency in MSC-1 (Panel A) and MSC-2 (Panel B) cell lines.

To further confirm the involvement of P2X7R in the permeabilization response, I performed the same experiment after a 2 hours pre-incubation of MSC-2 with 600 µM oATP, a potent irreversible P2X7R antagonist. As we can see in Figure 12, the inhibition of P2X7R completely abrogated the ethidium bromide uptake.

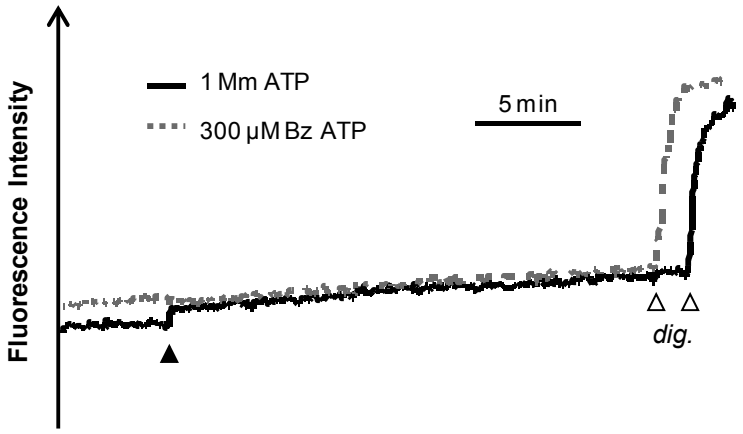

Figure 12. The inhibition on P2X7R abrogates Et Br uptake in MSC-2.
Figure 12 shows the tracers of MSC-2 cells pre-treated with oxo-ATP and stimulated with ATP and BzATP.

The pore associate to the P2X7R is permeable to lucifer yellow in both cell lines

I have verified if in MSC-1 and MSC-2 the pore associated to the P2X7 receptor was also permeable to higher molecular weight molecules than ethidium bromide.
I therefore performed the experiment with lucifer yellow (MW 457 Da) a fluorescent dye that in particular conditions, such as the opening of the P2X7R pore, enters the cell that becomes visible at the fluorescence microscope.
I acquired images in both phase-contrast and fluorescence. To analyze the data I compared the stimulated conditions (1 mg/ml lucifer yellow and 1 mM ATP or 300 μM BzATP) with two negative controls: one in the absence of the stimulation ("lucifer yellow"), and another without both lucifer - yellow and nucleotide ("control").
Figure 13 and 14 show that:

- In the "negative control" any fluorescence was observed.
- In the "lucifer–yellow" condition, no significant permeabilization to the dye was detectable.
- In the presence of both fluorescent dye and stimulus (1 mM ATP or 300 μM BzATP), MSC-1 and MSC-2 underwent permeabilization of the plasma membrane to lucifer yellow which was observable as fluorescence emission.

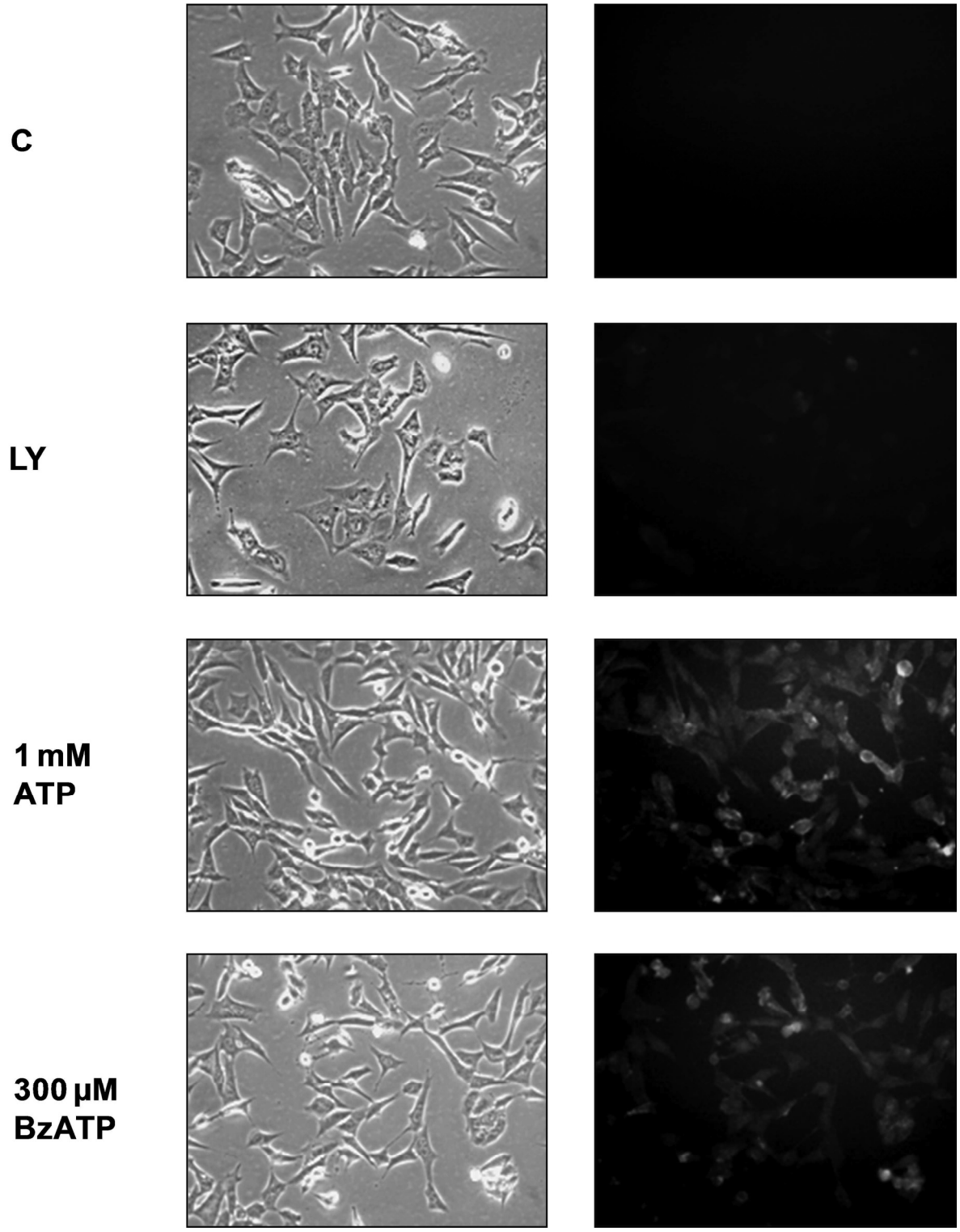

Figure 13. MSC-1 images in phase contrast and fluorescence.

The first couple of images show the negative control of MSC-1. The second couple of images show the cells in the presence of 1mg/ml of lucifer yellow. The forth and the fifth couples of images represent cells stimulated with ATP or BzATP in the presence of 1mg/ml lucifer yellow.

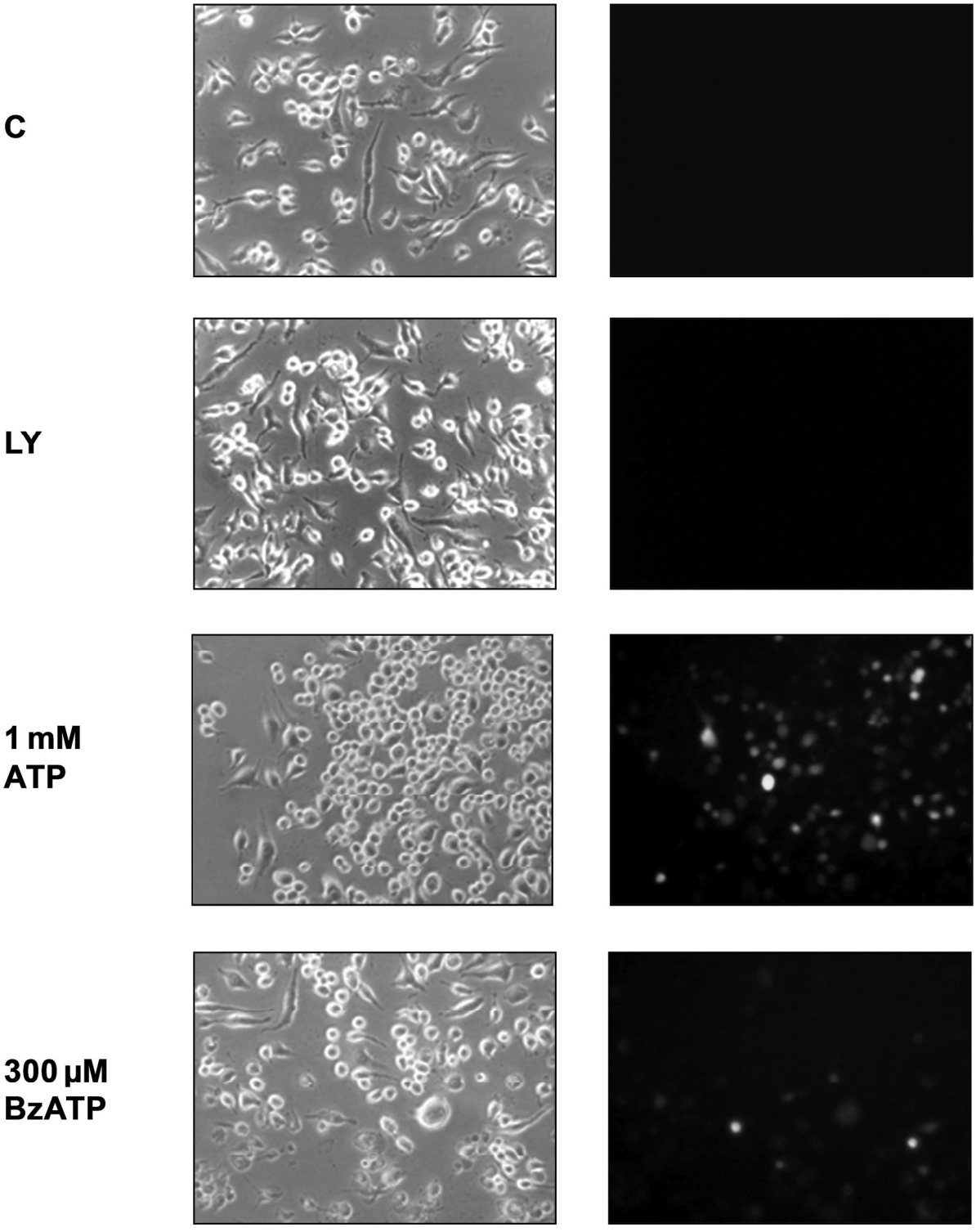

Figure 14. MSC-2 images in phase contrast and fluorescence.

The first couple of images show the negative control of MSC-1. The second couple of images show the cells in the presence of 1mg/ml of lucifer yellow. The forth and the fifth couples of images represent cells stimulated with ATP or BzATP in the presence of 1mg/ml lucifer yellow.

The stimulation of MSC-2 with ATP or BzATP induces depolarization of the plasma membrane

I verified if the stimulation of purinergic receptors and in particular P2X7, could affect the plasma membrane potential in MSC-2 cell line. To detect the phenomenon I labeled cells with bisoxonol, a fluorescent dye that binds the membrane phospholipids. In case of membrane depolarization an increased fluorescence emission of the bisoxonol occurs and is detectable by a spectro-fluorimeter. I normalized data to the depolarization induced by 20 mM KCl which completely depolarizes the membrane and I considered as a 100% response.

The stimulation of MSC-2 with 1 mM ATP induced 100% depolarization of plasma membrane (Figure 15) and the dose dependency curve shows that the nucleotide lead the maximum effect even at the concentration of 300 µM.

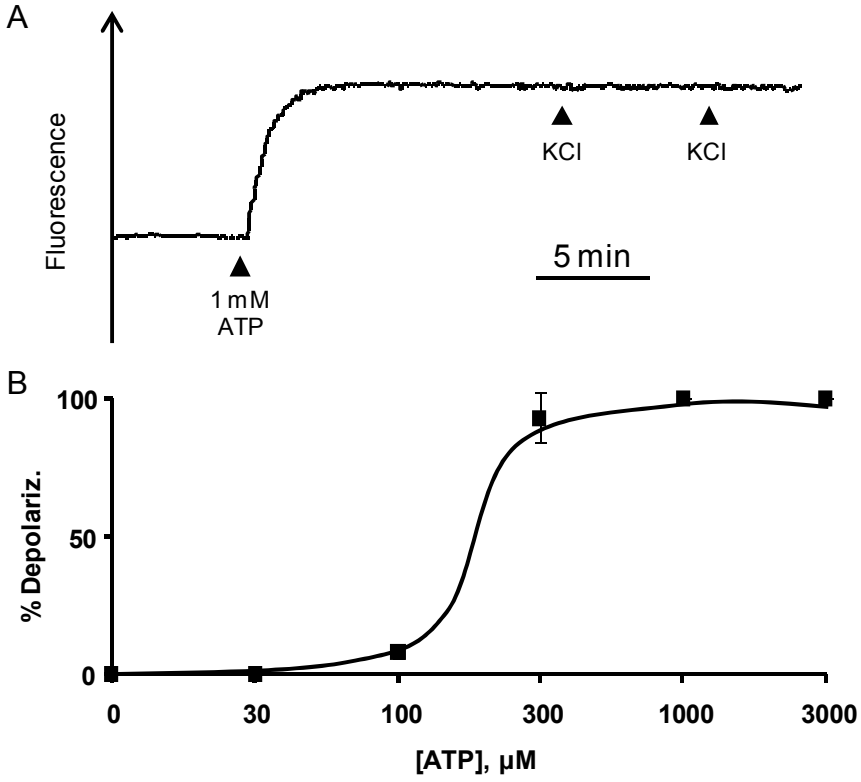

Figure 15. Plasma membrane depolarization induced by ATP.

Panel A shows the trace of MSC-2 cell line stimulated with 1 mM ATP. Cells were also treated with 20 mM KCl in order to evaluate the 100 % response. Panel B shows the ATP-dose dependence curve.

As shown in Figure 16 the depolarization was mainly due to the P2X7R activation, as even the stimulation with 300 μM BzATP induced a 100% response. The dose dependence curve shows that the agonist was completely effective even at the concentration of 100 μM.

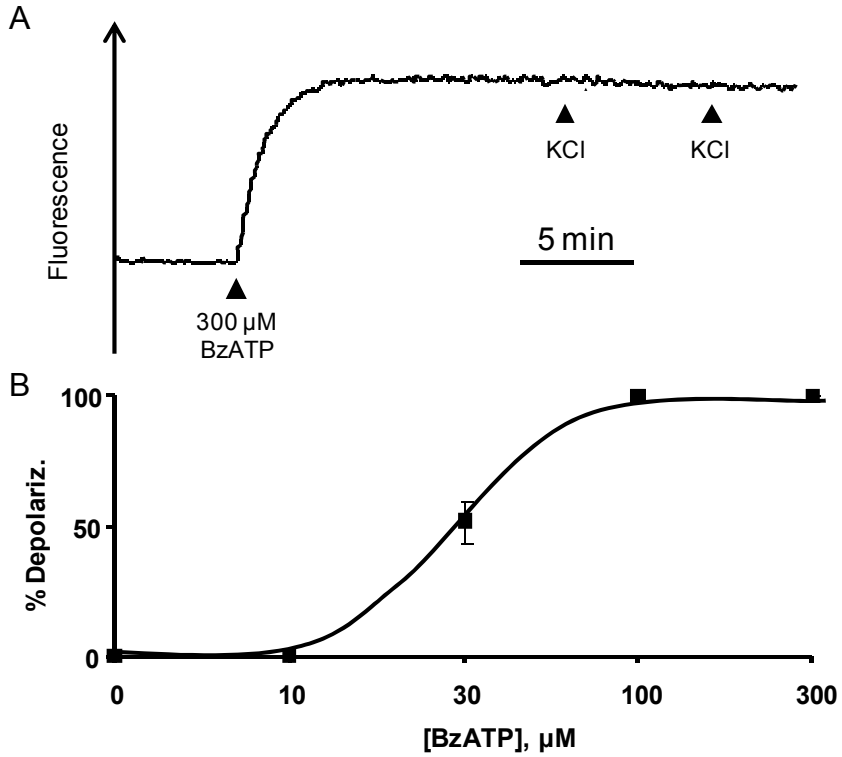

Figure 16. Plasma membrane depolarization induced by BzATP.

Panel A shows the trace of MSC-2 cell line stimulated with 300 μM BzATP. Cells were also treated with 20 mM KCl in order to evaluate the 100 % response. Panel B shows the BzATP-dose dependence curve.

The stimulation with ATP and BzATP induces cell swelling and blebbing in MSC-1 and MSC-2 cell lines

It is well stated that the dramatic upsetting of intracellular ion homeostasis caused by prolonged opening of the P2X7R pore, activates a chain of events leading to cell swelling, plasma membrane blebbing, mitochondria uncoupling, failure of oxidative phosphorylation and eventual cell death. Observing cells by the inverted microscope Nikon Eclipse TE300 I have verified that the stimulation with ATP and BzATP induced cell swelling and blebbing in MSC-1 and MSC-2.

As shown in Figure 17 the effect of 1 mM ATP was detectable even in the first minutes following the treatment. Cells underwent a continuative re-arrangement of the plasma membrane, followed by an intensive blebbing.

It would be interesting to verify if this was only a transient or an irreversibile effect.

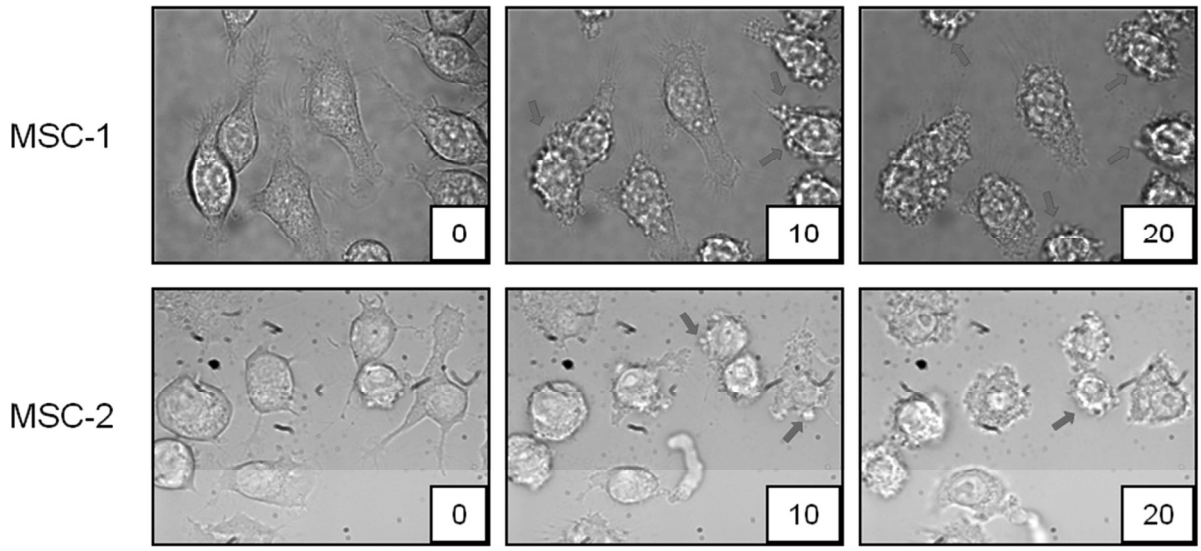

Figure 17. Phase-contrast images (100 X) of stimulation with 1 mM ATP in Na^+ Ca^{2+} buffer solution.

Cells were stimulated for 20 minutes with the nucleotide in a thermosttated chamber. I acquired images at 0, 10 and 20 miunutes. Red arrows indicate the morphological changes underwent by cells.

I also stimulated both cell lines with 300 μM BzATP. As shown in Figure 18 the effect of the agonist was comparable to the effect induced by the stimulation with ATP, suggesting the involvement of the P2X7 receptor in the phenomenon.

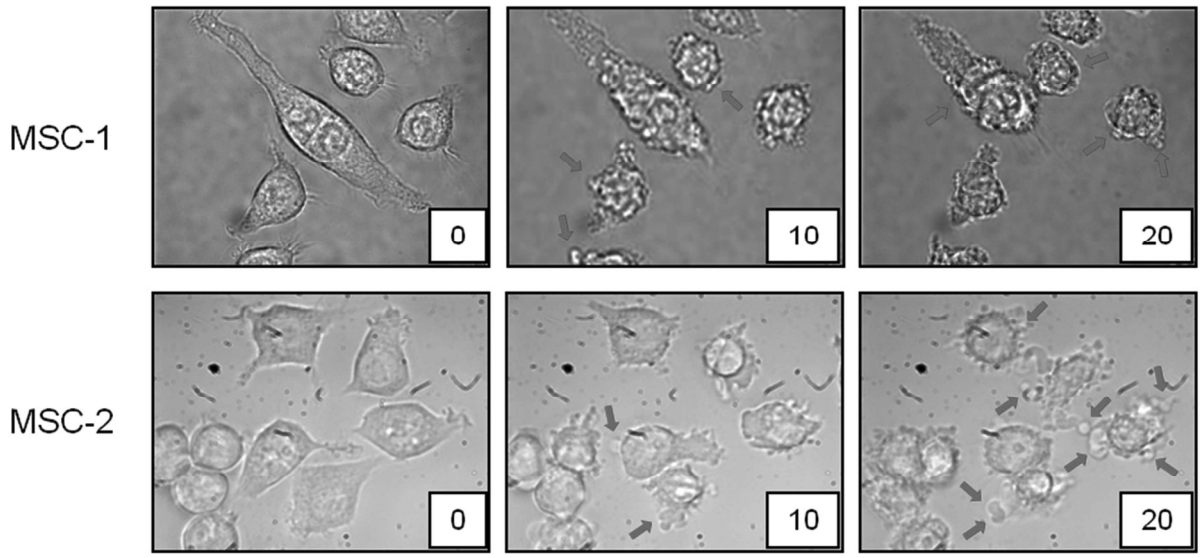

Figure 18. Phase-contrast images (100 X) of stimulation with 300 μM BzATP in Na^+ Ca^{2+} buffer solution.

Cells were stimulated for 20 minutes with the agonist. Red arrows indicate the morphological changes underwent by cells.

In order to further evaluate the involvement of P2XRs, and in particular P2X7, I have stimulated MSC-2 in a Na^+-0,5 mM EGTA buffer solution. As shown in Figure 19 the absence of the extracellular calcium does not affect the response to 1 mM ATP, suggesting the involvement of the PY subfamily. On the contrary in case of stimulation with BzATP in the same conditions, the blebbing response was partially abrogated, further highlighting the involvement of P2X7 receptor.

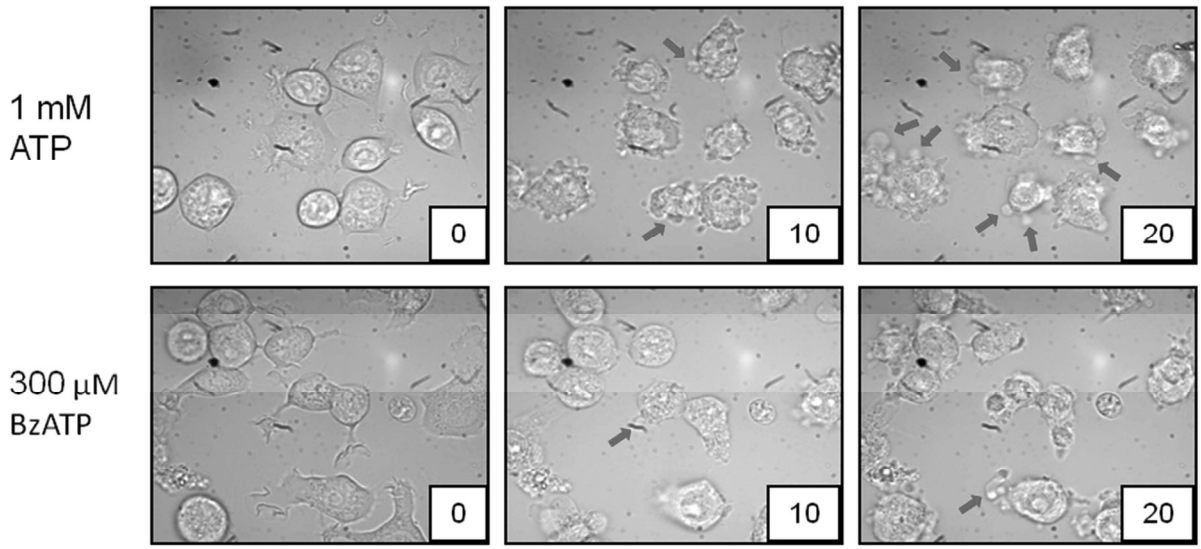

Figure 19. Phase-contrast images (100 X) of stimulation of MSC-2 cell line in Na^+ - 0,5 mM EGTA buffer solution.

Cells were stimulated for 20 minutes with ATP or BzATP in absence of extracellular calcium. Red arrows indicate the morphological changes, in particular blebbing, underwent by cells.

The stimulation of P2 receptors induces a moderate LDH release by MSC-1 and MSC-2

It is generally agreed that prolonged openings of the P2X7R pore is inevitably coupled to cell death [146]. There are however notable exception as for example human neuroblastoma cells, that despite the expression of a fully functional P2X7R pore, do not die even after prolonged exposures to high ATP concentrations [147]. Based on the result obtained by the imaging experiment I wondered whether the stimulation of MSC-1 and MSC-2 with nucleotides could have induced cell necrosis. In order to investigate the phenomenon I measured the release of the cytoplasmic marker lactic dehydrogenase (LDH) after chronic stimulation with ATP and BzATP.
As shown in Figure 20 although the prolonged exposure (eight hours) to 3 mM ATP induced morphological changes in MDSCs cell lines, a modest release of LDH was detected (Figure 21), evidence that the P2X7R pore opening was uncoupled from cytotoxicity. This data could explain why MDSCs can survive in highly inflammatory environment such as the tumor milieu.

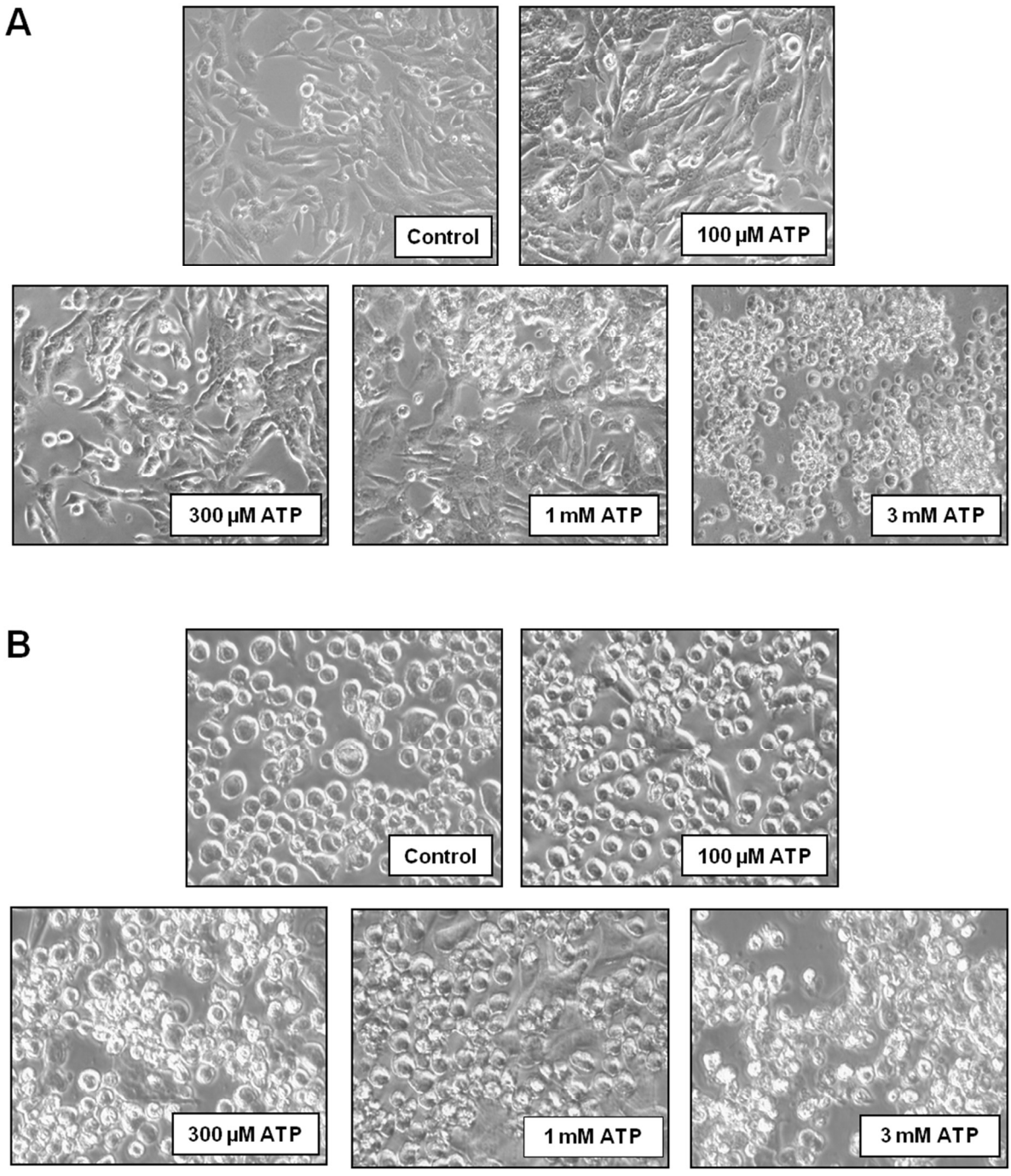

Figure 20. Phase-contrast images of chronic stimulation of MSC-1 and MSC-2 with ATP. Cells were stimulated for 8 hours with several ATP concentrations, images (20 X objective) were acquired at the end of the incubation time (Panel A shows MSC-1, Panel B shows MSC-2).

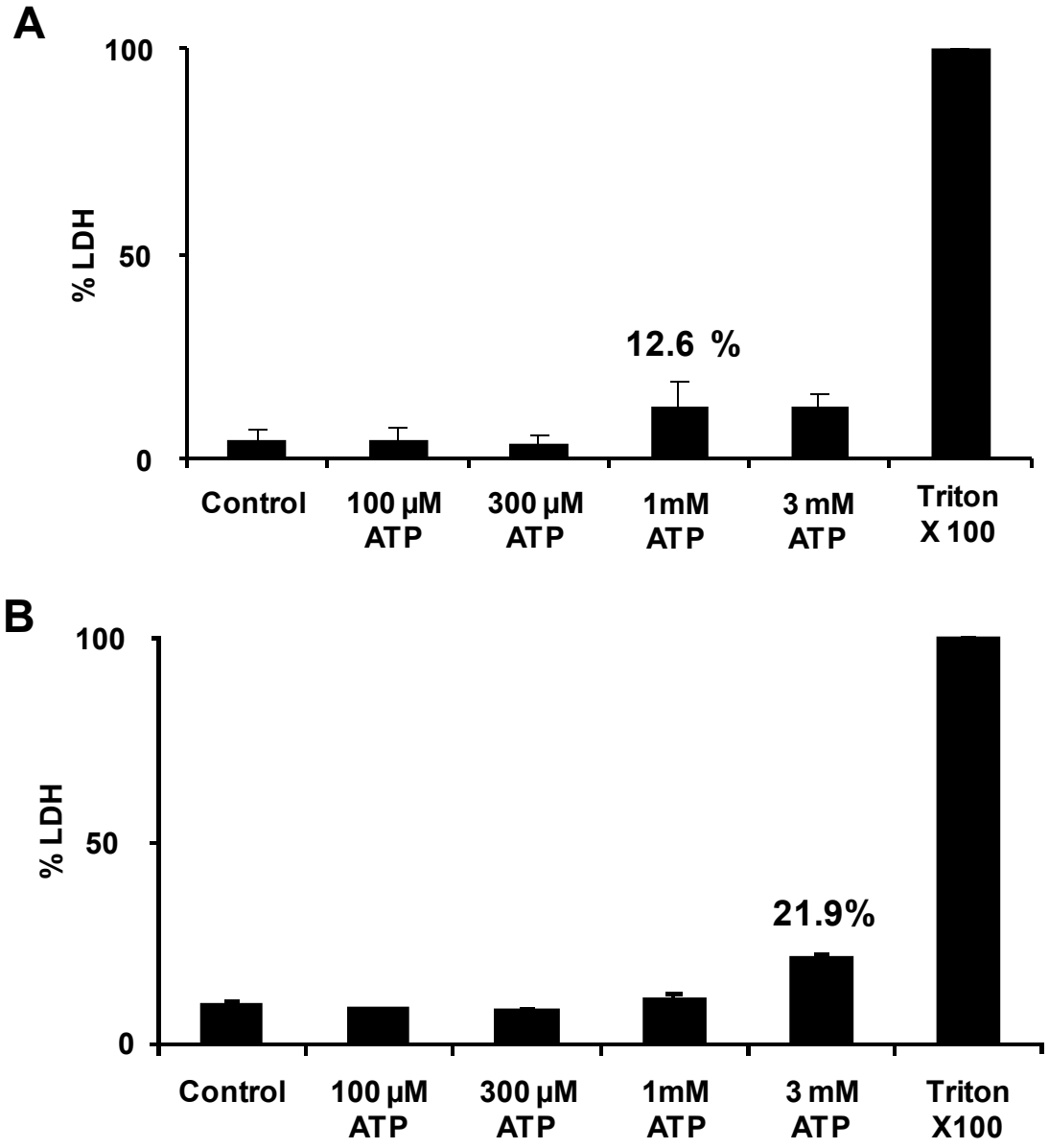

Figure 21. Chronic stimulation of MSC-1 and MSC-2 with ATP induces modest LDH release.

Cells were incubated at 37° C for 8 h in the presence of increasing ATP concentrations. LDH activity is expressed as % of total activity related to the enzyme released by Triton X-100 (Panel A shows MSC-1, Panel B shows MSC-2).

I have also measured the LDH release from MSC-1 cell line after chronic stimulation with BzATP. As shown in Figure 22 even the prolonged activation of P2X7R agonist did not lead cytotoxicity

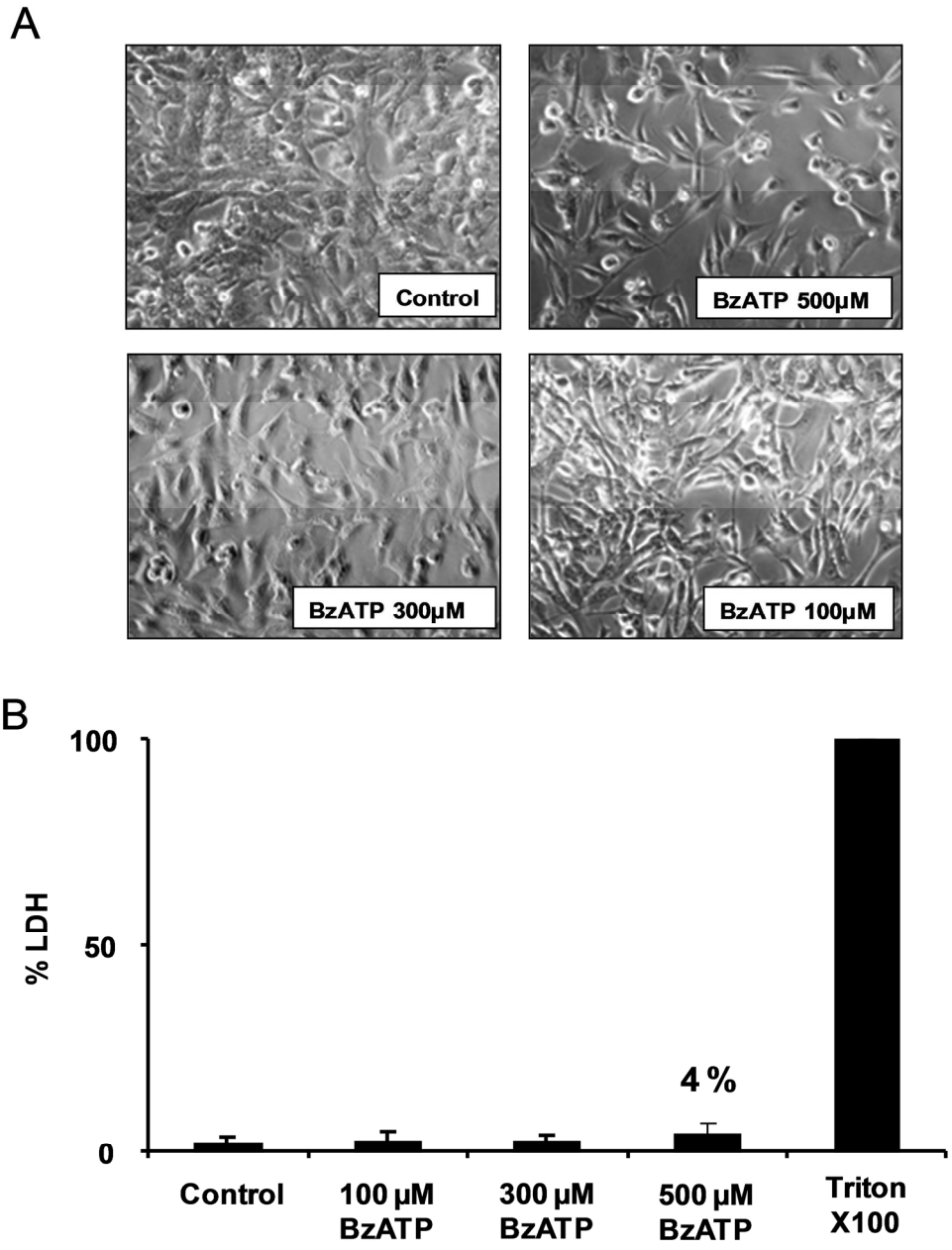

Figure 22. Phase-contrast images and LDH release from MSC-1 after chronic stimulation with BzATP.

Cells were incubated at 37° C for 8 h in the presen ce of increasing BzATP concentrations. Phase-contras images(20 X objective) were acquired at the end of the incubation time (Panel A). LDH activity is expressed as % of total activity related to the enzyme released by Triton X-100 (Panel B).

The stimulation of P2X7R triggers IL-1β release in both cell lines

In myelomonocytic cells P2X7R is well known to be coupled to inflammasome activation and IL-1β release [152]. To check whether this is also the case for MSC-1 and MSC-2 lines, these cells were primed with LPS for 4 h, followed by the usual BzATP challenge. As shown in Figure 23 A and B, P2X7R stimulation caused IL-1β release, especially at the higher concentration of 300 μM. Cytokine release was minimal, albeit clearly detectable in MSC-1 and substantially larger in MSC-2.

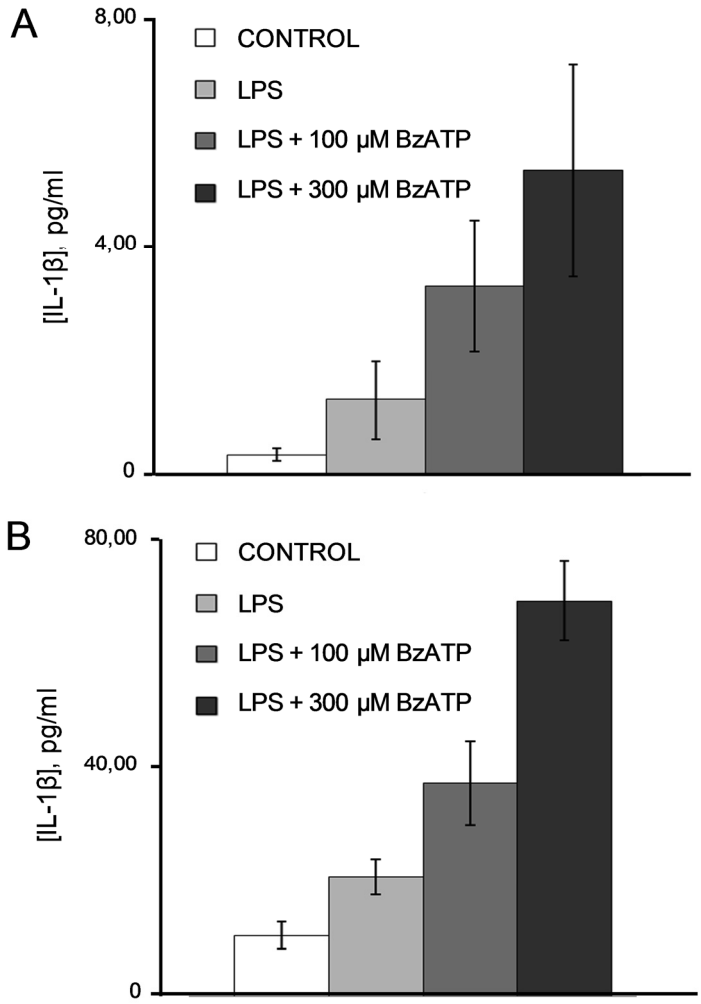

Figure 23. P2X7R-dependent IL-1β secretion from MSC-1 and MSC-2 lines.
Cell lines were primed for 4 hours with 1μg/ml LPS and then stimulated for 30 minutes with BzATP. At the end of this incubation time, cell free supernatants were assayed for IL-1β concentration with Mouse IL-1 beta Quantikine ELISA kit (RandD Systems, Abingdon, UK) (Panel A refers to MSC-1 and Panel B to MSC-2).

P2X7R stimulation induces the release of TGF-β1 in MSC-1 and MSC-2

P2X7R has been reported to support the release of TGF-β1 from astrocytes. I evaluated if the BzATP stimulation, with or without the LPS priming, could have induced the cytokine release in both cell lines.

Figure 24 A and B show that the stimulation of P2X7R induced TGF-β1 secretion in both cell lines. It should be noted that the release level of this immunosuppressive agent was already elevated under basal conditions and the amount of the cytokine detected in the medium was significantly higher in MSC-1 than MSC-2. This data is supported by Bronte and colleagues' observation by which MSC-1 cell line is constitutively suppressive. In the contrary the stimulation with IL-4 is required to induce the same effect in MSC-2.

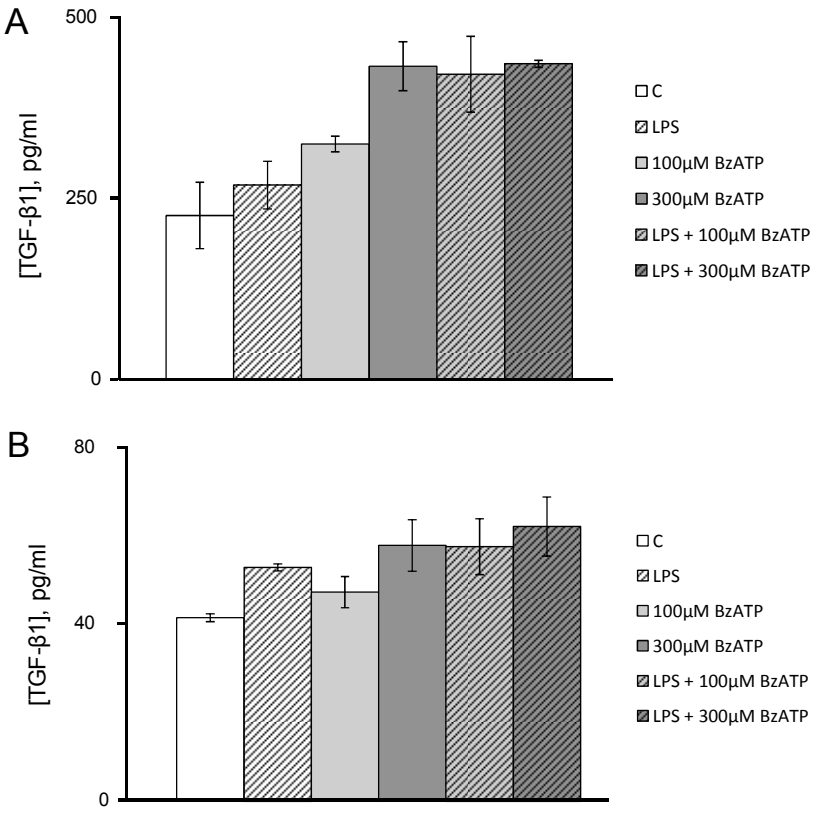

Figure 24. P2X7R-dependent TGF-β1 secretion from MSC-1 and MSC-2 lines.

Cell lines were primed for 4 hours with 1 μg/ml LPS and stimulated for 30 minutes with BzATP Stimulations were performed also without the priming with LPS. At the end of the incubation time, cell free supernatants were assayed for TGF-β1 concentration with Mouse TGF-β1 Quantikine ELISA (RandD Systems, Abingdon, UK). Data refers to 5 x 10^5 cells (Panel A refers to MSC-1 and Panel B to MSC-2).

The stimulation of P2X7R increases the intracellular ROS concentration in both cell lines

The ROS production is an important phenomenon related to the immune suppressive activity of MDSCs. P2X7R has been reported to support release of ROS from macrophage. By the measurement of the fluorescence level induced by the DCFDA, I observed that the stimulation with BzATP, even without the priming with LPS, increased the intracellular ROS concentration in both cell lines. The effect was particularly evident in MSC-2.

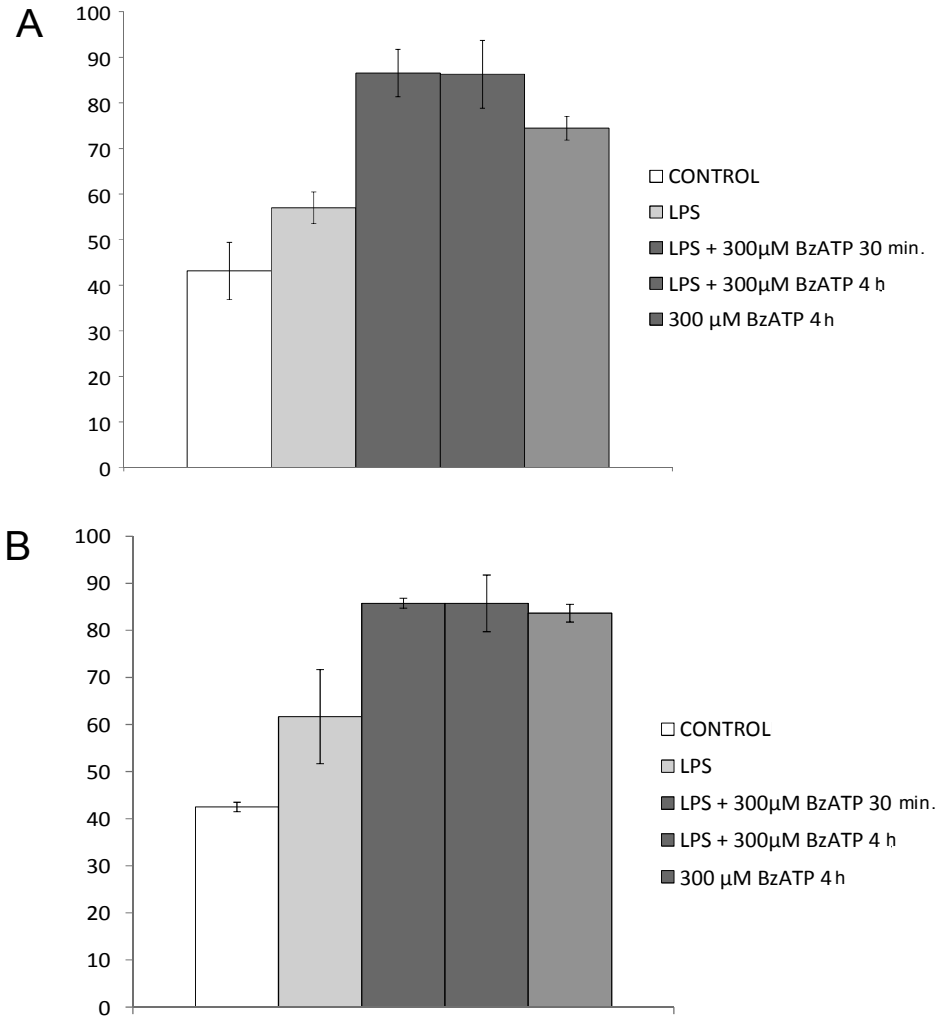

Figure 25. Stimulation of P2X7R leads ROS production in MSC-1 and MSC-2 cell lines. Panel A (MSC-1) and panel B (MSC-2) show the percentage of reactive oxygen species (ROS) with the oxidation-sensitive dye Dichlorodihydrofluorescein diacetate (DCFDA) as described in Materials and Methods. Results are expressed as % of the highest [ROS] detected related to the stimulation with 500µM H_2O_2 (not shown).

The stimulation of P2X7R increases ARG-1 expression in both cell lines

In collaboration with Prof. Pistoia's group (Laboratory of Oncology, Istituto Giannina Gaslini, Genoa) we have check whether the P2X7R stimulation could affect the expression of ARG-1 in MSC-1 and MSC-2 cell lines. As shown in Figure 26 A, in MSC-1 line the stimulation with BzATP, even without the priming with LPS, increased the expression of ARG-1. On the contrary in MSC-2 line (Figure 26 B), the stimulation of P2X7R triggered the same effect only after a 4h priming with LPS.

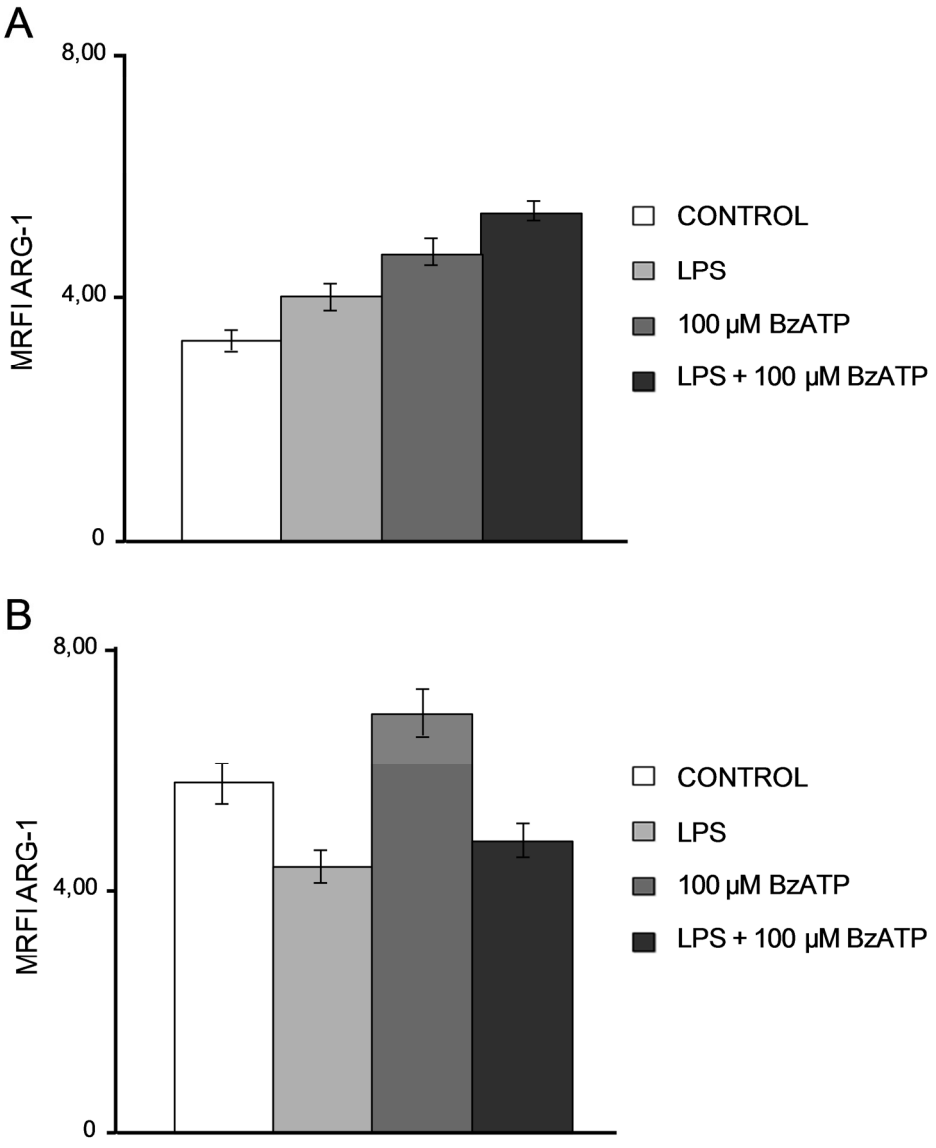

Figure 26. Stimulation of P2X7R leads ROS production in MSC-1 and MSC-2 cell lines. Cells were primed with 1µg/ml LPS for 4 hours, followed by stimulation with 100 µM BzATP for 30 min. Panel A (MSC-1) and panel B (MSC-2) show the expression of ARG-1 detected as described in Materials and Methods. Results are expressed as the mean fluorescent intensity ± SD from at least three different experiments performed.

Extracellular ATP is detectable in neuroblastoma tumor microenvironment

Some of the data of this thesis were used for a publications with the research group of Prof. Pistoia (Istituto Giannina Gaslini, Genova). In this work we investigated the MDSCs population that accumulates in Neuroblastoma and we found that P2X7R is involved in the modulation of the activity of these cells. Neuroblastoma (NB) is a malignant neoplasia originating from the sympathetic nervous system. About 50% of NB patients present metastatic disease at diagnosis and only one third of them survives at 5 years despite surgery, radiotherapy and aggressive chemotherapy followed by autologous hematopoietic rescue.

A breakthrough in *in vivo* ATP studies has been the development of the pmeLUC probe. This probe can be transfected into reporter or tumor cells, that can be then inoculated into experimental animal models to monitor by BLI changes in the eATP concentration at inflammatory or tumor sites [159].

In order to detect extracellular ATP in NB microenvironment, in collaboration with the group of Prof. Pistoia, the murine NB NXS2 cell line was stably transfected with the pmeLUC probe (NXS2-pmeLUC), and i.v. injected into immunocompetent syngeneic A/J mice. Bioluminescence imaging (BLI) analysis of mice disclosed a diffuse luminescence in the peritoneal cavity, associated with specific light-emitting spots in the kidneys, adrenal gland and ovaries, i.e. at sites of tumor metastasisis (Fig. 27 Panel A). BLI was carried out for up to 26 d after tumor cell inoculum (days 12, 19 and 26), showing an increased emission intensity as tumor progressed. At the different time points, some mice (three for each) were sacrificed, tumor masses excised and analyzed for luminescence emission. Direct BLI of the excised masses, consistently showed that light-emitting foci coincided with tumor masses (Fig. 27 panel B). These results indicate that extracellular ATP was specifically detected within tumor masses in NB bearing mice in amounts that increased in parallel with tumor progression.

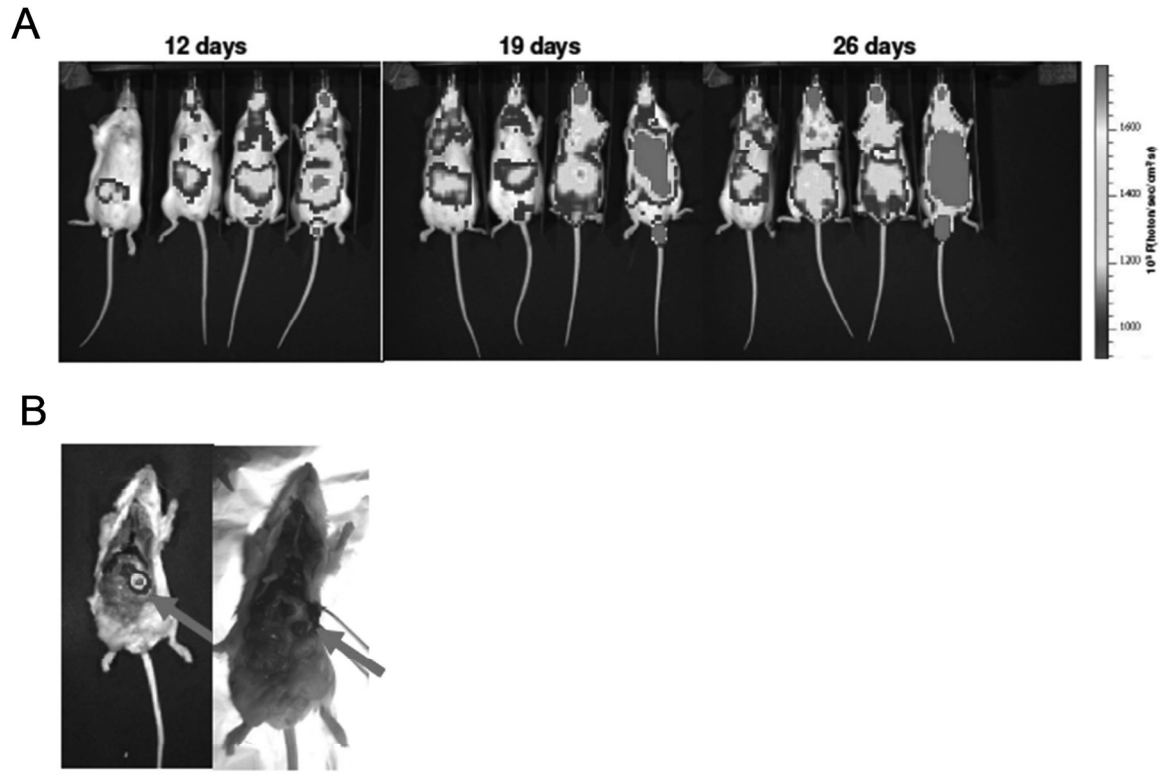

Figure 27. ATP detection in NB tumor microenvironment by pmeLUC probe.
Immunocompetent A/J mice (n=4) were i.v. injected with pmeLUC-NXS2 cells ($2x10^5$ cells/mouse). Panel A shows the animals imaged by bioluminescence 12, 19 and 26 days after tumor cell inoculum. Panel B shows a representative animal subjected to post-mortem macroscopic analysis. A light-emitting metastasis localized in the abdominal cavity is indicated by red arrow. This is a representative experiment out of three performed.

MSC-1 and MSC-2 cell lines release ATP in the extracellular microenvironment

Based on the evidence that ATP accumulates in the tumor milieu, I wondered if MDSCs could release the nucleotide in the extracellular microenvironment.
Figure 28 shows that both cell lines under basal conditions released ATP in the extracellular environment. The amount of ATP detected for MSC-2 was quite higher than for MSC-1.

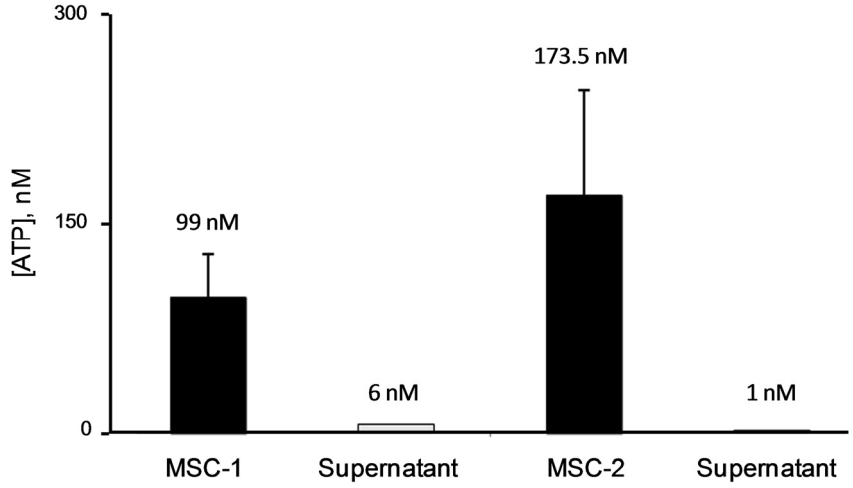

Figure 28. Concentration of ATP released by MSC-1 and MSC-2.
Cells were plated overnight in a 96 well plate, at the moment of the analysis supernatants were collected. The [ATP] released was measured both in cells and supernatants with the luciferine-luciferase assay. The level of the fluorescence detected was compared with a standard ATP curve created for every single experiment. The low amount of ATP detected in the supernatant could be mainly due to the degradation of the nucleotide by environmental agents (temperature, pH…) but we could not exclude even the involvement of other agents such as ectonucleotidases. The data is the result of three experiments, 10 wells each.

MSC-2 cell line express the protein of CD39

Based on the observation that both cell lines released ATP in the extracellular microenvironment and on the work of Ryzhov and colleague that hypothesized the involvement of the adenosine in the immunesuppressive activity of MDSC, I verified the expression of two ectonucleotidases in both cell lines [148].

CD39 and CD73 are two important membrane-bound enzymes involved in the metabolism of extracellular nucleotides. CD39 catalyzes the hydrolysis of ATP and ADP in adenosine–monophosphate (AMP), that is then converted in adenosine by CD73. Deaglio and colleague have recently related the expression of both enzymes with the suppressive activity of Treg cells [7].

As shown in Figure 29 the only enzyme detected was CD39, whose protein was expressed in MSC-2.

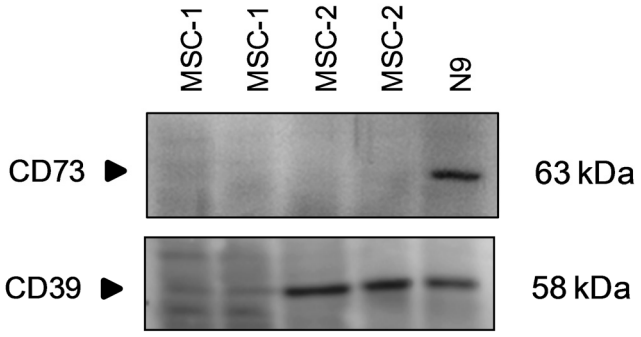

Figure 29. Identification of the proteins of CD39 and CD73.

Figure 29 shows the protein expression of CD39 and CD73 in MSC-1 and MSC-2. Equal amounts of protein (30 µg) were loaded in each lane and incubated with either primary antibody. Mouse microglial lysates (N9) served as a positive control.

In vitro generation of BM-MDSC

During the second year of the PhD course I had the opportunity to spend a research period in Prof. Bronte's group in Padova, where I learned how to *in vitro* differentiate murine bone marrow in MDSCs [149].

I collected BM form C57black6 wild type and P2X7 KO mice and I stimulated cells for 4 days with 40 ng/ml GM-CFS and 40 ng/ml IL-6. To confirm the differentiation in MDSCs I analyzed the expression of both markers CD11b and Gr-1. The level of expression was comparable to the values suggested by Marigo and colleagues.

Figure 30 shows that after the differentiation the percentage of MDSCs did not change from wild type and P2X7 KO mice, suggesting that P2X7R expression was not involved in the differentiation process.

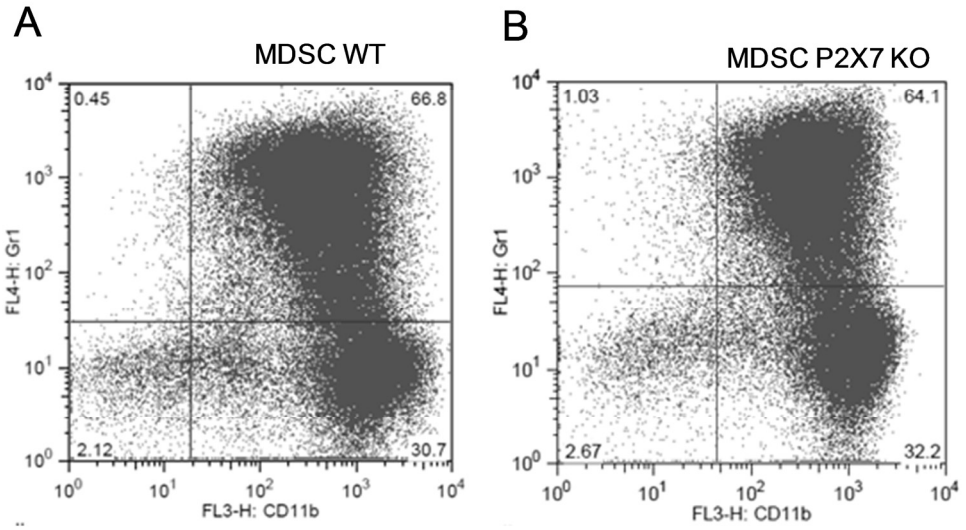

Figure 30. FACS Analysis of CD11b and Gr-1 expression in wild type and P2X7KO MDSC.

I stained wild type and P2X7KO MDSC with 1:100 PerCP/Cy5.5 anti CD11b and 1:100 APC anti Gr-1, as reported in Materials and Methods. I acquired data with FACSCalibur (BD Biosciences, Mountain View, CA, U.S.A.) and analyzed them with the program FlowJo (Tree Star, Inc.).

MDSCs express the protein of PX3, P2X5, P2Y6 AND P2X7R

By Western Blot I verified the expression of the proteins P2X3, P2X5, P2Y6 and P2X7 receptors in BM-MDSCs (Figure 30 A and B). Quite interestingly the protein of these P2Rs subtypes was detectable only after the differentiation of the BM in MDSCs. Moreover Figure 31 B shows that the P2X7R expression decreased in response to prolonged stimulation with ATP. This phenomenon could explain how MDSCs can survive even in highly inflammatory environments.

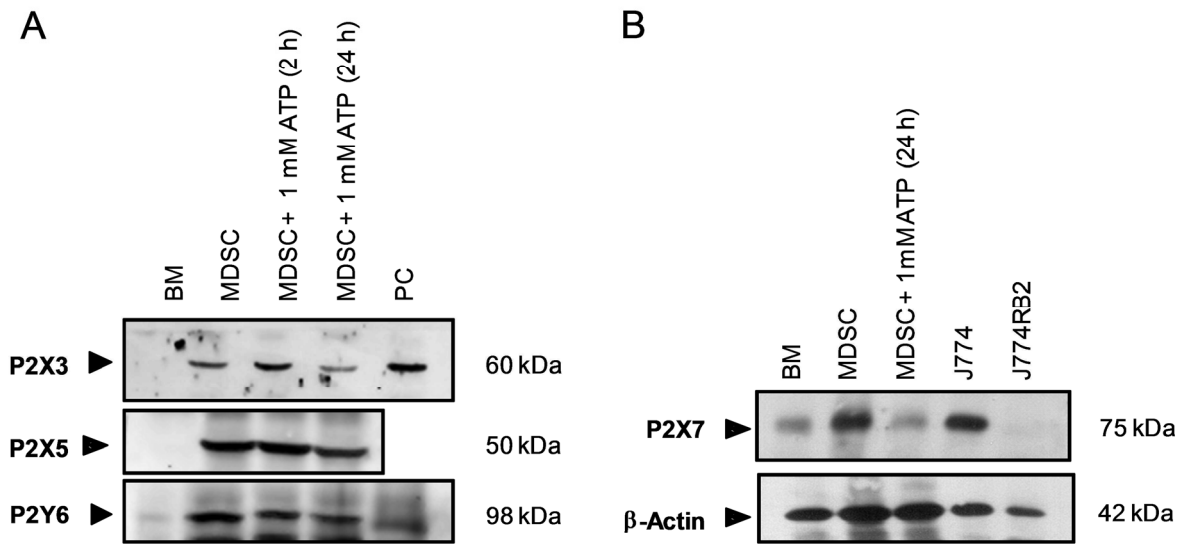

Figure 31. Identification of P2 receptors proteins in BM and MDSC.
Panel A shows the protein expression of P2X3, P2X5 and P2Y6 receptors in MDSC. Panel B shows the P2X7R expression normalized to β-Actin. Equal amounts of protein (30 µg) were loaded in each lane and incubated with either primary antibody. Murine microglial lysates (N9) or murine macrophages cell line (J774) served as a positive control.

MDSCs release ATP in the extracellular microenvironment

With the luciferine lucifase assay I evaluated wether even BM-derived MDSCs could release ATP in the extracellular milieu.

Figure 32 shows that under basal conditions both wild type and P2X7KO cells released ATP in the extracellular environment. The amount nucleotide releases by wild type MDSCs was quite higher than the concentration released by P2X7 KO cells.

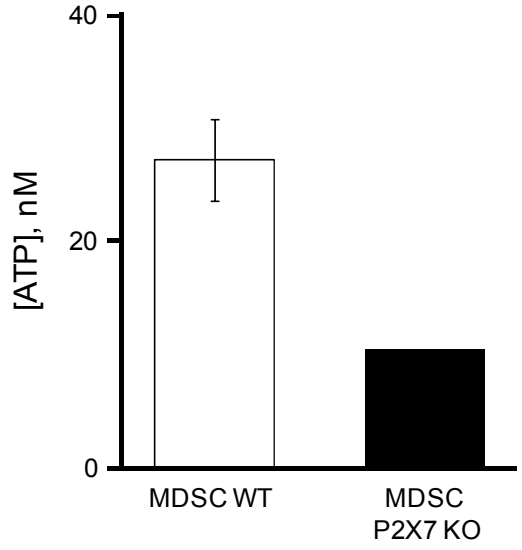

Figure 32. Concentration of ATP released by wild type and P2X7 KO MDSCs.

Cells were seeded in a 96 well plate and the [ATP] released was measured with the luciferine-luciferase assay. The level of the fluorescence detected was compared with a standard ATP curve created for every single experiment.

ATP and UTP have chemotactic effect on MDSC

There are evidences that MDSCs can migrate in the tumor site where exert their suppressive activity. It is well stated that nucleotides have chemotactic effect on different cell types. With a trans-well plate, I investigated whether ATP and UTP could have induced the same effect on MDSC. Figure 33 shows that, even if ATP and UTP increased the mobility of MDSCs, a real chemotactic effect was detectable.

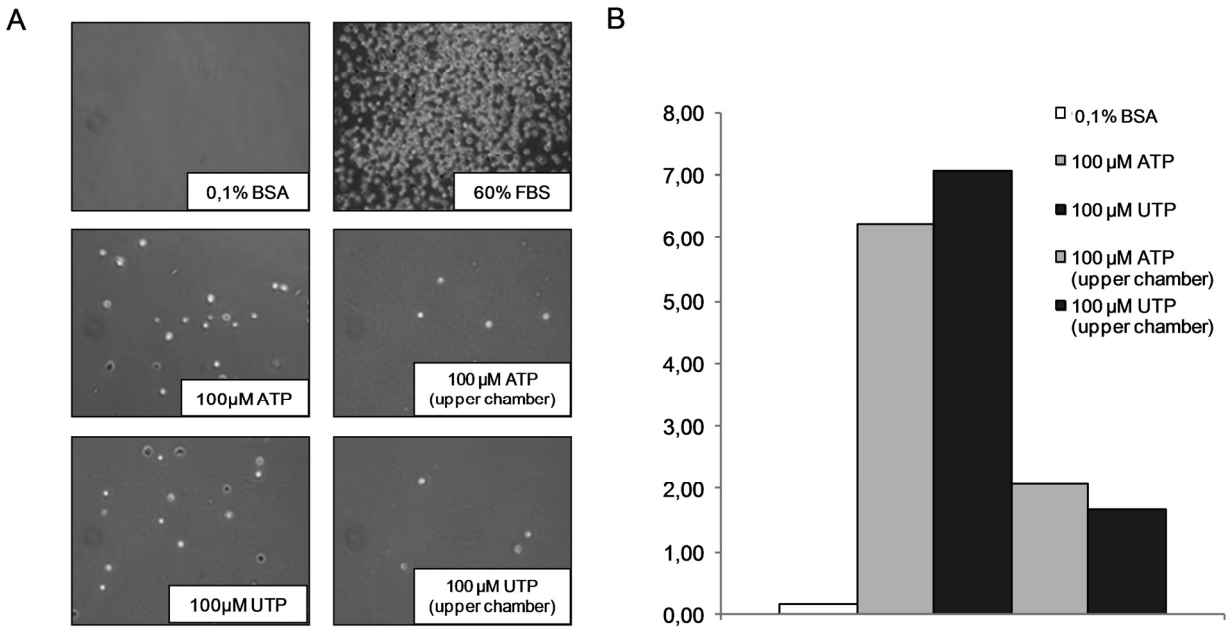

Figure 33. Chemotactic effect of ATP and UTP on MDSC.

After a 2h serum starvation, cells were seeded on the upper chamber of a trans-well plate. Each well was filled with the respective condition (0,1% BSA as negative control, 60% FBS as positive control, ATP, UTP). In order to discriminate the real chemotactic effect from the increased cell mobility due to the presence of nucleotides, I stimulated two wells with ATP and UTP in the upper chamber. After 3 hours from the stimulation the number of cells detected in the lower chamber was counted. Panel A shows the phase-contrast images of the lower chamber after the incubation time (20X). Panel B shows the number of cells counted.

MDSCs express the protein of CD39 and CD73

By Western blot I verified the expression of CD39 and CD73 in BM-MDSCs. As shown in Figure 34, MDSCs express the protein of CD39 (ectonucleoside triphosphate diphosphohydrolase-1) and CD73 (ecto-5′-nucleotidase).

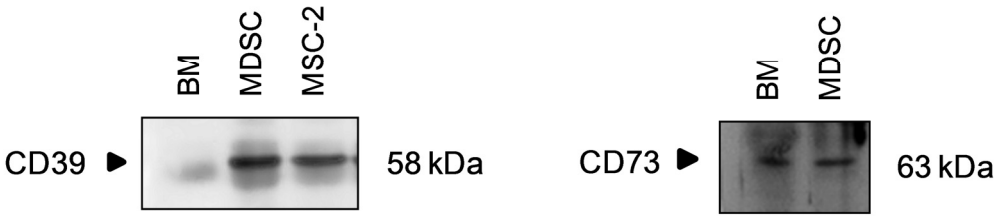

Figure 34. Identification of the proteins of CD39 and CD73.

Figure 34 shows the protein expression of CD39 and CD73 in MDSC. Equal amounts of protein (30 µg) were loaded in each lane and incubated with either primary antibody. MSC-2 cell line served as a positive control for CD39 expression.

The stimulation with ATP or adenosine increases the expression of CD39

I investigated whether the stimulation of MDSCs with 300 μM ATP or adenosine could affect the expression of CD39 in MDSCs. I stimulated cells for 2 or 24 hours and I evaluated the level of the protein by FACS. As shown in Figure 35 the 2 h stimulation with ATP and the 24 h stimulation with adenosine increased the expression of CD39.

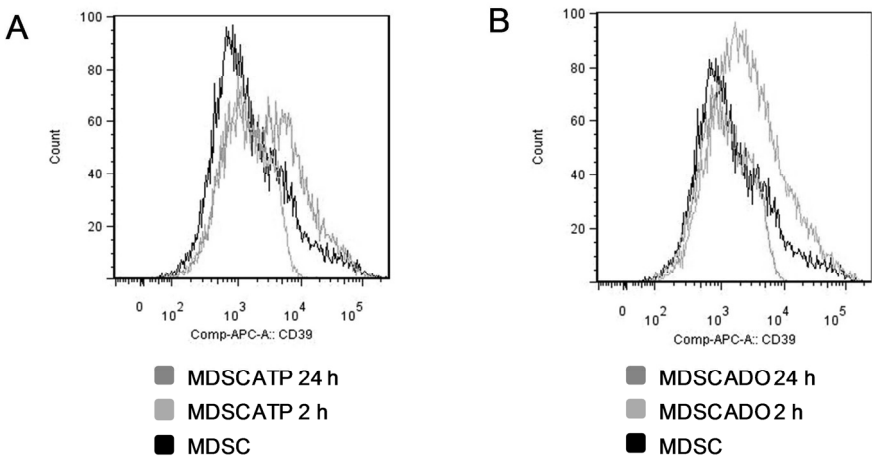

Figure 35. CD39 expression in MDSCs.
I stimulated MDSC for 2 and 24 hours with 300 μM ATP or adenosine (ADO) respectively. I stained cells with 1:100 APC anti CD39, I acquired samples with FACSCalibur (BD Biosciences, Mountain View, CA, U.S.A.) and analyzed the data with the program FlowJo (Tree Star, Inc.).

MDSCs express functional CD39 and CD73

A recently revealed immunesuppressive mechanism of MDSCs action is that by expressing CD73 (ecto-5′-nucleotidase) and converting AMP in adenosine. I hypothesized that MDSCs could even hydrolyze ATP/ADP into AMP, therefore by TLC assay I verified whether ecto-enzyme CD39 was functional in these cells.

As shown in Figure 36 the ectonucleoside triphosphate diphosphohydrolase-1 (CD39) was really functional and it hydrolyzed ADP in AMP. Moreover I verified that AMP was converted in adenosine and quite interestingly an high amount of inosine was detectable.

The role of inosine in the immune system is still controversial, but several works relate the molecule to immunesuppressive events [150].

Based on the observation that the stimulation with ATP increased CD39 expression in MDSCs, I evaluated if it could even affect the nucleotidase activity of cells. Quite interestingly I found that after ATP pre-stimulation, adenosine and inosine became detectable earlier (after 10 minutes of incubation) than in the unstimulated cells.

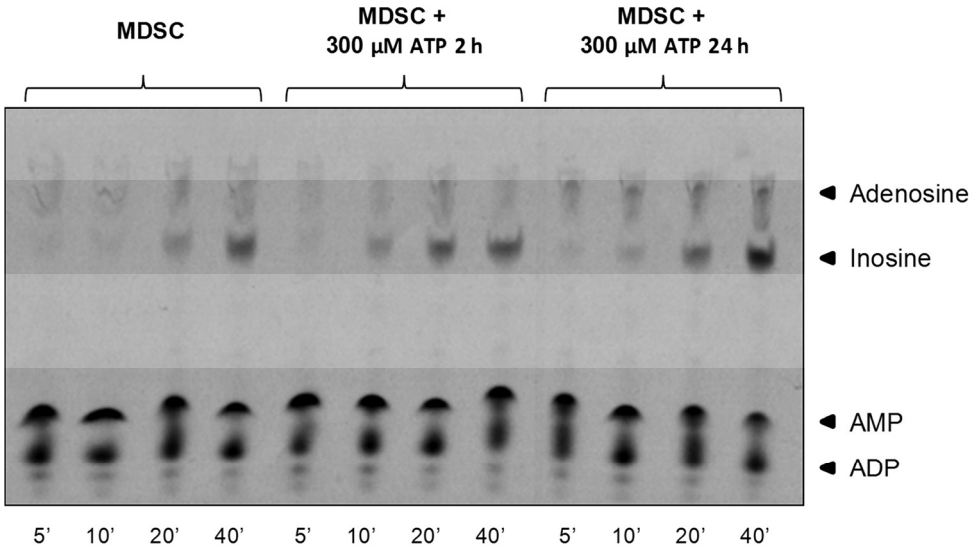

Figure 36. Hydrolysis of extracellular ^{14}C-radiolabeled ADP to adenosine and inosine.
Figure 36 shows the autoradiography of the products of the hydrolysis reactions that converts ADP in AMP, adenosine and inosine.

The stimulation of MDSCs with ATP or adenosine increases their immunosuppressive activity in vitro

In order to test whether ATP and adenosine would be involved in the suppressive mechanism of MDSCs, I evaluated how the stimulation of cells with these agonists could affect their suppressive activity on T cells proliferation.
I pre-stimulated MDSCs for 2 and 24 hours with 300 μM ATP or 300 μM adenosine respectively and I co-cultured them for 72 hours with CFSE-labeled splenocytes activated with Dynabeads. At the end of the incubation time I collected splenocytes and I measured the CFSE dilution in $CD4^+$ and $CD8^+$ cells.
As shown in Figures 37 and 38 the stimulation of MDSCs with ATP or adenosine increased MDSCs suppressive activity on $CD4^+$ and $CD8^+$ cells. The effect was more evident in the ratios 1:4 and 1:8.

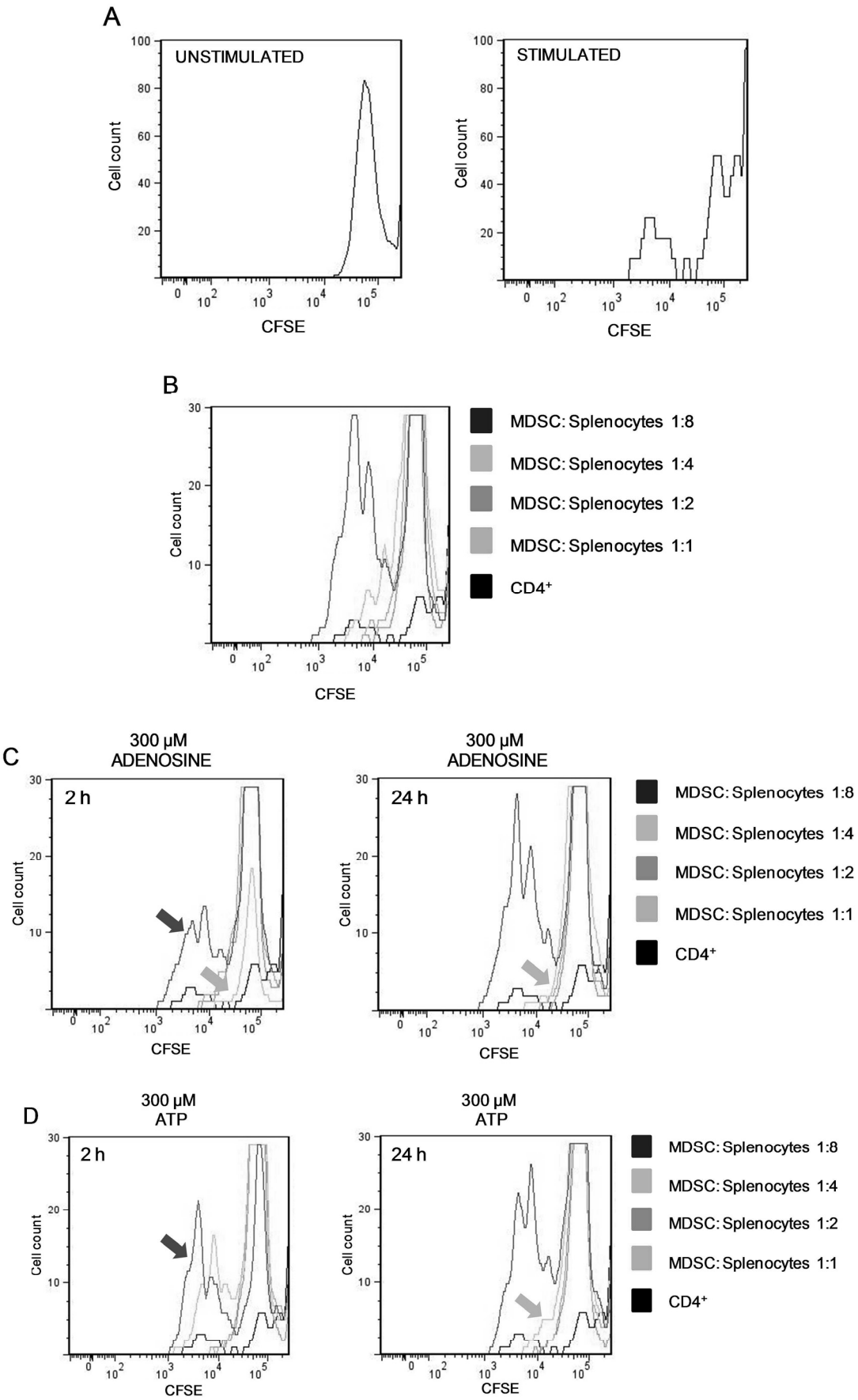
A
UNSTIMULATED
STIMULATED
Cell count
CFSE
B
MDSC: Splenocytes 1:8
MDSC: Splenocytes 1:4
MDSC: Splenocytes 1:2
MDSC: Splenocytes 1:1
CD4+
C
300 µM
ADENOSINE
2 h
24 h
D
300 µM
ATP

Figure 37. MDSCs–mediated immune suppression on $CD4^+$ T cells.

- Panel A shows CFSE-labeled splenocytes, gated on $CD4^+$ lymphocytes, unstimulated (left plot) and stimulated (right plot) with Dynabeads. Stimulation induced cell proliferation, detectable as CFSE-dilution.
- Panel B shows CFSE-labeled splenocytes, gated on $CD4^+$ lymphocytes, stimulated with Dynabeads, with MDSC in different ratios. The most suppressive ratios are 1:1 and 1:2.
- Panel C: Pre-stimulated MDSCs with 300 μM adenosine for 2 h (left plot) or 24 hours (right plot) add to the splenocytes stimulated with Dynabeads. Gate on $CD4^+$ lymphocytes. Adenosine 2 h increased MDSCs suppressive activity in the ratio 1:4 (light green arrow) and 1:8 (dark green arrow). Adenosine 24 h increased MDSCs suppressive activity in the ratio 1:4 (light green arrow).
- Panel C: Pre-stimulated MDSCs with 300 μM ATP for 2 h (left plot) or 24 hours (right plot) add to the splenocytes stimulated with Dynabeads. Gate on $CD4^+$ lymphocytes. ATP 2 h increased MDSCs suppressive activity in the ratio 1:8 (dark green arrow). ATP 24 h increased MDSCs' suppressive activity in the ratio 1:4 (light green arrow).

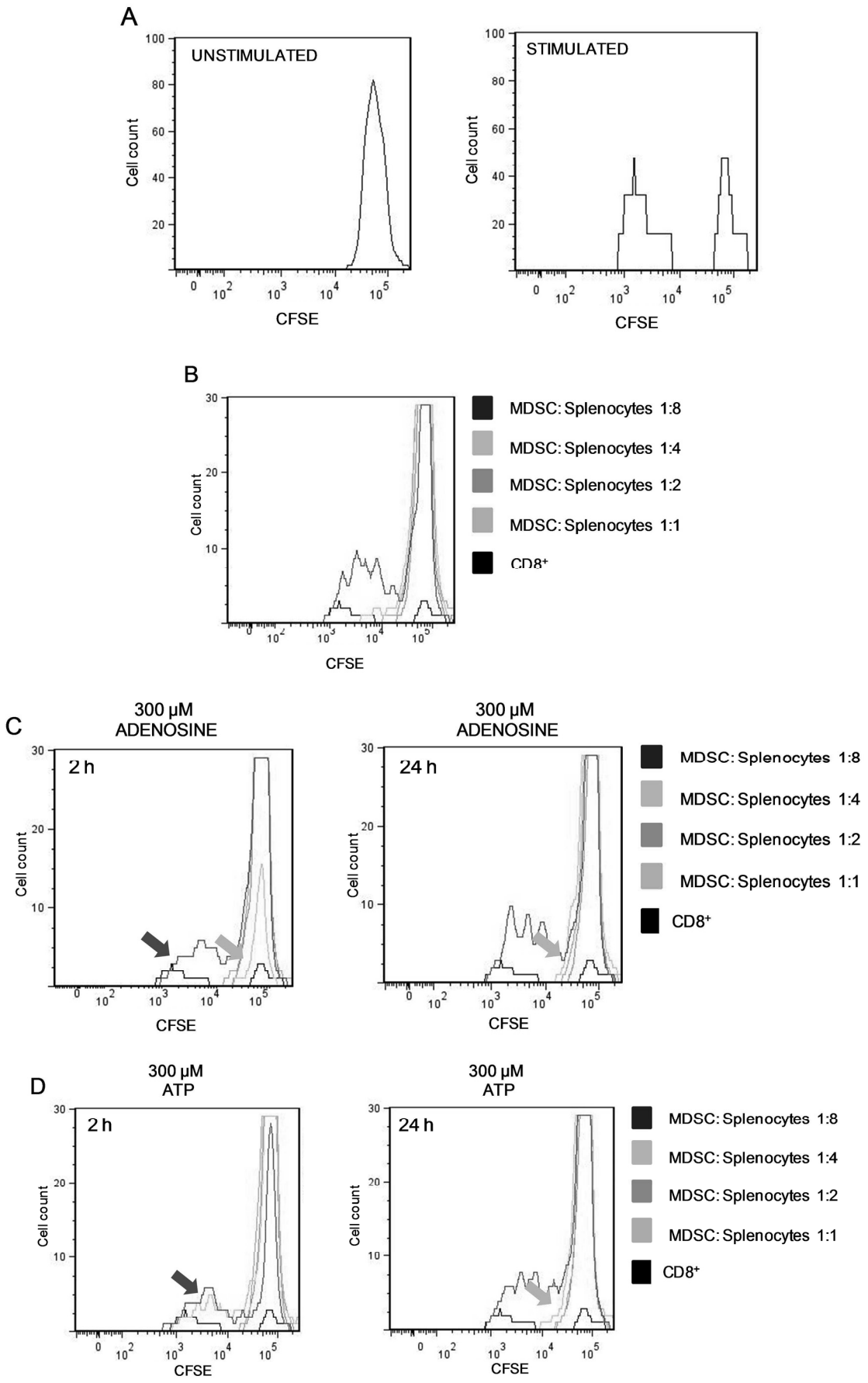
A
UNSTIMULATED
STIMULATED
Cell count
CFSE
B
MDSC: Splenocytes 1:8
MDSC: Splenocytes 1:4
MDSC: Splenocytes 1:2
MDSC: Splenocytes 1:1
CD8+
C
300 µM
ADENOSINE
2 h
24 h
D
300 µM
ATP

Figure 38. MDSCs–mediated immune suppression on $CD8^+$ T cells.

- Panel A shows CFSE-labeled splenocytes, gated on $CD8^+$ lymphocytes, unstimulated (left plot) and stimulated (right plot) with Dynabeads. Stimulation induced cell proliferation, detectable as CFSE-dilution.
- Panel B shows CFSE-labeled splenocytes, gated on $CD8^+$ lymphocytes, stimulated with Dynabeads, with MDSC in different ratios. The most suppressive ratios are 1:1 and 1:2.
- Panel C: Pre-stimulated MDSCs with 300 μM adenosine for 2 h (left plot) or 24 hours (right plot) add to the splenocytes stimulated with Dynabeads. Gate on $CD8^+$ lymphocytes. Adenosine 2 h increased MDSCs suppressive activity in the ratio 1:4 (light green arrow) and 1:8 (dark green arrow). Adenosine 24 h increased MDSCs suppressive activity in the ratio 1:4 (light green arrow).
- Panel C: Pre-stimulated MDSCs with 300 μM ATP for 2 h (left plot) or 24 hours (right plot) add to the splenocytes stimulated with Dynabeads. Gate on $CD8^+$ lymphocytes. ATP 2 h increased MDSCs suppressive activity in the ratio 1:8 (dark green arrow). ATP 24 h increased MDSCs' suppressive activity in the ratio 1:4 (light green arrow).

Identification of Myeloid Derived Suppressor Cells from neuroblastoma-bearing mice

In order to identify MDSCs subsets in the NB-bearing mice, in collaboration with Prof. Pistoia's group, A/J mice were i.v. injected with the syngeneic murine NB NXS2 cell line. Single cell suspensions obtained from spleen, BM and PB were analyzed by flow cytometry. Control spleen, BM and PB were obtained from tumor-free (naïve) animals. We found that the percentage of $CD11b^{+}/Gr\text{-}1^{+}$ cells in the spleen (Figure 39 A) and in the PB (Figure 39 B) of NB-bearing mice was significantly higher compared to naive mice.

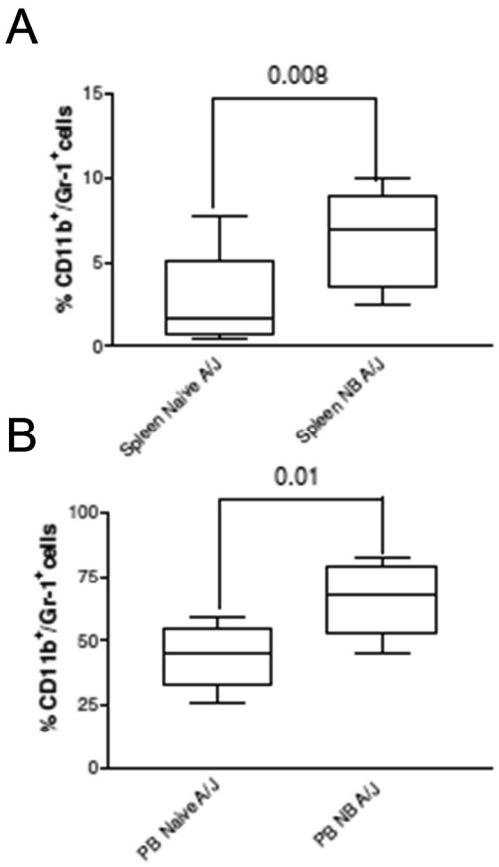

Figure 39. Accumulation of myeloid derived suppressor cells in neuroblastoma tumor-bearing mice.

Single cell suspension isolated from spleen, peripheral blood (PB) and bone marrow (BM) of naïve and NB tumor bearing mice (mice/group n=15) were stained with CD11b and anti-Gr-1 antibodies and subjected to flow cytometry analysis.

Panels A and B show the percentage of CD11b+/Gr-1+ cells in spleen and PB from naïve and tumor bearing mice. P values were calculated using Unpaired t test with Welch's correction.

Identification of Granulocytic and Monocytic Myeloid Derived Suppressor Cells subsets from neuroblastoma-bearing mice

On the basis of the differential expression of Ly-6G and Ly-6C markers, a recent report identified two distinct subsets of MDSCs i.e. G-MDSCs and M-MDSCs from tumor bearing mice [30]. In order to investigate the presence of these MDSC subsets, splenic CD11b+ cells from NB-bearing and naïve mice were enriched in the G-MDSCs and M-MDSCs fractions by immunomagnetic sorting. We found that amount of G-MDSCs and M-MDSCs isolated from NB-bearing mice was significantly higher compared to that isolated from naïve mice (Figure 40).

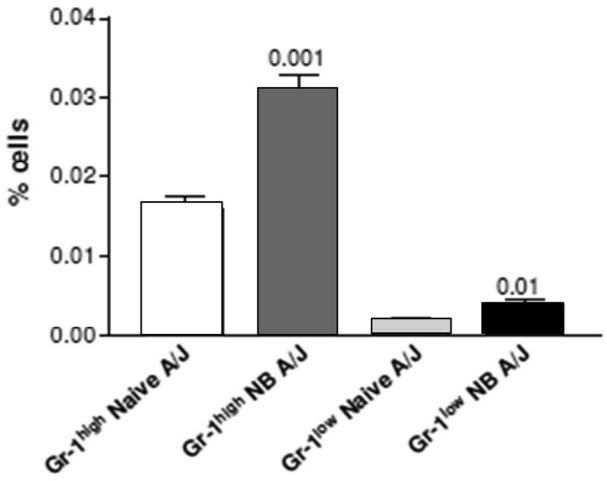

Figure 40. Accumulation of M-MDSC and G-MDSC in neuroblastoma tumor-bearing mice.

Single cell suspension isolated from spleen, peripheral blood (PB) and bone marrow (BM) of naïve and NB tumor bearing mice (mice/group n=15) were stained with CD11b and anti-Gr-1 antibodies and subjected to flow cytometry analysis.

Figure 40 shows the percentage of MDSC-Gr ^{high} (G-MDSC) and MDSC-Gr^{low} (M-MDSC) isolated from naïve and NB mice.

P2X7R is expressed in Granulocytic and Monocytic Myeloid Derived Suppressor Cells subsets in neuroblastoma-bearing mice.

In collaboration with Pistoia's group we evaluated the P2X7R expression in MDSCs isolated from tumor bearing mice. Figure 41 A shows that both NB G-MDSCs and M-MDSCs express P2X7R mRNA. Immunofluorescence analysis revealed a predominantly cytosolic, diffuse, staining in both MDSC subsets (Panel B). Interestingly however, NB M-MDSCs also showed a clear and specific patchy P2X7R fluorescence on the plasma membrane. No similar fluorescence pattern was ever detected in Naïve G-MDSCs and M-MDSCs, or from NB G-MDSCs. These results suggest an enhanced and specific plasma membrane localization of the P2X7R in M-MDSCs.

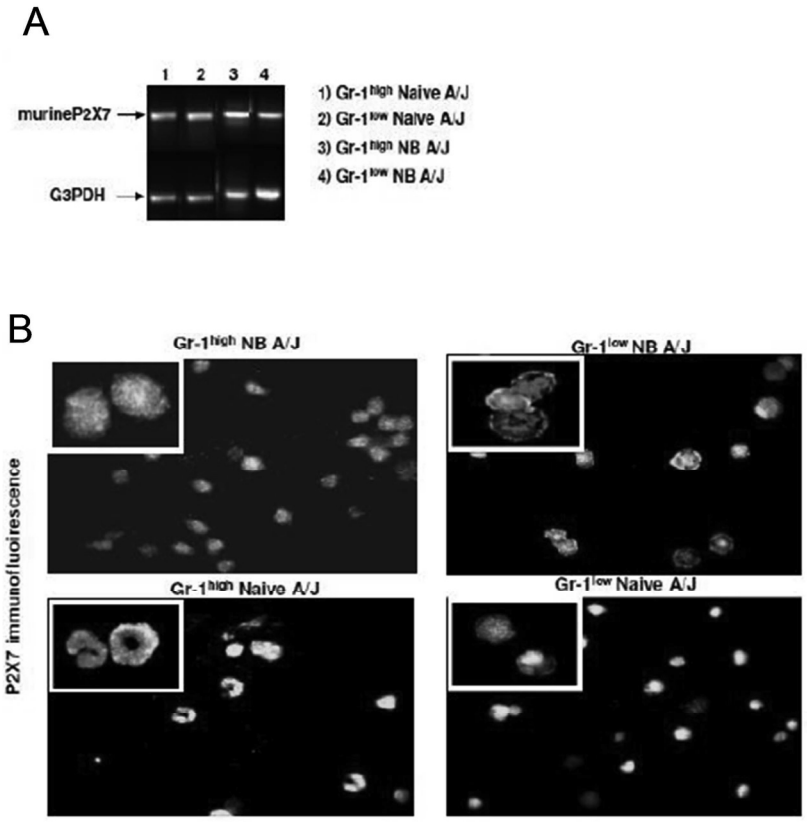

Figure 41. P2X7R expression in M-MDSCs and G-MDSCs in neuroblastoma bearing mice.

Panel A shows the expression of murine P2X7 mRNA in M-MDSCs and G-MDSCs. RT-PCR was performed as described in Materials and Methods. GA3PDH amplification was used as positive control. Panel B shows P2X7 expression and localization in M-MDSCs and G-MDSCs by fluorescence microscopy. Original magnification 40X, inset panels 100X.

P2X7 receptor is more functional in M-MDSCs

One of the earliest changes occurring after P2X7R activation is the collapse of plasma membrane potential due to Na+ influx. As shown in Figure 42 A and B, the stimulation with BzATP caused a large plasma membrane depolarization in both MDSC subsets. Interestingly, P2X7R-dependent plasma membrane depolarization was larger in NB M-MDSCs than in Naïve M-MDSCs or G-MDSCs, whether from NB or naïve mice (Panel B). Changes in fluorescence were fully abrogated by the P2X7R blocker oATP (Panels A and B). Figure 42 C shows plasma membrane potential collapse of HEK293-P2X7 or HEH293-mock, used as positive and negative control, respectively.

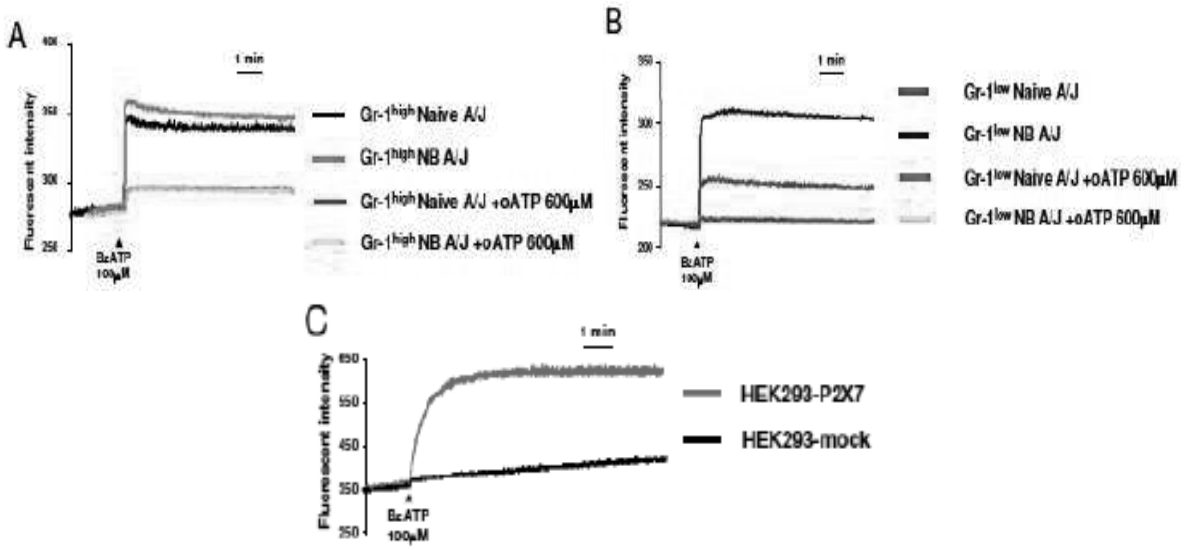

Figure 42. P2X7R-associated plasma membrane permeability changes in M-MDSCs and G-MDSCs from neuroblastoma bearing mice.

Panels A-C show BzATP-mediated induction of plasma membrane depolarization in Ca^{2+}-containing medium. Changes in plasma membrane potential were measured with bisoxonol as described in Materials and Methods.

Panel A shows the tracers of Naïve G-MDSCs (black trace), NB G-MDSCs (orange trace), naïve G-MDSCs (red trace) and NB G-MDSCs (cyan trace) pre-treated with oxo-ATP.

Panel B shows the traces of Naïve M-MDSCs (green trace), NB M-MDSCs (blue trace), Naïve M-MDSCs (red trace) and NB M-MDSCs (cyan trace) pre-treated with oxo-ATP.

Panel C shows the traces of HEK293-P2X7 (red trace) and HEK293-Mock (black trace) cells used as positive and negative control respectively.

Functional characterization of Granulocytic and Monocytic Myeloid Derived Suppressor Cells subsets from neuroblastoma-bearing mice

Naïve and NB G-MDSCs and M-MDSCs subsets were then tested for ARG-1 expression, ROS and TGF-β1 secretion. Figure 43 A shows that NB M-MDSCs expressed significantly higher levels of ARG-1 in comparison to naïve M-MDSCs (P=0.0001). In contrast, no ARG-1 expression was detected in naïve and NB G-MDSCs. Figure 43 B shows that NB M-MDSCs and NB G-MDSCs had an enhanced ability to release ROS compared to naïve MDSCs. Furthermore in NB M-MDSCs produced a strikingly higher amount of ROS compared to NB G-MDSCs. As shown in Figure 43 C, no significant difference in TGF-β1 secretion was detected in NB and Naïve MDSCs, but in both animal models M-MDSCs secreted significantly higher amounts of TGF-β in comparison to G-MDSCs

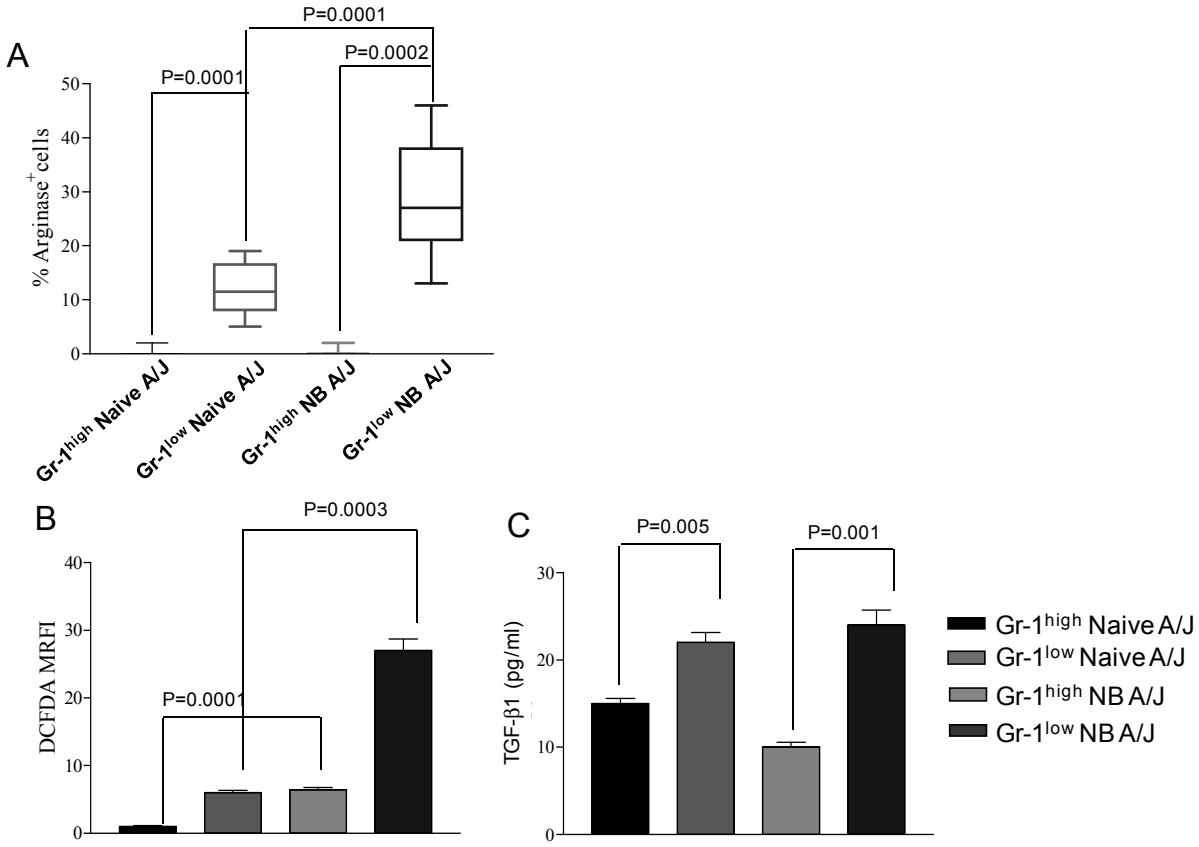

Figure 43. Mechanisms of suppressive activity of M-MDSCs and G-MDSCs in neuroblastoma bearing mice.

Panel A shows the percentage of ARG-1+ M-MDSCs and G-MDSCs. Data are expressed as mean value of ARG-1+ cells counted in 10 fields/slide. P values were calculated using Unpaired t test with Welch's correction.

Panel B shows the level of reactive oxygen species (ROS) of M-MDSCs and G-MDSCs labelled with the oxidation-sensitive dye Dichlorodihydrofluorescein diacetate (DCFDA) as described in Materials & Methods. Results are expressed as the mean fluorescent intensity ± SD from three different experiments performed.

Panel C shows the level of TGF-β1 produced by M-MDSCs and G-MDSCs as assessed by ELISA. Conditioned media from triplicate cultures were tested in duplicate. Data are expressed as mean value ± SD. P value was calculated using Unpaired t test with Welch's correction.

M-MDSCs are more tumorigenic than G-MDSCs

In some experiments, we also tested whether NB M-MDSCs and NB G-MDSCs promoted in vivo tumor progression. As shown in Figure 44 A the size of tumors generated by co-inoculation of NB NXS2-LUC and NB M-MDSCs was significantly higher compared to tumors developed by co-injection of NB cells and NB G-MDSCs. Figure 44 B represents the size of tumors measured as BLI.

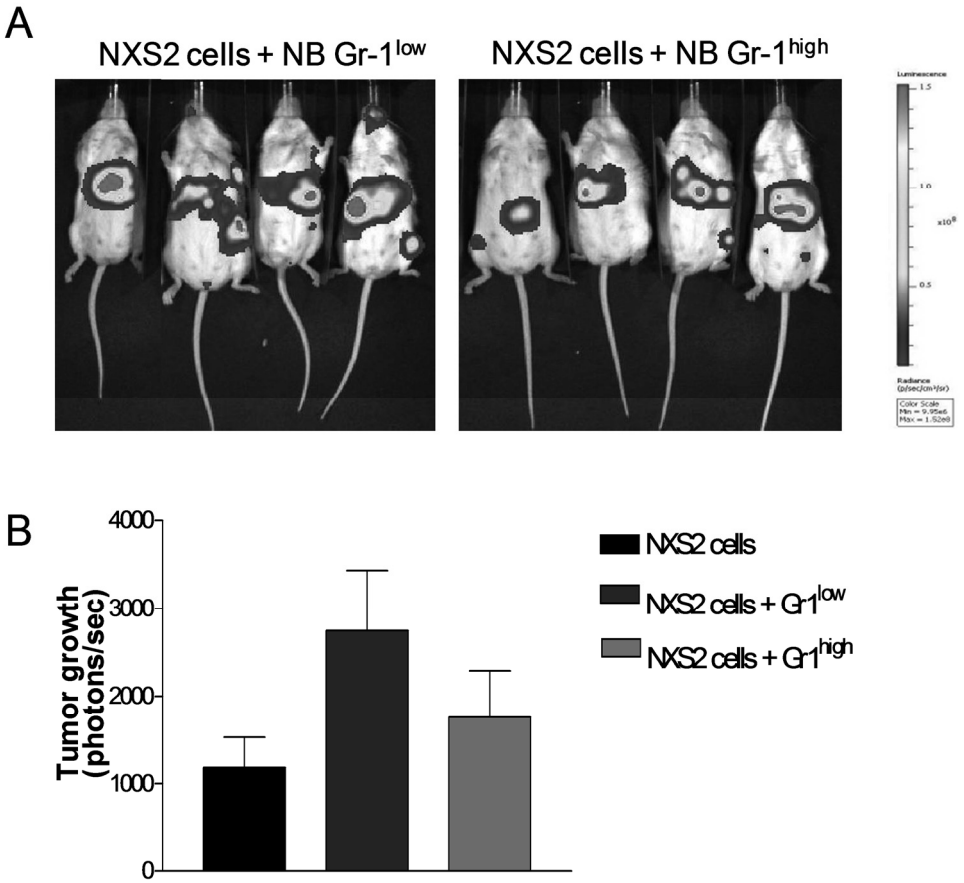

Figure 44. Tumors size detected with BLI.

Panel A shows four representative animals i.v. inoculated with NXS2 transfected with luciferase (NXS2-Luc) in combination with Gr-1high or Gr-1low MDSCs (1:1; $2x10^5$ cells/mouse) and imaged by bioluminescence 26 days after tumor cell inoculum. Tumor volume is expressed as mean luminescence value ± SD. P value was calculated using Unpaired t test with Welch's correction (Panel B).

DISCUSSION

The tumor induced-tolerance is a well established phenomenon that promotes tumor growth and expansion, resulting in the inability of the host immune system to effectively destroy the malignancy.

Although in the last years many attempts to potentiate the immune response (immunotherapy) have been performed, most of them have not been effective.

The first goal to shed light on this observation was the identification in 2007 of a new cell population, defined Myeloid Derived Suppressor Cells (MDSCs) [13], that accumulates in cancer and during bacterial or parasitic infections. Considered a major contributor to the failure of immunotherapies, MDSCs induce a potent suppression of tumor immunity (innate and adaptative).

The accumulation and activation of these cells are driven by multiple factors secreted by the tumor, many of which detectable even during chronic inflammation. Several laboratories are now working to understand the exact mechanism of MDSCs immunosuppressive activity, groups have found that ROS [153] and Arg-1 [154] are involved but many other factors may probably play a role.

Extracellular ATP is generally considered the prototypical danger signal, as it accumulates at inflammatory sites and within the tumor milieu at concentrations that may reach the hundred micromolar range. On the contrary, the nucleotide is almost undetectable in the interstitium of healthy tissues [155]. ATP is released into the tumor microenvironment by cancer cells and infiltrating inflammatory cells through different mechanisms including granule exocytosis, plasma membrane channels or lysis [22].

Moreover the nucleotide can be hydrolyzed in adenosine by CD39/(ENTPD1) and CD73/ecto-5'-nucleotidase, expressed in many different cell types included Tregs. In these cells the adenosine produced by CD39/73-mediated cleavage of ATP, acts on T effector cells resulting in cell cycle arrest [119]. Furthermore a recent work has shown the expression of functional CD73 in MDSCs, suggesting the involvement of the adenosine in their immunosuppressive activity [148].

Purinergic receptors (P2) are membrane receptors activated by extracellular ATP. Involved in many cellular functions such as vascular reactivity, apoptosis and

cytokine secretion, P2 receptors have been divided into two subclasses: P2X and P2Y [121].

P2Y are metabotropic receptors coupled to G proteins. Expressed in endothelial cells, dendritic cells, muscle, as well as neurons, monocytes, macrophages and B lymphocytes these receptors are activated by low concentrations of ATP.

P2X receptors are ligand-gated ion channels whose activation leads the passage of ions through plasma membrane. Under physiological conditions P2X receptors activation results in Na^+ and Ca^{2+} influx and K^+ efflux across the cell membrane.

In this subfamily is included P2X7 receptor, widely express in the body such as in immune cells [128], neurons and microglia [130]. Like all the P2XRs subfamily, under physiological stimulation P2X7R generates the selective channel for cations. On the contrary a sustained activation promotes the characteristic channel-to-pore transition leading the formation of a non-selective pore permeable to aqueous solutes of MW up to 900 Da. Furthermore P2X7R doesn't undergo desensitization, therefore the pore remains open until the agonist is present in the extracellular environment, to close after the removal of the same. This latter event triggers cell death, via apoptosis or necrosis depending on the cell type and the given experimental conditions. Caspase and metalloproteinase activation are involved in this process [146] [132] [156].

P2X7R is over-expressed in several human malignancies including chronic B lymphocytic leukemia and NB, a pediatric tumor with grim prognosis in its metastatic presentation at diagnosis [133] [134] [157].

Based on all these observations I wondered if MDSCs expressed P2 receptors and what was the role of extracellular ATP and adenosine in the immunosuppressive activity.

In two MDSCs cell lines, MSC-1 and MSC-2 [151] I have verified the mRNA expression of P2X3, P2X4, P2X5, P2X7, P2Y6, P2Y12 and P2Y13 receptors.

In both cell lines is detectable the protein of P2X3R, P2X5R and P2X7R, that is highly expressed in MSC-2.

The stimulation with ATP and BzATP induces a large $[Ca^{2+}]_i$ response and the rise is over 10 times larger in MSC-2 than in MSC-1line. The $[Ca^{2+}]_i$ increase is mainly due to the influx of the ion from the extracellular space, as it is almost entirely abrogated by chelation of extracellular Ca2+. In MSC-1 the BzATP dose-dependency curve is biphasic, witnessing the activation of at least two P2 receptor subtypes: one with

higher affinity responsible for the $[Ca^{2+}]_i$ increase at low agonist concentrations, and another with lower affinity, probably P2Y receptors. In line with this hypothesis I have verified that the stimulation with UTP triggers a transient calcium response in both cell lines.

P2X7R is fully functional as the stimulation with BzATP causes a massive uptake of EtBr and Lucifer yellow. It is worth of notice that also in this case MSC-2 line presents a larger response than MSC-1.

Further evidence of the P2X7R functionality is the plasma membrane depolarization triggered by the stimulation of MSC-2 with ATP and BzATP.

MDSCs accumulate in tumor microenvironment where they are likely exposed to high concentration of ATP. Quite interestingly I observed that although the P2X7R activation triggers swelling and blebbing, the phenomenon is uncoupled from cytotoxicity (modest amount of LDH release is detectable). This could explain how MDSCs can survive also in highly inflammatory environments.

I have also verified that in basal conditions both cell lines release ATP in the extracellular space and the amount of nucleotide detectable is particularly elevated in MSC-2.

As regard the immunosuppressive activity I have observed that the stimulation of P2X7R triggers the release of IL-1β, ROS and TGFβ and increases the expression of ARG-1.

In the second part of the work I focused my attention on BM-MDSCs in witch I verified the protein expression of P2X3R, P2X5R, P2Y6R and P2X7R. As further evidence that P2X7R is uncoupled from citotoxicity, I observed that the chronic exposition of cells to high ATP concentration, leads a decreased expression of the receptor.

Even BM-MDSCs release ATP in the extracellular space and P2X7R might play a role since the amount of nucleotide detected in wild type MDSCs is higher than in P2X7 KO cells.

It is stated that suppressor cells originate in bone marrow and migrate into the tumor site where exert their activity. In order to further explain this phenomenon I interestingly observed that nucleotides, in particular ATP and UTP, have chemotactic effect on BM-MDSCs.

In 2011 Ryzhov and colleague found the expression of functional CD73/ecto-5'-nucleotidase in MDSCs. They also hypothesizes the involvement of adenosine in the suppressive activity.

In line with their hypothesis I verified that BM-MDSCs express both CD73/ecto-5'-nucleotidase and CD39/(ENTPD1). Moreover I presented the first evidence that these cells can hydrolyze extracellular ADP in AMP, adenosine and quite surprisingly even an high amount of inosine is detectable. The role of inosine in inflammation is still controversial, but there are evidences that relate the molecule to immunosuppressive phenomena [150].

I furthermore observed that the stimulation of BM-MDSCs with ATP increases the protein expression of CD39 resulting an increased production of adenosine and inosine.

The main question that this work aimed to response was if ATP and adenosine would have played a role in the immunosuppressive activity of MDSCs.

At this regard I observed that the stimulation with 300 μM ATP or 300 μM adenosine increases the BM-MDSCs suppressive activity on the proliferation of $CD4^+$ and $CD8^+$ T effector cells.

Further evidences of the involvement of ATP and P2X7R in the functionality of MDSCs are the results obtained in collaboration with Istutito Giannina Gaslini (Genova) in a murine model of Neuroblastoma (NB).

A breakthrough in *in vivo* ATP studies has been the development of the pmeLUC probe that allows continuous monitoring of the extracellular ATP concentration in animal models for an extended length of time. Using this strategy, we have shown that levels of eATP increase with time in NXS2-pmeLUC NB tumors, thus paralleling tumor progression and metastasis dissemination. In agreement with a recent study showing the presence of $CD11b^+Gr\text{-}1^+$ MDSCs in the spleen, PB and BM of Neuro-2a NB bearing mice [160], we found that $CD11b^+Gr\text{-}1^+$ cells are enriched in the spleen and PB of NXS2 NB-bearing mice compared to naïve animals. Furthermore, NB M-MDSCs expressed higher levels of ARG-1, and produced higher amounts of ROS and TGF-β1 in comparison to NB G-MDSCs. In addition we observed that the size of tumors generated by co-inoculation of NB cells and M-MDSCs was higher compared to that of control tumors (only NB cells) and tumors developed by co-injection of NB cells and G-MDSCs. Furthermore we found that although P2X7R was expressed to about the same level by M-MDCS and G-MDSC subsets isolated from the spleen of

NB bearing mice or naive animals, quite interestingly the subcellular location was different. In M-MDSCs from NB-bearing mice P2X7R was clearly expressed on the plasma membrane, while in G-MDSCs from tumor-bearing mice and in G-MDSCs and M-MDSCs from naïve animals it was mainly localized in the cytosol or in the nucleus. This sub-cellular location, in agreement with the results obtained with the *in vitro* stimulation, suggests that P2X7R may be more functional in NB MDSCs compared to the other Gr-1 subsets. Our study provides the first evidence that ATP modulates MDSCs responses via a P2X7R dependent mechanism.

Based upon all the results, we propose a *scenario* whereby the extracellular ATP plays an important role in accumulation and functions of MDSCs.
Suppressor cells express functional P2 receptors and both ecto-enzymes CD39/ CD73. The stimulation of P2X7R triggers release of immunosuppressive cytokines and quite interestingly is uncoupled from citotoxicity. Moreover this thesis presents the first evidence that in MDSCs the adenosine produced by CD39/73-mediated cleavage of ATP, acts on T effector cells resulting in cell cycle arrest.

REFERENCES

1. Coley W. (1894) Treatment of inoperable malignant tumors with the toxines of erysipelas and the bacillus prodigiosus. Trans Am Surg Assoc 12:183–212
2. Burnet M. (1964) Immunological Factors in the Process of Carcinogenesis. Br Med Bull 20:154-8
3. Ravetch J.V. (2000) Lanier LL. Immune inhibitory receptors. Science 290:84–89
4. Gabrilovich D. (2004) Mechanisms and functional significance of tumour-induced dendritic cell defects Nat Rev Immunol 12: 941-52
5. Kusmartsev S., Gabrilovich D. (2006) Effect of tumor-derived cytokines and growth factors on differentiation and immune suppressive features of myeloid cells in cancer. Cancer Metastasis Rev 25:323–331
6. Nishikawa H., Sakaguchi S. (2010) Regulatory T cells in tumor immunity. Int J Cancer 127:759–767
7. Deaglio S., Dwyer K.M., Gao W., Friedman D., Usheva A., Erat A., Chen J.F., Enjyoji K., Linden J., Oukka M., Kuchroo V.K., Strom T.B. and Robson S.C. (2007) Adenosine generation catalyzed by CD39 and CD73 expressed on regulatory T cells mediates immune suppression. J Exp Med 204: 1257-1265
8. Fridlender Z.G., Sun J., Kim S. et al. (2009) Polarization of tumor associated neutrophil phenotype by TGF-beta: “N1” versus “N2” TAN. Cancer Cell 16:183–194
9. Shurin M.R., Naiditch H., Zhong H., Shurin G.V. (2011) Regulatory dendritic cells: new targets for cancer immunotherapy. CancerBiol Ther 11:988–992
10. Gabrilovich D.I., Ostrand-Rosenberg S., Bronte V. (2012) Coordinated regulation of myeloid cells by tumours. Nat Rev Immunol 12:253–268
11. Ostrand-Rosenberg S. (2010) Myeloid-derived suppressor cells: more mechanisms for inhibiting antitumor immunity. Cancer Immunol Immunother 59:1593–1600
12. Young P.P., Ardestani S., Li B. (2010) Myeloid cells in cancer progression: unique subtypes and their roles in tumor growth, vascularity, and host immune suppression. Cancer Microenviron 4:1–11

13. Gabrilovich D., Bronte V., Chen S.H., Colombo M.P., Ochoa A., Ostrand-Rosenberg S., Schreiber H. (2007) The terminology issue for myeloid-derived suppressor cells. Cancer Res 67:425
14. Gabrilovich, D., Velders M. P., et al. (2001) Mechanism of immune dysfunction in cancer mediated by immature gr-1(+) myeloid cells. J Immunol 9: 5398-406
15. Strober S. (1998) Natural suppressor (NS) cells, neonatal tolerance, and total lymphoid irradiation: exploring obscure relationships. Annu Rev Immunol 2:219–237
16. Gabrilovich D., Nagaraj S. (2009) Myeloid-derived suppressor cells as regulators of the immune system. Nat Rev Immunol 9:162–174
17. Movahedi K., Guilliams M., Van den Bossche J., Van den Bergh R., Gysemans C., Beschin A., De Baetselier P., Van Ginderachter J.A. (2008) Identification of discrete tumor-induced myeloid-derived suppressor cell subpopulations with distinct T cell-suppressive activity. Blood 111:4233–4244
18. Zhou Z., French D.L., Ma G., Eisenstein S., Chen Y., Divino C.M., Keller G., Chen S.H., Pan P.Y. (2010) Development and function of myeloid-derived suppressor cells generated from mouse embryonic and hematopoietic stem cells. Stem Cells 28:620–632
19. Marigo I., Dolcetti L., Serafini P. et al. (2008) Tumor-induced tolerance and immune suppression by myeloid derived suppressor cells. Immunol Rev 222:162–179
20. Montero A.J., Diaz-Montero C.M., Kyriakopoulos C.E. et al. (2012) Myeloid-derived suppressor cells in cancer patients: a clinical perspective. J Immunother 35:107–115
21. Filipazzi P., Huber V., Rivoltini L. (2012) Phenotype, function and clinical implications of myeloid-derived suppressor cells in cancer patients. Cancer Immunol Immunother 61:255–263
22. Di Virgilio F. (2012) Purines, purinergic receptors, and cancer. Cancer Res 72:5441-7
23. Sevko A., Sade-Feldman M., Kanterman J. et al. (2012) Cyclophosphamide promotes chronic inflammation-dependent immunosuppression and prevents anti-tumor response in melanoma. J Invest Dermatol 67:10019–10026
24. Meyer C., Sevko A., Ramacher M. et al. (2011) Chronic inflammation promotes myeloid-derived suppressor cell activation blocking antitumor

immunity in transgenic mouse melanoma model. Proc Natl Acad Sci U S A 108:17111–17116

25. Bunt S.K., Yang L., Sinha P. et al. (2007) Reduced inflammation in the tumor microenvironment delays the accumulation of myeloid derived suppressor cells and limits tumor progression. Cancer Res 67:10019–10026
26. Haverkamp J.M., Crist S.A., Elzey B.D. et al. (2011) In vivo suppressive function of myeloid-derived suppressor cells is limited to the inflammatory site. Eur J Immunol 41:749–759
27. Barreda D.R., Hanington P.C., Belosevic M. (2004) Regulation of myeloid development and function by colony stimulating factors. Dev Comp Immunol 28:509–554
28. Maione P., Rossi A., Di Maio M. et al. (2009) Tumor-related leucocytosis and chemotherapy-induced neutropenia: linked or independent prognostic factors for advanced non-small cell lung cancer? Lung Cancer 66:8–14
29. Revoltella R.P., Menicagli M., Campani D. (2012) Granulocyte-macrophage colony-stimulating factor as an autocrine survival growth factor in human gliomas. Cytokine 57:347–359
30. [[L., Peranzoni E., Ugel S. et al. (2010) Hierarchy of immunosoppressive strength among myeloid-derived suppressor cell subsets is determined by GM-CSF. Eur J Immunol 40:22–35
31. Lechner M.G., Liebertz D.J., Epstein A.L. (2010) Characterization of cytokine-induced myeloid-derived suppressor cells from normal human peripheral blood mononuclear cells. J Immunol 185:2273–2284
32. Kujawski M., Kortylewski M., Lee H., Herrmann A., Kay H., Yu H. (2008) Stat3 mediates myeloid celldependent tumor angiogenesis in mice. J Clin Invest 118:3367–3377
33. Shojaei F., Wu X., Qu X., Kowanetz M., Yu L., Tan M., Meng Y.G., Ferrara N. (2009) G-CSF-initiated myeloid cell mobilization and angiogenesis mediate tumor refractoriness to anti-VEGF therapy in mouse models. Proc Natl Acad Sci U S A 106:6742–6747
34. Sica A., Bronte V. (2007) Altered macrophage differentiation and immune dysfunction in tumor development. J Clin Invest 117:1155–1166
35. Corzo C.A., Condamine T., Lu L., Cotter M.J., Youn J.I., Cheng P., Cho H.I., Celis E., Quiceno D.G., Padhya T., McCaffrey T.V., McCaffrey J.C.,

Gabrilovich D. (2010) HIF-1alpha regulates function and differentiation of myeloid-derived suppressor cells in the tumor microenvironment. J Exp Med 207:2439–2453

36. Li H., Han Y., Guo Q., Zhang M., Cao X. (2009) Cancer-expanded myeloid-derived suppressor cells induce anergy of NK cells through membrane-bound TGF-beta 1. J Immunol 182:240–249
37. Liu C., Yu S., Kappes J., Wang J., Grizzle W.E., Zinn K.R., Zhang H.G. (2007) Expansion of spleen Myeloid- Derived Suppressor Cells represses NK cell cytotoxi-city in tumor-bearing host. Blood 109:4336–4342
38. Sinha P., Clements V.K., Bunt S.K., Albelda S.M., Ostrand-Rosenberg S. (2007) Cross-talk between myeloid derived suppressor cells and macrophages subverts tumor immunity toward a type 2 response. J Immunol 179:977–983
39. Rodríguez P.C., Ochoa A.C. (2006) T cell dysfunction in cancer: role of myeloid cells and tumor cells regulating amino acid availability and oxidative stress. Semin Cancer Biol 16:66–72
40. Bronte V., Zanovello P. (2005) Regulation of immune responses by L-arginine metabolism. Nat Rev Immunol 5:641–654
41. Rodríguez P.C., Zea A.H., Culotta K.S. et al. (2002) Regulation of T cell receptor CD3zeta chain expression by L-arginine. J Biol Chem 277:21123–21129
42. Whiteside T.L. (2004) Down-regulation of zeta-chain expression in T cells: a biomarker of prognosis in cancer? Cancer Immunol Immunother 53:865–878
43. Boniface J.D., Poschke I., Mao Y. et al. (2011) Tumor-dependent down-regulation of the ζ-chain in T-cells is detectable in early breast cancer and correlates with immune cell function. Int J Cancer 131:129–139
44. Ezernitchi A.V., Vaknin I., Cohen-Daniel L. et al. (2006) TCR zeta down-regulation under chronic inflammation is mediated by myeloid suppressor cells differentially distributed between various lymphatic organs. J Immunol 177:4763–4772
45. Baniyash M. (2004) TCR zeta-chain downregulation: curtailing an excessive inflammatory immune response. Nat Rev Immunol 4:675–687
46. Bronte V., Serafini P., Mazzoni A., Segal D.M., Zanovello P. (2003) L-arginine metabolism in myeloid cells controls T-lymphocyte functions. Trends Immunol 24:302–306

47. Rodriguez P.C. et al. (2005) Arginase I in myeloid suppressor cells is induced by COX-2 in lung carcinoma. J Exp Med 202:931–939
48. Cederbaum S.D., Yu H., Grody W.W., Kern R.M., Yoo P., Iyer R.K. (2004) Arginases I and II: do their functions overlap? Mol Genet Meta 81:S38–44.
49. Srivastava M.K., Sinha P., Clements V.K., Rodriguez P., Ostrand-Rosenberg S. (2010) Myeloid-derived suppressor cells inhibit T-cell activation by depleting cystine and cysteine. Cancer Res 70:68–77
50. Boulland M. L., J. Marquet, et al. (2007) Human IL4I1 is a secreted L-phenylalanine oxidase expressed by mature dendritic cells that inhibits T-lymphocyte proliferation. Blood 1: 220-7
51. Taylor M.W., Feng G.S.(1991) Relationship between interferon-gamma, indoleamine 2,3-dioxygenase, and tryptophan catabolism. FASEB J 5:2516–2522
52. Uyttenhove C., Pilotte L., Theate I., Stroobant V., Colau D., Parmentier N., Boon T., Van den Eynde B.J. (2003) Evidence for a tumoral immune resistance mechanism based on tryptophan degradation by indoleamine 2,3-dioxygenase. Nat Med 9:1269–1274
53. Hwu P., Du M.X., Lapointe R., Do M., Taylor M.W., Young H.A. (2000) Indoleamine 2,3-dioxygenase production by human dendritic cells results in the inhibition of T cell proliferation. J Immunol 164:3596–3599
54. Munn D.H., Shafizadeh E., Attwood J.T., Bondarev I., Pashine A., Mellor A.L. (1999) Inhibition of T cell proliferation by macrophage tryptophan catabolism. J Exp Med 189:1363–1372
55. Lob S., Konigsrainer A., Rammensee H.G., Opelz G., Terness P. (2009) Inhibitors of indoleamine-2,3- dioxygenase for cancer therapy: can we see the wood for the trees? Nat Rev Cancer 9:445–452
56. Mansoor M.A., Svardal A.M., Ueland P.M. (1992) Determination of the in vivo redox status of cysteine, cysteinylglycine, homocysteine, and glutathione in human plasma. Anal Biochem 200:218–229
57. Gout P.W., Buckley A.R., Simms C.R., Bruchovsky N. (2001) Sulfasalazine, a potent suppressor of lymphoma growth by inhibition of the x(c)- cystine transporter: a new action for an old drug. Leukemia 15:1633–1640

58. Gmunder H., Eck H.P., Benninghoff B., Roth S., Droge W. (1990) Macrophages regulate intracellular glutathione levels of lymphocytes. Evidence for an immunoregulatory role of cysteine. Cell Immunol 129:32–46
59. Gmunder H., Eck H.P., Droge W. (1991) Low membrane transport activity for cystine in resting and mitogenically stimulated human lymphocyte preparations and human T cell clones. Eur J Biochem 201:113–117
60. Iwata S., Hori T., Sato N., Ueda-Taniguchi Y., Yamabe T., Nakamura H., Masutani H., Yodoi J. (1994) Thiolmediated redox regulation of lymphocyte proliferation. Possible involvement of adult T cell leukemia-derived factor and glutathione in transferrin receptor expression. J Immunol 152:5633–5642
61. Szuster-Ciesielska A., Hryciuk-Umer E., Stepulak A., Kupisz K., Kandefer-Szerszen M. (2004) Reactive oxygen species production by blood neutrophils of patients with laryngeal carcinoma and antioxidative enzyme activity in their blood. Acta Oncol 43:252–8
62. Sauer H., Wartenberg M., Hescheler J. (2001) Reactive oxygen species as intracellular messengers during cell growth and differentiation. Cell Physiol Biochem 11:173–86
63. Wu G., Morris S.M. Jr. (1998) Arginine metabolism: nitric oxide and beyond. Biochem J 336:1–17
64. Otsuji M., Kimura Y., Aoe T., Okamoto Y., Saito T. (1996) Oxidative stress by tumor-derived macrophages suppresses the expression of CD3 zeta chain of T-cell receptor complex and antigen-specific Tcell responses. Proc Natl Acad Sci USA 93:13119–24
65. Agostinelli E., Seiler N. (2006) Non-irradiation-derived reactive oxygen species (ROS) and cancer: therapeutic implications. Amino Acids 31:341–55
66. Kusmartsev S., Nagaraj S., Gabrilovich DI. (2005) Tumor-associated CD8+ T cell tolerance induced by bone marrow-derived immature myeloid cells. J Immunol 175:4583–92
67. Schmielau J., Finn O.J. (2001) Activated granulocytes and granulocyte-derived hydrogen peroxide are the underlying mechanism of suppression of T-cell function in advanced cancer patients. Cancer Res 61:4756–60
68. Nagaraj S., Gupta K., Pisarev V., Kinarsky L., Sherman S., Kang L., Herber D.L., Schneck J., Gabrilovich D. (2007) Altered recognition of antigen is a mechanism of CD8+ T cell tolerance in cancer. Nat Med 13:828–835

69. Nagaraj S., Schrum A.G., Cho H.I., Celis E., Gabrilovich D. (2010) Mechanism of T cell tolerance induced by myeloid-derived suppressor cells. J Immunol 184:3106–3116
70. Sakuishi K., Jayaraman P., Behar S.M., Anderson A.C., Kuchroo V.K. (2011) Emerging Tim-3 functions in antimicrobial and tumor immunity. Trends Immunol 32:345–9
71. Hanson E.M., Clements V.K., Sinha P., Ilkovitch D., Ostrand-Rosenberg S. (2009) Myeloid-derived suppressor cells down-regulate L-selectin expression on CD4+ and CD8+ T cells. J Immunol 183:937–44
72. Bunt S.K., Clements V.K., Hanson E.M., Sinha P., Ostrand-Rosenberg S. (2009) Inflammation enhances myeloid-derived suppressor cell cross-talk by signaling through Toll-like receptor 4. J Leukoc Biol 85:996–1004
73. Yang R., Cai Z., Zhang Y., Yutzy WHt., Roby K.F., Roden R.B. (2006) CD80 in immune suppression by mouse ovarian carcinoma-associated Gr-1+CD11b+ myeloid cells. Cancer Res 66:6807–15
74. Collins M., Ling V., Carreno B.M. (2005) The B7 family of immune-regulatory ligands. Genome Biol 6:223
75. Chen W., Jin W., Hardegen N., Lei K.J., Li L., Marinos N., McGrady G., Wahl S.M. (2003) Conversion of peripheral CD4+CD25– naive T cells to CD4+CD25+ regulatory T cells by TGF-b induction of transcription factor Foxp3. J Exp Med 198:1875–86
76. Ghiringhelli F., Puig P.E., Roux S. et al. (2005) Tumor cells convert immature myeloid dendritic cells into TGF-b-secreting cells inducing CD4+CD25+ regulatory T cell proliferation. J Exp Med 202:919–29
77. Huang B., Pan P.Y., Li Q., Sato A.I., Levy D.E., Bromberg J., et al. (2006) Gr-1+CD115+ immature myeloid suppressor cells mediate the development of tumor-induced T regulatory cells and T-cell anergy in tumor-bearing host. Cancer Res 66:1123–31
78. Serafini P., Mgebroff S., Noonan K., Borrello I. 2008, Myeloid-derived suppressor cells promote crosstolerance in B-cell lymphoma by expanding regulatory T cells. Cancer Res 68:5439–49
79. Gabrilovich D.I., Velders M., Sotomayor E., Kast W.M. (2001) Mechanism of immune dysfunction in cancer mediated by immature Gr-1+ myeloid cells. J Immunol 166:5398–406

80. Kusmartsev S., Nagaraj S., Gabrilovich D. (2005) Tumor-associated CD8+ T cell tolerance induced by bone marrow-derived immature myeloid cells. J Immunol 175:4583–92
81. Kusmartsev S., Nefedova Y., Yoder D., Gabrilovich D. (2004) Antigen-specific inhibition of CD8+ T cell response by immature myeloid cells in cancer is mediated by reactive oxygen species. J Immunol 172:989–99
82. Movahedi K., et al. (2008) Identification of discrete tumor-induced myeloid-derived suppressor cell subpopulations with distinct T-cell suppressive activity. Blood 111:4233–4244
83. Nagaraj S, et al. (2007) Altered recognition of antigen is a novel mechanism of CD8+ T cell tolerance in cancer. Nat Med 13:828–835
84. Song X., et al. (2005) CD11b+/Gr-1+ immature myeloid cells mediate suppression of T cells in mice bearing tumors of IL-1beta-secreting cells. J Immunol 175:8200–8208
85. Waris G., Ahsan H. (2006) Reactive oxygen species: role in the development of cancer and various chronic conditions. J Carcinog 5:14
86. Kusmartsev S., Gabrilovich D. (2005) STAT1 signaling regulates tumor-associated macrophage-mediated T cell deletion. J Immunol 174:4880–4891
87. Mantovani A., Sozzani S., Locati M., Allavena P., Sica A. (2002) Macrophage polarization: tumor-associated macrophages as a paradigm for polarized M2 mononuclear phagocytes. Trends Immunol 23:549–555
88. Muller A.J., Prendergast G.C. (2007) Indoleamine 2,3-dioxygenase in immune suppression and cancer. Curr. Cancer. Drug Targets 7:31–40
89. Chalmin F., Ladoire S., Mignot G., Vincent J., Bruchard M., Remy-Martin J.P., et al. (2010) Membrane associated Hsp72 from tumor-derived exosomes mediates STAT3-dependent immunosoppressive function of mouse and human myeloid-derived suppressor cells. J Clin Invest 120:457–71
90. Sinha P., Clements V., Ostrand-Rosenberg S. (2005) Reduction of myeloid-derived suppressor cells and induction of M1 macrophages facilitate the rejection of established metastatic disease. J Immunol 174:636–45
91. Solito S., Bronte V., Mandruzzato S. (2010) Antigen specificity of immune suppression by myeloid-derived suppressor cells. J Leukoc Biol 184:3106–16

92. Nagaraj S., Nelson A., Youn J., Cheng P., Quiceno D., Gabrilovich D. (2012) Antigen-specific CD4+ T cells regulate function of myeloid-derived suppressor cells in cancer via retrograde MHC class II signaling. Cancer Res. 174:636–45
93. Nefedova Y., Huang M., Kusmartsev S., Bhattacharya R., Cheng P., Salup R., et al. (2004) Hyperactivation of STAT3 is involved in abnormal differentiation of dendritic cells in cancer. J Immunol 172:464–74
94. Kortylewski M., Kujawski M., Wang T., Wei S., Zhang S., Pilon-Thomas S., et al. (2005) Inhibiting Stat3 signaling in the hematopoietic system elicits multicomponent antitumor immunity. Nat Med 11:1314–21
95. Chan L.L., Cheung B.K., Li J.C., Lau A.S. (2001) A role for STAT3 and cathepsin S in IL-10 down-regulation of IFN-gamma-induced MHC class II molecule on primary human blood macrophages. J Leukoc Biol 88:303–11
96. Poschke I., Mougiakakos D., Hansson J., Masucci G.V., Kiessling R. (2010) Immature immunosoppressive CD14+HLA-DR-/low cells in melanoma patients are Stat3 hi and overexpress CD80, CD83, and DC-sign. Cancer Res 70:4335–45
97. Solito S., Falisi E., Diaz-Montero C.M., Doni A., Pinton L., Rosato A., et al. (2011) A human promyelocyticlike population is responsible for the immune suppression mediated by myeloid-derived suppressor cells. Blood 175:4338–46
98. Xiang X., Poliakov A., Liu C., Liu Y., Deng Z.B., Wang J., et al. (2009) Induction of myeloid-derived suppressor cells by tumor exosomes. Int J Cancer 124:2621–33
99. Donkor M.K., Lahue E., Hoke T.A., Shafer L.R., Coskun U., Solheim J.C., et al. (2009) Mammary tumor heterogeneity in the expansion of myeloid-derived suppressor cells. Int Immunopharmacol 9:937–48
100. Harizi H., Juzan M., Pitard V., Moreau J., Gualde N. (2002) Cyclooxygenase-2-issued prostaglandin e(2) enhances the production of endogenous IL-10, which down-regulates dendritic cell functions. J Immunol 68:2255–63
101. Sinha P., Clements V.K., Fulton A.M., Ostrand-Rosenberg S. (2007) Prostaglandin E2 promotes tumor progression by inducing myeloid-derived suppressor cells. Cancer Res 67:4507–13
102. Lazarowski E.R., Boucher R.C. and Harden T.K. (2000) Constitutive release of ATP and evidence for major contribution of ecto-nucleotide pyrophosphatase

and nucleoside diphosphokinase to extracellular nucleotide concentrations. J Biol Chem 275: 31061-31068

103. Sosnovskii A.S., Kubatiev A. A. (1993) Platelet aggregation and ATP release from dense platelet granules in immobilized rats. Bull of Exp Biol and Med 116: 809-811
104. Bodin P., Bailey D. and Burnstock G. (1991) Increased flow-induced ATP release from isolated vascular endothelial cells but not smooth muscle cells. Br J Pharmacol 103: 1203-1205
105. Suadicani S.O., Brosnan C.F. and Scemes E. (2006) P2X7 receptors mediate ATP release and amplification of astrocytic intercellular Ca2+ signaling. J Neurosci 26: 1378-1385
106. Sabirov R.Z., Dutta A.K. and Okada Y. (2001) Volume dependent ATP-conductive large-conductance anion channel as a pathway for swelling-induced ATP release. J Gen Physiol 118: 251-266
107. Coco S., Calegari F., Pravettoni E., Pozzi D., Taverna E., Rosa P., Matteoli M. and Verderio C. (2003) Storage and release of ATP from astrocytes in culture. J Biol Chem 278: 1354-1362
108. Schenk U., Westendorf A.M., Radaelli E., Casati A., Ferro M., Fumagalli M., Verderio C., Buer J., Scanziani E. and Grassi F. (2008) Purinergic control of T cell activation by ATP released through pannexin-1 hemichannels. Sci Signal 1:6
109. Holton P., Hilton S.M. (1954) Antidromic vasodilatation and blood flow in the rabbit's ear. J Physiol 125:138-147
110. Di Virgilio F., Chiozzi P., Ferrari D., Falzoni S., Sanz J.M., Morelli A., Torboli M., Bolognesi G., Baricordi O.R. (2001) Nucleotide receptors: an emerging family of regulatory molecules in blood cells. Blood 97:587-600
111. Ferrari D., Chiozzi P., Falzoni S., Hanau S. and Di Virgilio F. (1997) Purinergic modulation of interleukin-1 beta release from microglial cells stimulated with bacterial endotoxin. J Exp Med 185: 579-582
112. Lazarowski E.R., Boucher R.C., Harden T.K. (2003) Mechanisms of release of nucleotides and integration of their action as P2X- and P2Y- receptor activating molecules. Mol Pharmacol 64:785-795

113. Satterwhite C.M., Farrelly A.M., Bradkey M.E. (1999) Chemotactic, mitogenic and angiogenic actions of UTP on vascular andothelial cells. J Physiol 276:1091-1097
114. Erlinge D. (2004) Extracellular ATP: a central plyer in the regulation of vascular smooth muscle phenotype. Focus on “Dual role of PKA in Phenotype modulation of vascular smooth muscle cells by extracellular ATP”. Am J Physiol Cell Physiol 287:260-262
115. Lemoli R.M., Ferrari D., Fogli M., Rossi L., Pizzirani C., Forchap S., Chiozzi P., Vaselli D., Bertolini F., Foutz T., Aluigi M., Baccarini M., Di Virgilio F. (2004) Extracellular nucleotides are potent stimulators of human hematopoietic stem cells in vitro and in vivo. Blood 104:1662-1670
116. Elliott M.R., Chekeni F.B., Trampont P.C., Lazarowski E.R., Kadl A., Walk S.F., Park D., Woodson R.I., Ostankovich M., Sharma P., Lysiak J.J., Harden T.K., Leitinger N. and Ravichandran K.S. (2009) Nucleotides released by apoptotic cells act as a findme signal to promote phagocytic clearance. Nature 461: 282-286
117. Rubartelli A. and Lotze M.T. (2007) Inside, outside, upside down: damage-associated molecular-pattern molecules (DAMPs) and redox. Trends Immunol 28: 429-436
118. Berchtold S., Ogilvie A.L., Bogdan C., Muhl-Zurbes P., Ogilvie A., Schuler G. and Steinkasserer A. (1999) Human monocyte derived dendritic cells express functional P2X and P2Y receptors as well as ecto-nucleotidases. FEBS Lett 458: 424-428
119. Deaglio S., Dwyer K.M., Gao W., Friedman D., Usheva A., Erat A., Chen J.F., Enjyoji K., Linden J., Oukka M., Kuchroo V.K., Strom T.B. and Robson S.C. (2007) Adenosine generation catalyzed by CD39 and CD73 expressed on regulatory T cells mediates immune suppression. J Exp Med 204: 1257-1265
120. Ralevic V. and Burnstock G. (1998) Receptors for purines and pyrimidines. Pharmacol Rev 50:413-492
121. Abbracchio M.P. and Burnstock G. (1994) Purinoceptors: are there families of P2X and P2Y purinoceptors? Pharmacol Ther 64: 445-475
122. Abbracchio M.P., Burnstock G., Boeynaems J.M., Barnard E.A., Boyer J.L., Kennedy C., Knight G.E., Fumagalli M., Gachet C., Jacobson K.A. and Weisman G.A. (2006) International Union of Pharmacology LVIII: update on

the P2Y G protein-coupled nucleotide receptors: from molecular mechanisms and pathophysiology to therapy. Pharmacol Rev 58: 281-341

123. Newbolt A., Stoop R., Virginio C., Suprenant A., North R.A., Buell G., Rassendren F. (1998) Membrane topology of an ATP-gated ion channel (P2X receptor). J Biol Chem 273:15177-15182
124. Torres G.E., Egan T.M., Voigot M.M. (1998) Hetero-oligometric assembly of P2X receptor subunits. Specificities exisit with regard to possible partners. J Biol Chem 274:6653-6659
125. Eickorst A.N., Berson A., Cockayne D., Lester H.A., Khakh B.S. (2002) Control of P2X(2) channel permeability by the cytosolic domain. J Gen Physiol 120:119-131
126. North R.A. (2002) Molecular Physiology of P2X receptors. Physiol Rev 82:1013-1067
127. Wiley J.S., Gargett C.E., Zhang W., Snook M.B., Jamieson G.P. (1998,) Partial agonists and antagonists reveal a second permeability state of human lymphocyte P2Z/P2X7 channel. Am J Phisiol 275:1224-31
128. Mutini C., Falzoni S., Ferrari D., Chiozzi P., Morelli A., Baricordi O.R., Collo G., Ricciardi-Castagnoli P., Di Virgilio F. (1999) Mouse dendritic cells express the P2X7 receptor: characterization and possible participation in antigen presentation. J Immunol 163:1958-1965
129. Falzoni S., Munerati M., Ferrari D., Spisani S., Moretti S., Di Virgilio F. (1995) The P2X receptor of human macrophage cells. J Clin Invest 95:1207-1216
130. Ferrari D., Villalba M., Chiozzi P., Falzoni S., Ricciardi-Castagnoli P., Di Virgilio F. (1996) Mouse microglial cells express a plasma membrane pore gated by extracellular ATP. J Immunol 156:1531-1539
131. Dubyak G.R., Clifford E.E., Humphreys B.D., Kertesy S.B., Martin K.A. (1996) Expression of multiple ATP receptor subtypes during the differentiation and inflammatory activation of myeloid leukocytes. Drug Dev Res 39:269-278
132. Ferrari D., Los M., Bauer M.K., Vandenabele P., Wesselborg S., Schulze-Osthoff K. (1999) P2X purinoreceptor ligation induces activation of caspases with distinct roles in apoptotic and necrotic alterations of cell death. FEBS 447:71-75
133. Adinolfi E., Melchiorri L., Falzoni S., Chiozzi P., Morelli A., Tieghi A., Cuneo A., Castoldi G., Di Virgilio F., Baricordi O.R. (2002) P2X7 receptor expression in

evolutive and indolent forms of chronic B lymphocytic leukemia. Blood 99:706-8

134. Raffaghello L., Chiozzi P., Falzoni S., Di Virgilio F., Pistoia V. (2006) The P2X7 Receptor Sustains the Growth of Human Neuroblastoma Cells through a Substance P-Dependent Mechanism. Cancer Res 66:907-14
135. Baricordi O.R., Melchiorri L., Adinolfi E., Falzoni S., Chiozzi P., Buell G., Di Virgilio F. (1999) Increased proliferation rate of lymphoid cells transfected with the P2X7 ATP receptor. J Biol Chem 274: 33206-8
136. Wilhelm K., Ganesan J., Muller T., Dürr C., Grimm M., Beilhack A., Krempl C.D., Sorichter S., Gerlach U.V., Jüttner E., Zerweck A., Gärtner F., Pellegatti P., Di Virgilio F., Ferrari D., Kambham N., Fisch P., Finke J., Idzko M., Zeiser R. (2010) Graft-versus-host disease is enhanced by extracellular ATP activating P2X7R. Nat Med 16:1434-8
137. Suprenant A., Rassendren F., Kawashima E., North R.A., Buell G.N. (1996) The cytolitic P2X receptor for extracellular ATP identified as P2X receptor. Science 272:735-738
138. Wiley J.S., Chen R., Jamieson G.P. (1993) The ATP4- receptor-operated channel (P2X class) of human lymphocytes allows Ba2+ and ethidium+ uptake:inhibition of fluxes by suramin. Ach Biochem. Biophysl 305:54-60
139. Kim M., Spelta V., Sim J., North R.A., Suprenant A. (2001) Differential assembly of rat purinergic P2X7 receptor in immune cells of the brain and periphery. J Biol Chem 276:23262-23267
140. Adinolfi E., Kim M., Young M.T., Di Virgilio F. (2003) Tyrosine phosphorilation of Hsp90 within the P2X7 receptor complex negatively regulates P2X7 receptors. J Biol Chem 278:37344-3735
141. Smart M.L., Gu B., Panchal R.O., Wiley J., Cromer B., Williams D.A., Petrou S. (2003) P2X7 receptor cell surface expression and cytolitic pore formation are regulated by a distal C-terminal region. J Biol Chem 278:8853-8860
142. Gu B.J., Zhang W., Worthington R.A., Sluyter R., Dao-Ung P., Petru S., Barden J.A., Wiley J.S. (2001) A Glu-496 to Ala polymorphism leads of fully functional loss of function of the human P2X7 receptor. J Biol Chem 276:11135-11142
143. Wiley J.S., Dao-Ung L.P., Li C., Shemon A.N., Gu B.J., Smart M.L., Fuller SJ., Barden J.A., Petrou S., Sluyter R. (2003) An Ile-568 to Asn polymorphysm

prevents normal trafficking and function of the human P2X7 receptor. J Biol Chem 278:17108-17113

144. Cabrini G., Falzoni S., Forchap S., Pellegatti P., Balboni A., Agostini P., Cuneo A., Castaldi G., Baricordi O.R., Di Virgilio F. (2005) A His-155 to Tyr polymorphism confers gain-of-function to the human P2X7 receptor of human leukemic lymphocytes. J Immunol 175:82-9115

145. Greenberg S., Di Virgilio F., Steinberg T. H. and Silverstein, S. C. (1988) Extracellular nucleotides mediate Ca2+ fluxes in J774 macrophages by two distinct mechanisms. J Biol Chem 263:0337-10343.

146. Di Virgilio F. (1995) The P2Z purinoceptor: an intriguing role in immunity, inflammation and cell death. Immunol Today 16:524-528

147. Raffaghello L., Chiozzi P., Falzoni S., Di Virgilio F. and Pistoia V. (2006) The P2X7 receptor sustains the growth of human neuroblastoma cells through a substance P-dependent mechanism. Cancer Res 66:907-914

148. Ryzhov S., Novitskiy S. V., Goldstein A. E., Biktasova A., Blackburn M. R., Biaggioni I., Dikov M. M. and Feoktistov I. (2011) Adenosinergic regulation of the expansion and immunosuppressive activity of CD11b+Gr1+ cells. J Immunol 187:6120-6129

149. Marigo I., Bosio E., Solito S., Mesa C., Fernandez A., Dolcetti L., Sonda N., Bicciato S., Falisi E., Calabrese F., Basso G., Zanovello P., Ugel S., Cozzi E., Mandruzzato S. and Bronte V. (2010) Tumor-Induced tolerance and immune suppression depend on the C/EBPb transcription factor Immunity 32:790–802

150. Hasko´ G., Sitkovsky M. V. and Szabo´ C. (2004) Immunomodulatory and neuroprotective effects of inosine TRENDS in PharmSci 25:152-157

151. Apolloni E., Bronte V., Mazzoni A., Serafini P., Cabrelle A., Segal D.M., Young H.A., Zanovello P. (2000) Immortalized myeloid suppressor cells trigger apoptosis in antigen-activated T lymphocytes. J Immunol. 165:6723-30

152. Di Virgilio, F. (2013) The therapeutic potential of modifying inflammasomes and NOD-like receptors. Pharmacol Rev 65:872-905

153. Kusmartsev S. and Gabrilovich D.I. (2003) Inhibition of myeloid cell differentiation in cancer: the role of reactive oxygen species. J Leukoc Biol. 74:186-96

154. Zea A.H., Rodriguez P.C., Atkins M.B., Hernandez C., Signoretti S., Zabaleta J., McDermott D., Quiceno D., Youmans A., O'Neill A., Mier J., Ochoa A.C.

(2005) Arginase-producing myeloid suppressor cells in renal cell carcinoma patients: a mechanism of tumor evasion. Cancer Res. 65:3044-8

155. Pellegatti P., Raffaghello L., Bianchi G., Piccardi F., Pistoia V., and Di Virgilio F. (2008) Increased level of extracellular ATP at tumor sites: in vivo imaging with plasma membrane luciferase. PLoS One 3:e2599
156. Surprenant A., Rassendren F., Kawashima E., North R. A., and Buell G. (1996). The cytolytic P2Z receptor for extracellular ATP identified as a P2X receptor (P2X7). Science 272:735-738
157. Di Virgilio F., Ferrari D. and Adinolfi E. (2009) P2X(7): a growth-promoting receptor-implications for cancer. Purinergic Signal 5:251-256
158. Pastorino F., Di Paolo D., Piccardi F., Nico B., Ribatti D., Daga A., Baio G., Neumaier C. E., Brignole C., Loi M., et al. (2008) Enhanced antitumor efficacy of clinical-grade vasculature-targeted liposomal doxorubicin. *Clin Cancer Res* 14: 7320-7329
159. Pellegatti P., Falzoni S., Pinton P., Rizzuto R., and Di Virgilio F. (2005) A novel recombinant plasma membrane-targeted luciferase reveals a new pathway for ATP secretion. *Mol Biol Cell* 16:3659-3665
160. Santilli G., PiotrowskamI., Cantilena S., Chayka O., D'Alicarnasso M., Morgenstern D. A., Himoudi N., Pearson K., Anderson J., Thrasher A. J., and Sala A. (2013) Polyphenol e enhances the antitumor immune response in neuroblastoma by inactivating myeloid suppressor cells. *Clin Cancer Res* 19:1116-1125

FULL PAPERS

1. 1 Gulinelli S., Salaro E., Vuerich M., Bozzato D., Pizzirani C., Bolognesi G., Idzko M., Di Virgilio F., Ferrari D. (2012) IL -18 associates to microvesicles shed from human macrophages by a LPS/TLR-4 independent mechanism in response to P2X receptor stimulation. Eur J Immunol. 42, 3334-45
2. 2 Giovanna Bianchi*, Marta Vuerich*, Patrizia Pellegatti, Danilo Marimpietri, Laura Emionite, Ilaria Marigo, Vincenzo Bronte, Francesco Di Virgilio*, Vito Pistoia*, Lizzia Raffaghello* (2014) The ATP/P2X7 axis modulates myeloid-derived suppressor cell functions in neuroblastoma microenvironment Cell Death and Dis. In Press

   *These authors had equally contributed to the paper.

POSTERS

1. 1 Vuerich M., Papalini F., Simonato F., Gulinelli S., Di Virgilio F., Bronte V., Ferrari D. Myeloid Derived Suppressor Cells express P2 receptors (
2. 2 Vuerich M., Simonato F., Papalini F.,Gulinelli S., Franceschelli P., Di Virgilio F., Ferrari D., Bronte V. Extracellular ATP Modulates Myeloid Derived Suppressor Cell Functions
3. 3 Pistoia V., Bianchi G., Marimpietri D., Emionite L., Vuerich M., Marigo I., Bronte V.,
4. Di Virgilio F., Raffaghello L. The ATP/P2X7 Axis Modulates Myeloid-Derived Suppressor Cell Functions in Neuroblastoma Microenvironment